Assessment of Type II Diabetes Mellitus

by

Melissa Barazandegan

B.Sc., Sharif University of Technology, 2007
M.Sc., Sharif University of Technology, 2009

A THESIS SUBMITTED IN PARTIAL FULFILLMENT OF
THE REQUIREMENTS FOR THE DEGREE OF

DOCTOR OF PHILOSOPHY

in

THE FACULTY OF GRADUATE AND POSTDOCTORAL STUDIES

(Chemical and Biological Engineering)

THE UNIVERSITY OF BRITISH COLUMBIA

(Vancouver)

November 2016

Abstract

Several methods have been proposed to evaluate a person's insulin sensitivity (ISI). However, all are neither easy nor inexpensive to implement. Therefore, the purpose of this research is to develop a new ISI that can be easily and accurately obtained by patients themselves without costly, time consuming and inconvenient testing methods. In this thesis, the proposed testing method has been simulated on the computerized model of the type II diabetic-patients to estimate the ISI. The proposed new ISI correlates well with the ISI called M-value obtained from the gold standard but elaborate euglycemic hyperinsulinemic clamp ($r = 0.927$, $p = 0.0045$).

In this research, using a stochastic nonlinear state-space model, the insulin-glucose dynamics in type II diabetes mellitus is modeled. If only a few blood glucose and insulin measurements per day are available in a non-clinical setting, estimating the parameters of such a model is difficult. Therefore, when the glucose and insulin concentrations are only available at irregular intervals, developing a predictive model of the blood glucose of a person with type II diabetes mellitus is important. To overcome these difficulties, under various levels of randomly missing clinical data, we resort to online Sequential Monte Carlo estimation of states and parameters of the state-space model for type II diabetic patients. This method is efficient in monitoring and estimating the dynamics of the peripheral glucose, insulin and incretins concentration when 10%, 25% and 50% of the simulated clinical data were randomly removed.

Variabilities such as insulin sensitivity, carbohydrates intake, exercise, and more make controlling blood glucose level a complex problem. In patients with advanced TIIDM, the control of blood glucose level may fail even under insulin pump therapy. Therefore, building a reliable model-based fault detection (FD) system to detect failures in controlling blood glucose level is critical. In this thesis, we propose utilizing a validated robust model-based FD technique for detecting faults in the insulin infusion system and detecting patients organ dysfunction. Our results show that the proposed technique is capable of detecting disconnection in insulin infusion systems and detecting peripheral and hepatic insulin resistance.

Preface

This thesis entitled "Assessment of type II diabetes mellitus" presents my research during my PhD studies at Chemical and Biological Engineering Department of the University of British Columbia. I led and performed my PhD research under the supervision of Professor K. E. Kwok and Professor R. B. Gopaluni. This thesis includes six Chapters. Contributions and collaborations to the published papers or submitted papers for publication are concisely explained in the following:

- A version of chapter 3 has been presented at the 37^{th} Canadian Medical and Biological Engineering Society (CMBES 37) and won the 3^{rd} place prize presentation award. A version of this chapter has been published first online. Melissa Barazandegan, Fatemeh Ekram, Ezra Kwok, Bhushan Gopaluni, "Simple Self-Administered Method for Assessing Insulin Sensitivity in Diabetic Patients", Journal of Medical and Biological Engineering, pp 1-9, First online: 08 April 2016 [1]. This paper has been prepared with close collaboration of Professor Kwok and Professor Gopaluni. They also have helped in revision of the final draft. Dr. Ekram helped in preparation of the initial drafts of the paper.

- A version of chapter 4 has been published. Melissa Barazandegan, Fatemeh Ekram, Ezra Kwok, Bhushan Gopaluni, Aditya Tulsyan, "Assessment of type II diabetes mellitus using irregularly sampled measurements with missing data", Bioprocess Biosyst Eng, Volume 38, Issue 4, pp 615-629, 2015 [2]. This paper has been published with

close collaboration of Professor Kwok and Professor Gopaluni. They also have helped in revision of the final drafts. Dr. Ekram helped in preparation of the first drafts of the paper and Mr. Tulsyan helped in preparing SIR particle filtering model under missing data.

- A version of chapter 5, Melissa Barazandegan, Ezra Kwok, Bhushan Gopaluni, "Model-Based Detection of Organ Dysfunction and Faults in Insulin Infusion Devices for Type 2 Diabetic Patients" has been presented and published as a proceeding paper in American Control Conference 2016 (ACC2016) [**?**]. This paper has been prepared with close collaboration of Professor Kwok and Professor Gopaluni. They also have helped in revision of the final drafts.

Table of Contents

List of Tables

List of Figures

Nomenclature

Model variables in the glucose sub-model

D	Oral glucose amount (mg)
G	Glucose concentration (mg/dl)
M	Multiplier of metabolic rates (dimensionless)
Q	Vascular blood flow rate (dl/min)
q	Glucose amount in GI tract (mg)
r	Metabolic production or consumption rate (mg/min)
Ra	Rate of glucose appearance in the blood stream(mg/min)
T	Transcapillary diffusion time constant (min)
t	Time (min)
V	Volume (dl)

Model variables in the insulin sub-model

I	Insulin concentration (mU/l)

M Multiplier of metabolic rates (dimensionless)

m Labile insulin mass (U)

P Potentiator (dimensionless)

Q Vascular blood flow rate (dl/min)

R Inhibitor (dimensionless)

r Metabolic production or consumption rate (mU/min)

S Insulin secretion rate (U/min)

T Transcapillary diffusion time constant (min)

t Time (min)

V Volume (dl)

X Glucose-enhanced excitation factor (dimensionless)

Y Intermediate variable (dimensionless)

Model variables in the glucagon sub-model

Γ Normalized glucagon concentration (dimensionless)

M Multiplier of metabolic rates (dimensionless)

r Metabolic production or consumption rate (dl/min)

t Time (min)

V Volume (dl)

Model variables in the incretins sub-model

Ψ	Incretins concentration (pmol/l)
r	Metabolic production or consumption rate (pmol/min)
t	time (min)
V	Volume (dl)

First superscript

Γ	Glucagon
B	Basal condition
G	Glucose
I	Insulin
M	ncretins

Second superscript

∞	Final steady state value

Metabolic rate subscripts

BGU	Brain glucose uptake
GGU	Gut glucose uptake
HGP	Hepatic glucose production

HGU Hepatic glucose uptake

$I\Psi R$ Intestinal incretins release

KGE Kidney glucose excretion

KIC Kidney insulin clearance

LIC Liver insulin clearance

$M\Gamma C$ Metabolic glucagon clearance

$P\Gamma C$ Plasma glucagon clearance

$P\Gamma R$ Pancreatic glucagon release

$P\Psi C$ Plasma incretins clearance

PGU Peripheral glucose uptake

PIC Peripheral insulin clearance

PIR Pancreatic insulin release

$RBCU$ Red blood cell glucose uptake

First superscripts

∞ Final steady state value

A Hepatic artery

B Brain

G Gut

H	Heart and lungs
L	Liver
P	Periphery
S	Stomach

Second subscripts (if required)

C	Capillary space
F	Interstitial fluid space
l	Liquid
s	Solid

Acknowledgements

All praise is due to God Almighty, the most gracious and the most merciful, who protects, preserves and supports us during day and night. Thank you, God, for your insight, guidance, companionship, integrity, and for all the sacrifices you made.

I would like to express my sincere thanks and appreciation to my doctoral supervisors, Professor Ezra Kwok and Professor Bhushan Gopaluni from Chemical and Biological Engineering Department at the University of British Columbia. You have been a tremendous mentor for me. I would like to thank you for encouraging my research and for allowing me to grow as a research scientist. Your advice on both research as well as on my career have been priceless.

I would like to thank my control group members who have been helpful and supportive friends during my Ph.D. appointment: Omid Vahidi, Fatemeh Ekram, and Aditya Tulsyan.

I would like to thank my parents, Mehdi and Mojgan, and especially my sister, Sogol, for their unconditional love, encouragement and support during my research.

Finally I would like to express my gratitude to my husband, Mohammadali, and my son, Aubtin, for being so supportive throughout my graduate program.

Dedication

This thesis is dedicated to the loveliest creature on earth, my mother, who sacrificed herself for me, to my father for all his support, to my sweet sister, to my lovely husband and to my beloved son.

Chapter 1

Introduction

1.1 Background

Diabetes Mellitus is one of the leading diseases in the developed world. According to the International Diabetes Federation, the prevalence of diabetes is growing rapidly in the world. Diabetes mellitus occurs when the blood glucose levels are not regulated due to the impaired insulin secretion, action or both. Insulin is a key hormone secreted from β-cells in the pancreas that regulates glucose homeostasis [3–6]. Diabetes mellitus is generally categorized into three groups [7]:

- Type I diabetes or insulin dependent diabetes mellitus (IDDM), in which the body is unable to produce insulin due to the autoimmune destruction of the beta cells in the pancreas. Therefore, the body becomes insulin dependent and daily insulin doses must be supplied to the type I diabetic patients to survive. Most often, it occurs in childhood, but the disease can also develop in adults in their late 30s and early 40s.

- Type II diabetes or non-insulin dependent diabetes mellitus (NIDDM), in which the pancreas does not produce enough insulin or the human body cells become resistance against insulin [3]. Type II diabetic patients require gradual treatment and are not in emergency need of medical attention.

- Gestational diabetes, which develops during pregnancy (gestation). It occurs in preg-

nant women who have never had diabetes before. Gestational diabetes causes high blood glucose level that can affect woman's pregnancy and the baby's health.

A comparison of type I and type II diabetes is presented in table 1.1 [8].

Table 1.1: Comparison of type I and II diabetes [8]

Feature	Type I diabetes	Type II diabetes
Onset	Sudden	Gradual
Age at onset	Any age (Mostly in children)	Mostly in adults
Body habitus	Thin or normal	Often obese
Ketoacidosis	Common	Rare
Autoantibodies	Usually present	Absent
Endogenous insulin	Low or absent	Normal, decreased or increased
Concordance in identical twins	%50	%90
Prevalence	$\sim$ 10% of diabetic population	$\sim$ 90% of diabetic population

1.1.1 Glucose homeostasis

When the glucose, a simple sugar, is produced from digestion of carbohydrates in the gastrointestinal tract, it is absorbed by the body cells to provide the primary energy source. The blood glucose concentration is maintained at a constant level during fast by producing endogenous glucose through two main metabolic pathways [7]:

- **Gluconeogenesis**, in which glucose is generated from non-carbohydrate carbon substrates such as lactate, glycerol, and glucogenic amino acids. In this metabolic pathway, the endogenous glucose is produced by the liver and kidney and is released into the blood stream.

- **Glycogenolysis**, in which glucose is generated from breakdown of glycogen. In this metabolic pathway, the endogenous glucose is produced by the liver and muscles. The endogenous glucose produced by the liver is released into the blood stream while the produced glucose in muscle cells is consumed by themselves.

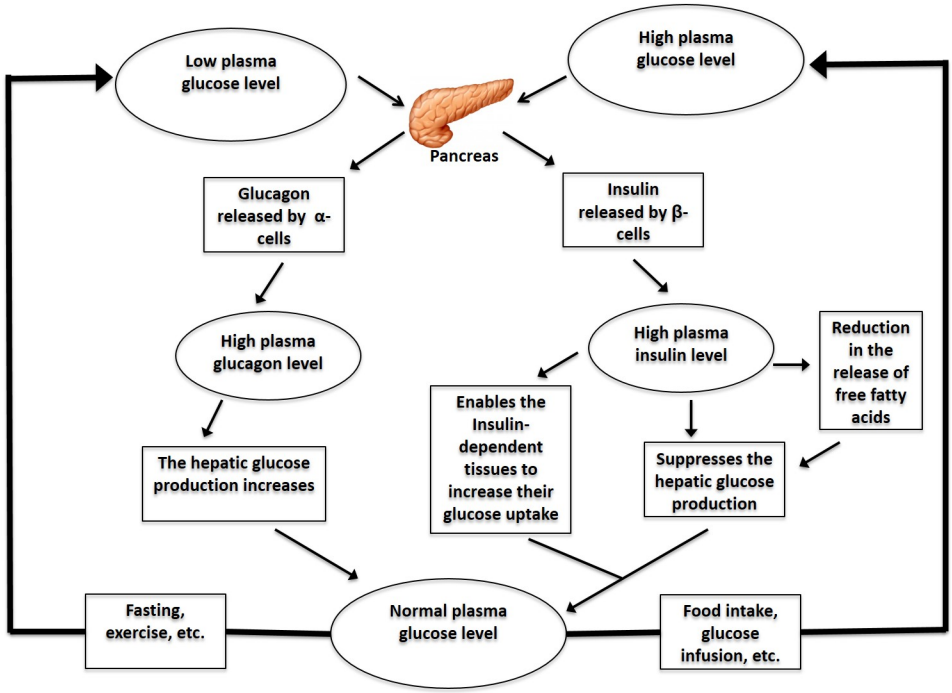

Figure 1.1: Glucose homeostasis control mechanism in the body [7]

Approximately 15% of endogenous glucose production released into the blood stream is derived from the kidney, and the remaining 85% is produced by the liver. [9].

In normal (non-diabetic) subjects, the blood glucose level is controlled within an approximate range of 60-150 mg/dl, despite disturbances such as exercise or intake of a meal containing carbohydrates [10]. The blood glucose level is regulated through feedback systems reacting mainly on glucose, insulin and glucagon concentrations. Insulin and glucagon are two hormones in the body secreted from the β and α cells of the pancreas, respectively. These hormones play an important role in glucose homeostasis in the body, however, the effects of glucagon are opposite to those of insulin (see Figure 1.1). Insulin contributes in lowering the blood sugar level by stimulating some body cells to absorb glucose, suppressing endogenous glucose production and inhibiting glucagon secretion. When the blood sugar

level is high, insulin is secreted from $\beta - cells$ of pancreas to:

- stimulate the body cells to absorb glucose
- suppress endogenous glucose production
- inhibit glucagon secretion from $\alpha - cells$ of pancreas

Conversely, when the blood glucose concentration is low, glucagon is secreted from $\alpha - cells$ of pancreas to:

- stimulate the liver to produce more glucose
- inhibit insulin secretion from $\beta - cells$ of pancreas

1.1.2 Type II diabetes mellitus and the related metabolic abnormalities

Type II diabetes occurs when the pancreas does not produce enough insulin or the human body cells become resistance against insulin [3]. Type II diabetes is characterized by multiple abnormalities in a number of body organs such as the liver, the pancreas, muscles and adipose tissues. These abnormalities are classified as follows:

- **Insulin resistance in peripheral tissues:** Peripheral tissues (*i.e.* muscle and adipose tissue cells) absorb blood glucose by sensing insulin hormone. Insulin resistance happens when the sensitivity of peripheral cells to the metabolic action of insulin is decreased due to genetic factors, environmental factors, obesity, hypertension, dyslipidemias, and/or coronary artery diseases [11]. Impairment of the following factors is known to be associated with insulin residence in peripheral tissues [9]:
  - The number of insulin receptors
  - The affinity of insulin receptors

  - Insulin intracellular signalling
  - The number of glucose transporters
  - Glucose transporter translocation on the cell membrane
  - Insulin stimulatory effects on glycogenesis
  - Insulin stimulatory effects on glycolysis

- **Reduced hepatic glucose uptake:** It is believed that reduce in hepatic glucose uptake rate is due to the impairment of insulin stimulation effect on glucose phosphorylation in the liver [12].

- **Impaired hepatic glucose production:** Many studies have confirmed that type II diabetic patients have impaired hepatic glucose production rate and low insulin-induced suppression of endogenous glucose production [13–17]. The impaired effect of insulin suppression on both pathways of endogenous glucose production (*i.e.* gluconeogenesis and glycogenolysis) have been demonstrated by Basu *et al.* [16, 17].

- **Impaired pancreatic insulin secretion:** Deficiency and failure in the pancreatic insulin production shows the development of overt diabetes [9]. Pancreatic insulin secretion in response to a glucose stimulus has a biphasic pattern. Early peak of insulin production and the overall insulin secretion rate are the two forms of defective pancreatic insulin secretion in type II diabetic patients[18–20].

- **Glucose resistance:** When the levels of glucose concentration is less than 130 mg/dl, glucose-induced stimulation of glucose disposal is normal in type II diabetic patients [21]. However, high levels of glucose concentration (particularly above 130 mg/dl) impair the glucose stimulation effect on glucose uptake rate in type II diabetic patients [22, 23].

1.1.3 Evaluation of the health status of diabetic patients

There are different clinical tests used for assessing the glucose metabolism in different body organs to evaluate the health status of diabetic patients. A brief explanation of some of these clinical tests is as follows [7]:

- **Oral glucose tolerance test (OGTT):** This test is usually used to diagnose diabetes, insulin resistance, impaired beta cell function, and sometimes reactive hypoglycemia and acromegaly, or rarer disorders of carbohydrate metabolism. First, the fasting plasma glucose is tested. Then, to determine how body is able to clear glucose from the blood, a glass of dissolved glucose in water is given to the patient and blood samples are taken afterwards up to four times to measure the blood glucose. Depending on different standards, the dose of glucose may vary from 50 gr to 100 gr.

- **Euglycemic hyperinsulinemic clamp (EHIC):** In this test, the plasma glucose concentration is held constant at basal levels by intravenous glucose infusion. Meanwhile, the plasma insulin concentration is raised and maintained at 100 $\mu U/ml$ by a continuous infusion of insulin. When the steady-state is achieved, the glucose infusion rate equals glucose uptake by all the tissues in the body. Therefore, for more sensitive insulin tissues, more glucose infusion is needed. The hyperinsulinemic clamps is a measure of insulin resistance.

- **Hyperglycemic clamp (HGC):** In this test, the plasma glucose concentration is raised to 125 mg/dl above basal levels by intravenous glucose infusion and no insulin injection. Since the plasma glucose concentration is held constant, at steady states, the rate of glucose infusion is an index of insulin secretion and glucose metabolism. The hyperglycemic clamps are often used to assess insulin secretion capacity.

- **Intravenous glucose tolerance test (IVGTT):** This test is similar to the OGTT test. However, instead of oral glucose consumption, glucose is infused intravenously into the patient's body. Then, variation of glucose concentration is measured from patient's blood samples. Measurements of glucose concentration show how the body clears glucose from the body.

- **Insulin suppression test:** Similar to the EHIC test, this test is used to measure insulin sensitivity. In this test, somatostatin is injected to suppress endogenous secretion of glucose and insulin while a constant rate of glucose and insulin is infused intravenously. Blood samples are taken from the subject in specific times during the test. At steady-states, the plasma insulin concentration is the same in all subjects, and the value of the plasma glucose concentration provides a direct estimate of insulin resistance. Body with high level of insulin resistance, has the higher value of the plasma glucose concentration at steady-state.

1.1.4 Qualitative and quantitative evaluation of abnormal metabolism behaviour in diabetic patients

As described in previous section, there are different clinical test that their results used to evaluate abnormal behaviour of body organs in diabetic patients. To quantify the medical condition of healthy and diabetic patients, many studies proposed different indices in the literature such as [7]:

- Insulin Sensitivity Index (ISI), which quantifies the ability of insulin to stimulate body glucose disposal.

- Glucose Effectiveness Index (GEI), which measures the ability of glucose per se to mediate its rate of disappearance and to inhibit hepatic glucose production.

Many different definitions for these two indices are reported in the literature. Direct measurements of insulin sensitivity are proposed via the following test in the literature:

- Euglycemic hyperinsulinemic clamp test [24, 25]
- Insulin Sensitivity Tolerance (IST) test [26–28]

In addition, indirect measurement of insulin sensitivity is proposed in the literature from frequently sampled intravenous glucose tolerance test (FSIVGTT) [29–35]. In this method, from the results of FSIVGTT test the parameters of the minimal model are determined [36]. Later, the obtained parameters are used to define insulin sensitivity and glucose effectiveness indices. Also, different surrogate indices for insulin sensitivity have been also defined in the literature using fasting insulin and glucose measurements as follows:

- Homeostasis model assessment (HOMA) [37–39],
- Quantitative insulin sensitivity check index (QUICKI) [25, 40–43]
- Oral Glucose Tolerance test (OGTT): Matsuda index [44], Stumvoll index [45], Avignon index [46], oral glucose insulin sensitivity index [47], Gutt index [48], and Belfiore index [49] are the insulin sensitivity indices obtained from this test by using different sampling protocols during OGTT test.

1.2 Thesis objectives

The application of dynamic mathematical modelling has increased in every aspect of our lives. Mathematical modelling of glucose metabolism in diabetic patient is helpful in providing reliable information without causing serious and irreversible harm to the subject. Most of the studies in the field of modelling of diabetes have addressed type I diabetes mellitus. However, type II diabetes is the most pervasive type which affects 90% of the

diabetes population around the world [50]. Type I diabetes mellitus is characterized by pancreas dysfunction, however, type II diabetic patients deal with multiple abnormalities in a number of body organs such as the liver, the pancreas, muscles and adipose tissues. Therefore, studying, modelling and simulating physiological behaviour of type II diabetic patients is much more complicated than type I diabetic patients.

In the light of aforementioned above, the goal of my Ph.D. research is to benefit our society in managing diabetes mellitus, which is one of the most prevalent diseases affecting at least 285 million people worldwide. The objective of my Ph.D. research mainly is focused on employing a clinically-relevant physiological model of type II diabetes mellitus to improve the management of blood glucose level and fault detection features suitable for monitoring and control. This objective can be achieved in the following three steps:

1. Type II diabetes is characterized by multiple abnormalities in a number of body organs. Insulin resistance is one of the abnormalities happening when the sensitivity of peripheral cells to the metabolic action of insulin is decreased. The ability of insulin to stimulate body glucose disposal can be characterized by an insulin sensitivity index (ISI). Several methods have been proposed for evaluating a person's insulin sensitivity from an oral glucose tolerance test (OGTT) and the euglycemic insulin clamp technique. However, none are easy or inexpensive to implement since the plasma insulin concentration, as a key variable for assessing the insulin sensitivity index (ISI), is required to be clinically measured at specific times. Therefore, my first thesis objective is using clinically-relevant physiological model of type II diabetes mellitus to develop a simple self-administered testing method for estimating the insulin sensitivity index that can be easily and accurately obtained by patients themselves without costly, time-consuming, and inconvenient testing methods.

2. Mathematical modelling of glucose metabolism in diabetic patient provides useful in-

formation to diabetic patients of dangerous metabolic conditions, enables physicians to review past therapy, estimates future blood glucose levels, and provides therapy recommendations.The insulin-glucose dynamics in type II diabetes mellitus can be modelled by using a stochastic nonlinear state-space model. Estimating the parameters of such a model is difficult as only a few blood glucose and insulin measurements per day are available in a non-clinical setting. Therefore, my second thesis objective is to develop a predictive model of the blood glucose of a person with type II diabetes mellitus when the glucose and insulin concentrations are only available at irregular intervals. The results of this study can be used to inform type II diabetic patients of their medical conditions, enable physicians to review past therapy, estimate future blood glucose levels, provide therapeutic recommendations and even design a stabilizing control system for blood glucose regulation.

3. Controlling blood glucose level for patient with type II diabetes mellitus (TIIDM) has been influenced by many variables with significant levels of variability, such as insulin sensitivity, carbohydrates intake, exercise, and more. These variabilities make controlling blood glucose level a complex problem. In patients with advanced type II diabetes mellitus, when the body fails to regulate blood glucose level, an external loop including an insulin pump and a glucose measurement device can be used in maintaining glucose regulation. However, the control of blood glucose level may fail even in patient with insulin pump therapy. Therefore, my third thesis objective is to build a reliable model-based fault detection system to detect failures in controlling blood glucose level. The results of this study is helpful to detect faults in the insulin infusion system and detect patient's organ dysfunction.

1.3 Thesis outline

My thesis is organized as follows:

- In chapter 2, the mathematical modelling developed by Vahidi *et al.* [7, 51] for type II diabetes is described. The Vahidi model results from initial work by Guyton *et al.* [52], which was updated by Sorensen [53]. This model is a much more detailed model compared to the compartmental minimal modelling (MINMOD) approach proposed by Bergman [36]. The MINMOD includes three nonlinear differential equations representing variations of plasma insulin and glucose concentrations. However, the Vahidi model consists of more compartments for better representation of the glucose and insulin concentrations in different parts of a human body. Their application of additional compartments allows for a more accurate simulation of the physiological dynamics and individual abnormalities for type II diabetic patients.

- In chapter 3, the feasibility of using the mathematical compartment model proposed by Vahidi *et al.* [7, 51] to estimate insulin sensitivity has been described. A simple method for conveniently estimating insulin sensitivity by patients themselves has been developed and evaluated.

- In chapter 4, the nonlinear states and the parameters of Vahidi model in the presence of 10%, 25% and 50% of randomly missing clinical observations have been estimated by implementing a Bayesian filtering method.

- In chapter 5, faults in insulin infusion system and organs dysfunction are detected in type II diabetic patients using the model-based fault detection technique based on a Sequential Monte Carlo (SMC) filtering method.

- Finally, chapter 6 summarizes the thesis and provides recommendations on future

works.

Chapter 2

Mathematical modeling of type II diabetes mellitus

2.1 Introduction

Glucose-insulin interactions in a healthy human body have been mathematically modelled in many studies. Initially, Bolie [54] and Ackerman *et al*. [55] proposed a simple linear model, and later, more complicated nonlinear models have been proposed. Among those approaches, the compartmental modelling approach is the most popular one. In this approach, different organs or parts of the body are represented by compartments, and the model equations are derived from the mass balance equations over each compartment. The compartmental minimal model (MINMOD) of Bergman *et al*. [36] has been widely used in many studies. The MINMOD includes three nonlinear differential equations representing variations of plasma insulin and glucose concentrations. Later, more complicated compartmental models have been proposed including more compartments for better understanding of the organ's behaviour [53, 56, 57].

The physiological behaviour of type I and type II diabetes can be developed by adjusting the structures of healthy human models. For, instance, since the pancreas in type I diabetic patients does not produce insulin hormone, type I diabetes mellitus model can be simply adjusted from healthy human models by setting the insulin production rate term to zero

[7].

However, using the similar approach for type II diabetes modelling is not as simple as type I diabetes modelling since type II diabetes is associated with multiple abnormalities in different body organs. In type II diabetic patients, all the body organs are still functioning and the organ's abnormalities affects the glucose metabolic rates, the glucose regulatory secretion rates, and the pancreatic insulin secretion rates. Therefore, type II diabetes mellitus model can be developed from the same structure of the healthy human model but with the modified parameters. This approach has been used by Dalla Man *et al.* [58] and Vahidi *et al.*. [7]. Vahidi model is based on a healthy human body model proposed by Sorensen [53], which is adjusted and validated for type II diabetes using available clinical data of diabetic patients.

In the following sections, the equations of Sorensen model are presented along with the parameters updated for type II diabetic patient by Vahidi [7, 53]. The description of the model variables can be found in Nomenclature.

2.2 The Sorensen model

Sorensen modified the compartmental model of glucose-insulin interactions in a healthy body developed by Guyton *et al.* [52]. In this, model, the regulatory effects of insulin and glucagon hormones on glucose metabolism are considered. However, the hormonal effects of epinephrine, cortisol, and growth hormone are assumed to be negligible. Also, the physiology of changes in amino acid and free fatty acid substrate levels are not considered. In this model, the physiologic parameters such as blood flow rates and capillary space volumes are selected to represent a typical 70 kg adult male.

The simplified blood circulatory system contributing significantly in glucose production and consumption is shown in Figure 2.1. The heart left ventricle pumps the Oxygen-rich

blood and deliver it to all body organs through the arteries. the body organs drain out deoxygenated blood and deliver it to the heart right atrium through the veins.

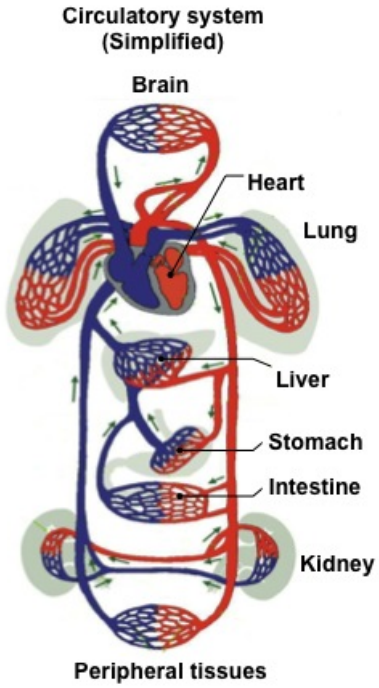

Figure 2.1: Simplified blood circulatory system [7]

The Sorensen model contains three main sub-models representing blood glucose, insulin and glucagon concentrations in the body and their interactions.

Each sub-model is divided into individual numbers of compartments representing specific parts or organs of a human body. The number of compartments is different in each sub-model. As can be seen in Figure. 2.2, the insulin sub-model has seven compartments: brain, liver, heart and lungs, periphery, gut, kidney, and pancreas. The blocks represent different compartments and the arrows indicate the blood flow directions.

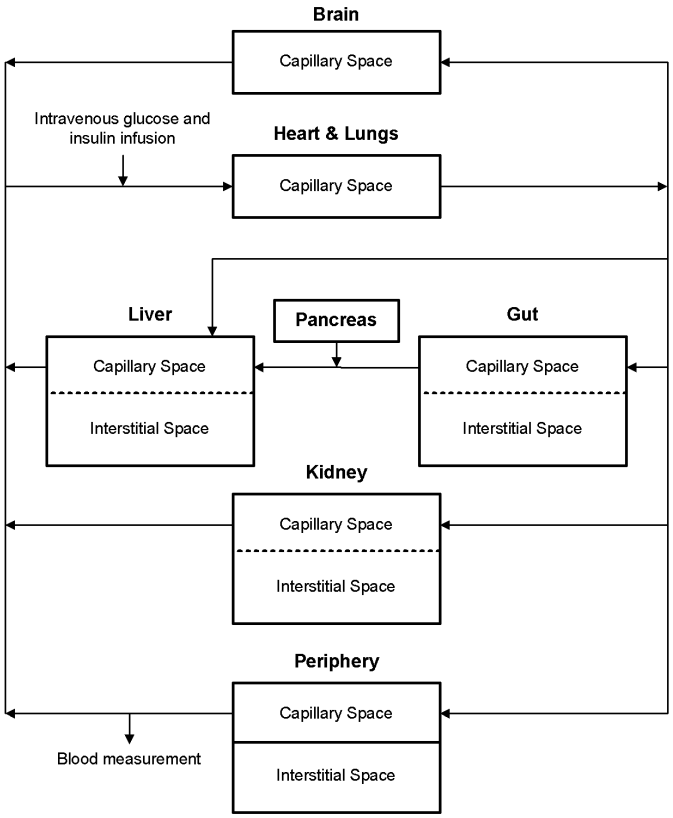

Figure 2.2: Shematic diagram of insulin submodel [51]

The glucose sub-model is similar to the insulin sub-model except that the pancreas compartment is excluded. The glucose sub-model can be seen in Figure. 2.3.

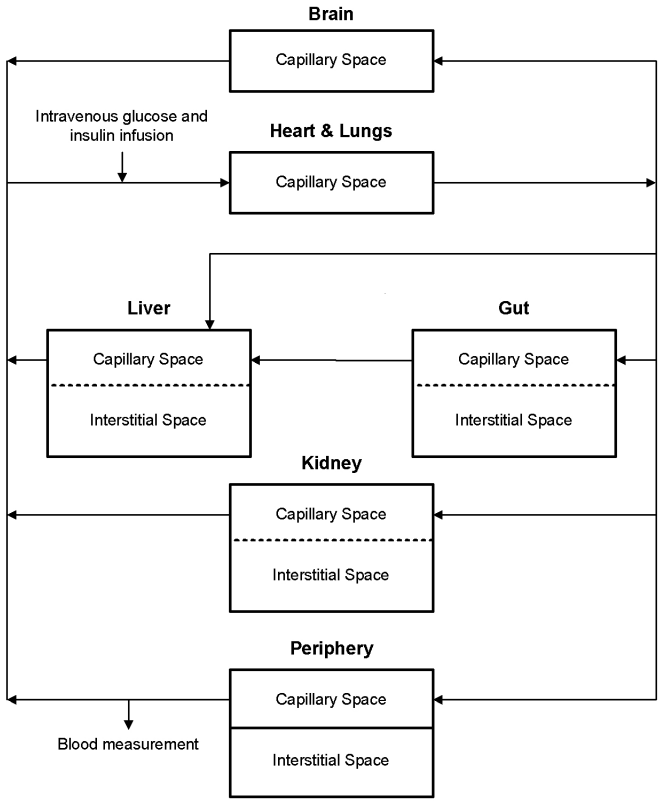

Figure 2.3: Shematic diagram of glucose submodel [7]

Since the glucagon concentration is considered to be identical in all parts of the body, only one compartment is used in the glucagon sub-model [59]. Each compartment is generally divided into the following three well-mixed spaces, which are shown in Figure 2.4:

- Capillary blood space
- Interstitial fluid space
- Intracellular space

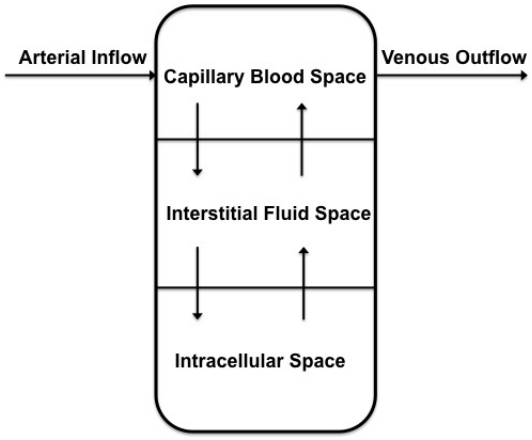

Figure 2.4: General representation of a compartment[7]

As can be seen from Figure 2.4, the capillary space is fed in by arterial blood inflow and drained by venous blood outflow. The blood components may diffuse through capillary walls to the interstitial fluid and from interstitial fluid to the intracellular space and vice versa. Due to the following reasons, maximum two of these sub-compartments are physiologically required to be considered in modelling of solute transport from the capillary blood space to the intracellular space (Figure 2.5):

- The capillary wall may not allowing fluid to pass through a solute and no extravascular exchange occurs. Therefore, both the interstitial fluid and the intracellular fluid spaces are omitted and only the capillary blood space is considered (Figure 2.5 a).
- The capillary wall may be very permeable to a solute leading to a fast equilibrium of the capillary blood and the interstitial fluid spaces. In this case, both of the capillary blood and the interstitial fluid spaces are considered as a combined sub-compartment with uniform solute concentration (Figure 2.5 b).
- The cell membrane may be very permeable to a solute leading to a fast equilibrium of the interstitial fluid and intracellular fluid spaces. Therefore, both of the

interstitial fluid and intracellular fluid spaces are combined and considered as one sub-compartment with uniform solute concentration (Figure 2.5 c).

- The capillary wall and cell membrane are both very permeableto a solute leading to a fast equilibrium of all three spaces. Therefore, all three spaces are combined and considered as one space with uniform solute concentration (Figure 2.5 d).

- The concentration of the solute in the intracellular fluid space restricts the rate of solute transport across the cell membrane. Therefore, the intracellular space is omitted (Figure 2.5 e).

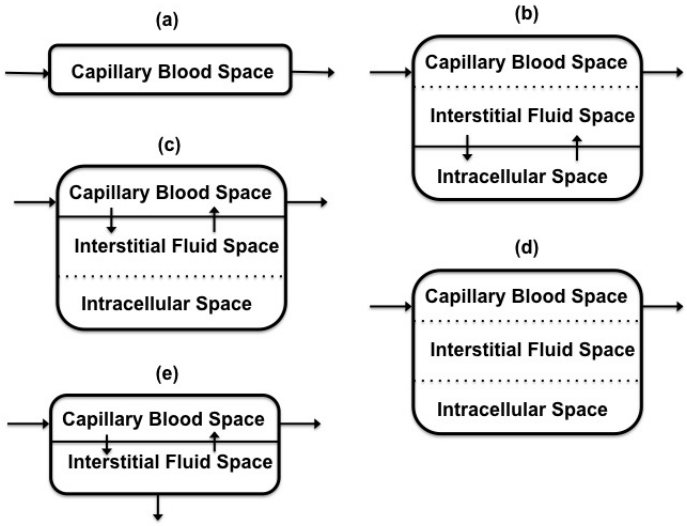

Figure 2.5: Simplified configurations of physiological compartments[7]

In the following sections, the mass balance equations over each sub-compartment are presented.

2.2.1 Glucose sub-model

As explained in section 2.2, the glucose sub-model is divided into six compartments: brain; liver; heart and lungs; periphery (muscles and adipose tissues); gastrointestinal (GI) tract (the stomach and intestinal system); and kidney. Mass balance equations over each sub-compartment results the following eight ordinary differential equations:

$$V_{BC}^{G}\frac{dG_{BC}}{dt} = Q_{B}^{G}(G_H - G_{BC}) - \frac{V_{BF}^{G}}{T_{B}^{G}}(G_{BC} - G_{BF}), \tag{2.1}$$

$$V_{BF}^{G}\frac{dG_{BF}}{dt} = \frac{V_{BF}^{G}}{T_{B}^{G}}(G_{BC} - G_{BF}) - r_{BGU}, \tag{2.2}$$

$$V_{H}^{G}\frac{dG_H}{dt} = Q_{B}^{G}G_{BC} + Q_{L}^{G}G_L + Q_{K}^{G}G_K + Q_{P}^{G}G_{PC} + Q_{H}^{G}G_H - r_{BCU}, \tag{2.3}$$

$$V_{G}^{G}\frac{dG_G}{dt} = Q_{G}^{G}(G_H - G_G) - r_{GGU}, \tag{2.4}$$

$$V_{L}^{G}\frac{dG_L}{dt} = Q_{A}^{G}G_H + Q_{G}^{G}G_G - Q_{L}^{G}G_L + r_{HGP} - r_{HGU}, \tag{2.5}$$

$$V_{K}^{G}\frac{dG_K}{dt} = Q_{K}^{G}(G_H - G_K) - r_{KGE}, \tag{2.6}$$

$$V_{PC}^{G}\frac{dG_{PC}}{dt} = Q_{P}^{G}(G_H - G_{PC}) - \frac{V_{PF}^{G}}{T_{P}^{G}}(G_{PC} - G_{PF}), \tag{2.7}$$

$$V_{PF}^{G}\frac{dG_{PF}}{dt} = \frac{V_{PF}^{G}}{T_{P}^{G}}(G_{PC} - G_{PF}) - r_{PGU}, \tag{2.8}$$

where G is the glucose concentration (mg/dl), Q is the vascular blood flow rate (dl/min), V is the volume (dl), T is the transcapillary diffusion time constant (min), r is the metabolic production or consumption rate (mg/min) and t is time (min). The subscripts of these variables refer to the body organs. Subscript B is the brain, subscript BC is the brain capillary space and subscript BF is the brain interstitial fluid space. Subscript A is the hepatic artery, subscript G is gut, subscript L is liver and subscript G is GI tract (stomach

and intestines). Subscript P is periphery, subscript PC is the periphery capillary space and subscript PF is the periphery interstitial fluid space.

The general form of the metabolic production and consumption rates in each organ is as follows [53]:

$$r = M^I(t)M^G(t)M^\Gamma(t)r^B, \tag{2.9}$$

where M^I, M^G and M^Γ are the independent multiplicative effect of insulin, glucose and glucagon on the metabolic rate, respectively. r^B is the basal metabolic rate and the multipliers have the following general form:

$$M^C = a + b\tanh[c(\frac{C}{C^B} - d)], \tag{2.10}$$

where a, b, c and d are the parameters of the model. C is the substance concentration and C^B is the basal concentration of the substance. The following equations are used to calculate the glucose metabolic rates [53]:

$$r_{BGU} = 70 \tag{2.11}$$

$$r_{RBGU} = 10 \tag{2.12}$$

$$r_{GGU} = 20 \tag{2.13}$$

$$r_{PGU} = M^I_{PGU}M^G_{PGU}r^B_{PGU}, \tag{2.14}$$

$$r^B_{PGU} = 35 \tag{2.15}$$

$$M^I_{PGU} = 7.03 + 6.52\tanh(0.338(\frac{I_{PF}}{I^B_{PF}} - 5.82) \tag{2.16}$$

$$M^G_{PGU} = \frac{G_{PF}}{G^B_{PF}} \tag{2.17}$$

$$r_{HGP} = M^I_{HGP} M^G_{HGP} M^\Gamma_{HGP} r^B_{HGP}, \tag{2.18}$$

$$r^B_{HGP} = 35 \tag{2.19}$$

$$\frac{d}{dt} M^I_{HGP} = 0.04(M^{I_\infty}_{HGP} - M^I_{HGP}) \tag{2.20}$$

$$M^{I_\infty}_{HGP} = 1.21 - 1.14 \tanh[1.66(\frac{I_L}{I^B_L} - 0.89)] \tag{2.21}$$

$$M^G_{HGP} = 1.42 - 1.14 \tanh[0.62(\frac{G_L}{G^B_L} - 0.497)] \tag{2.22}$$

$$M^\Gamma_{HGP} = 2.7 \tanh[0.39(\frac{\Gamma}{\Gamma^B}] - f \tag{2.23}$$

$$\frac{d}{dt} f = 0.0154[(\frac{2.7 \tanh[0.39(\frac{\Gamma}{\Gamma^B}] - 1}{2}) - f] \tag{2.24}$$

$$r_{HGU} = M^I_{HGU} M^G_{HGU} r^B_{HGU}, \tag{2.25}$$

$$r^B_{HGU} = 20 \tag{2.26}$$

$$\frac{d}{dt} M^I_{HGU} = 0.04(M^{I_\infty}_{HGU} - M^I_{HGU}) \tag{2.27}$$

$$M^{I_\infty}_{HGU} = 2.0 \tanh[0.55(\frac{I_L}{I^B_L}] \tag{2.28}$$

$$M^G_{HGU} = 5.66 + 5.66 \tanh[2.44(\frac{G_L}{G^B_L} - 1.48)] \tag{2.29}$$

$$\begin{aligned} {}_{KGE} &= 71 + 71 \tanh[0.11(G_K - 460)] \qquad 0 \le G_K < 460 \\ r_{KGE} &= 71 + 71 \tanh[0.11(G_K - 460)] \qquad G_K \ge 460 \end{aligned} \tag{2.30}$$

where r_{BGU} is brain glucose uptake rate, r_{RBGU} is red blood cell glucose uptake rate, r_{GGU} is gut glucose uptake rate, r_{HGP} is hepatic glucose production rate, r_{HGU} is hepatic glucose uptake rate, r_{KGE} is kidney glucose excretion rate, and r_{PGU} is peripheral glucose uptake rate. G, I and Γ are the concentration of glucose, insulin and glucagon, respectively.

Superscript B refers to the basal condition and ∞ refer to final steady state value.

In equation 2.17, the glucose multiplier of peripheral glucose uptake rate is different from other multipliers. It is a linear function of the peripheral glucose concentration and has the following general form:

$$M_{PGU}^{G} = a(\frac{G_{PF}}{G_{PF}^{B}}) + b \tag{2.31}$$

where a and b are the parameters of glucose multiplier of peripheral glucose uptake rate.

The glucose absorption model that calculates the glucose appearance rate into the blood stream following an oral glucose intake is considered in the gut compartment of the glucose sub-model as follows:

$$\frac{dq_{Ss}}{dt} = -k_{12}q_{Ss} + D\delta(t), \tag{2.32}$$

$$\frac{dq_{SI}}{dt} = -k_{empt}q_{Ss} + k_{12}q_{SI}, \tag{2.33}$$

$$\frac{dq_{int}}{dt} = -k_{abs}q_{int} + k_{empt}q_{SI}, \tag{2.34}$$

$$k_{empt} = k_{min} + \frac{k_{max} - k_{min}}{2}\{\tanh[\varphi_1(q_{Ss} + q_{SI} - x_1D)] - \tanh[\varphi_2(q_{Ss} + q_{SI} - x_2D)] + 2\}, \tag{2.35}$$

$$\varphi_1 = \frac{5}{2D(1 - x_1)}, \tag{2.36}$$

$$\varphi_2 = \frac{5}{2Dx_2}, \tag{2.37}$$

$$Ra = fk_{abs}q_{int}, \tag{2.38}$$

where $\delta(t)$ is the impulse function. x_1, x_2 and f are constant and their values are 0.9. 0.82, and 0.00236 respectively [58]. D is the amount of oral glucose intake (mg). The

parameters that are unknown and need to be estimated are k_{12}, k_{min}, k_{max}, and k_{abs}.

2.2.2 Incretins sub-model

The incretins production is calculated from the following differential equation:

$$\frac{d\psi}{dt} = \varsigma \; k_{empt} \; q_{S2} - r_{I\Psi P}, \tag{2.39}$$

where ψ is the amount of produced incretins, $k_{empt} \; q_{S2}$ is the rate of glucose entrance to the small intestine, $r_{I\Psi P}$ is the rate of incretins absorption into the blood stream, and ς is a constant. $r_{I\Psi P}$ is calculated from the following equation:

$$r_{I\Psi P} = \frac{\Psi}{\tau_\Psi}, \tag{2.40}$$

where τ_Ψ is the time constant of the incretins absorption process into the blood stream. The mass balance equation over the incretins compartment results in:

$$V^\Psi \frac{d\psi}{dt} = r_{I\Psi P} - r_{P\Psi C}, \tag{2.41}$$

where V^Ψ=11.31 (l) is the incretins distribution volume, Ψ is the blood incretins concentration and $r_{P\Psi C}$ the rate of plasma incretins clearance, which depends on the incretins concentration. The clearance rate is calculated from the following equation:

$$r_{P\Psi C} = r_{M\Psi C} \; \psi, \tag{2.42}$$

The parameters that are unknown and need to be estimated are ς, τ_Ψ, and $r_{M\Psi C}$.

2.2.3 Insulin sub-model

As explained in section 2.2, the insulin sub-model is divided into seven compartments: brain; liver; heart and lungs; periphery (muscles and adipose tissues); gastrointestinal (GI) tract (the stomach and intestinal system); kidney; and pancreas. Since pancreatic insulin production is a complex mechanism that cannot be described by simple mass balance equations, the insulin sub-model comprises mass balance equations over each sub-compartment except for the pancreas compartment. Therefore, a separate model is considered for the pancreas.

Mass balance equations over each sub-compartment results in the following equations:

$$V_B^I \frac{dI_B}{dt} = Q_B^I(I_H - I_B), \tag{2.43}$$

$$V_H^I \frac{dI_H}{dt} = Q_B^I I_B + Q_L^I I_L + Q_K^I I_K + Q_P^I I_{PV} - Q_H^I I_H, \tag{2.44}$$

$$V_G^I \frac{dI_G}{dt} = Q_G^I(I_H - I_G), \tag{2.45}$$

$$V_L^I \frac{dI_L}{dt} = Q_A^I I_H + Q_G^I I_G - Q_L^I I_L + r_{PIR} - r_{LIC}, \tag{2.46}$$

$$V_K^I \frac{dI_K}{dt} = Q_K^I(I_H - I_K) - r_{KIC}, \tag{2.47}$$

$$V_{PC}^I \frac{dI_{PC}}{dt} = Q_P^I(I_H - I_{PC}) - \frac{V_{PF}^I}{T_P^I}(I_{PC} - I_{PF}), \tag{2.48}$$

$$V_{PF}^I \frac{dI_{PF}}{dt} = \frac{V_{PF}^I}{T_P^I}(I_{PC} - I_{PF}) - r_{PIC}, \tag{2.49}$$

where I is the insulin concentration (mU/l), Q is the vascular blood flow rate (dl/min), V is the volume (dl), T is the transcapillary diffusion time constant (min), r is the metabolic production or consumption rate (mg/min) and t is time (min). The subscripts of the variables refer to the body organs. subscript B is the brain, subscript A is the hepatic

artery, subscript G is gut, subscript L is liver and subscript G is GI tract (stomach and intestines). Subscript P is periphery, subscript PC is the periphery capillary space and subscript PF is the periphery interstitial fluid space.

The following equations are used to calculate the insulin consumption rates:

$$r_{LIC} = 0.4[Q_A^I I_H + Q_G^I I_G + r_P IR] \tag{2.50}$$

$$r_{KIC} = 0.3 Q_K^I I_K \tag{2.51}$$

$$r_{PIC} = \frac{I_{PF}}{[(\frac{1-0.15}{0.15 Q_P^I}) - \frac{20}{V_{PF}^I}]} \tag{2.52}$$

where R is the inhibitor (dimensionless) and r is the metabolic production or consumption rate (mU/min). r_{KIC} is kidney insulin clearance rate, r_{LIC} is liver insulin clearance rate, r_{PIC} is peripheral insulin clearance rate and r_{PIR} is pancreatic insulin release rate.

Pancreatic insulin release

Pancreatic insulin release is mainly stimulated by blood glucose concentration changes. Insulin release pattern in response to a glucose concentration step change has a biphasic in a healthy pancreas (see Figure 2.6). As can be seen from Figure 2.6, there is a sharp release of insulin about 5-10 min in the first phase [7].

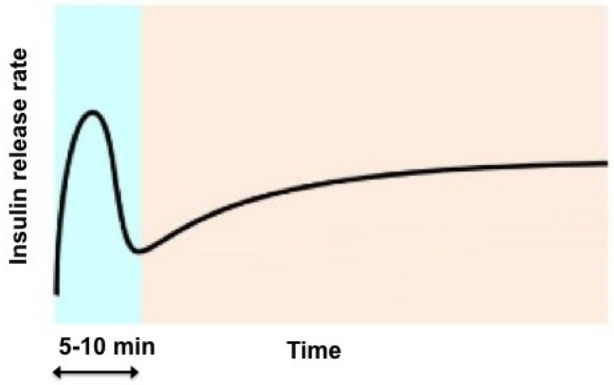

Figure 2.6: Biphasic response of a healthy pancreas to a glucose concentration step change [7]

To mimic the biphasic behaviour of pancreatic insulin secretion in response to a glucose stimulus, Landahl and Grodsky [60] proposed the pancreatic insulin release model presented in Figure 2.7.

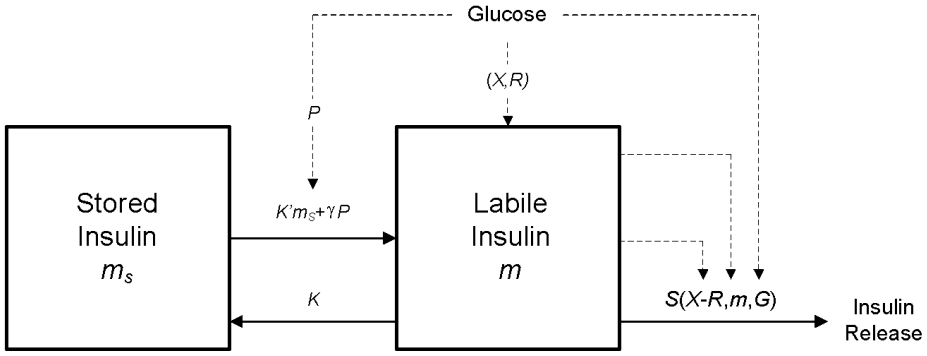

Figure 2.7: Schematic diagram of Landahl and Grodskys model [7]

In the pancreas model, insulin is exchanged between a small labile insulin unit and a large stored insulin unit. Glucose-stimulated factor, P, regulates the rate at which insulin flows into the labile compartment. The rate of insulin secretion from the labile insulin compartment is a function of the glucose concentration, the amount of labile insulin m, and

the instantaneous level of glucose-enhanced excitation factor X and its inhibitor R. The first phase insulin release is caused by an instantaneous increase in the glucose-enhanced excitation factor (X) followed by a rapid increase in its inhibitor (R). The second phase release results from the direct dependence of the insulin secretion rate (S) on the glucose stimulus and the gradual increase in the level of the labile compartment filling factor (P).

The pancreas model equations including mass balance equations over its compartments and correlations between variables results in:

$$\frac{dm}{dt} = K' m_S K m + \gamma P - S, \tag{2.53}$$

$$\frac{dm_S}{dt} = K m - K' m_S - \gamma P, \tag{2.54}$$

It is assumed that the capacity of the storage compartment is large enough and remains at steady state. For a glucose concentration of zero, P is set to zero. Therefore, the steady state mass balance equation around the storage compartment is:

$$K' m_S = K m_0, \tag{2.55}$$

where m_0 is the labile insulin quantity at a glucose concentration of zero. The rest of the equations for the pancreas model are:

$$\frac{dP}{dt} = \alpha(P_\infty - P), \tag{2.56}$$

$$\frac{dR}{dt} = \beta(X - R), \tag{2.57}$$

$$\begin{aligned} S = [N_1 Y + N_2(X - R) + \xi_1 \psi] m \quad x > R, \\ S = [N_1 Y + \xi_1 \psi] m \quad x \leq R, \end{aligned} \tag{2.58}$$

$$P_\infty = Y = X^{1.11} + \xi_2\psi, \tag{2.59}$$

$$X = \frac{G_H^{3.27}}{132^{3.27} + 5.93G_H^{3.02}} \tag{2.60}$$

P_∞ and Y reflect the glucose-induced stimulation effects on the liable compartment filling factor and the insulin secretion rate, respectively. The parameters that are unknown and need to be estimated are α, β, K, N_1, N_2, γ, ξ_1 and ξ_2.

2.2.4 Glucagon sub-model

The glucagon sub-model has one mass balance equation over the whole body as follows:

$$V^\Gamma \frac{d\Gamma}{dt} = r_{P\Gamma R} - r_{P\Gamma C}, \tag{2.61}$$

The metabolic rates for the glucagon sub-model are summarized below:

$$r_{P\Gamma C} = 9.1\Gamma \tag{2.62}$$

$$r_{P\Gamma R} = M^G_{P\Gamma R} M^I_{P\Gamma R} r^B_{P\Gamma R} \tag{2.63}$$

$$M^G_{P\Gamma R} = 1.31 - 0.61\tanh[1.06(\frac{G_H}{G_H^B} - 0.47)] \tag{2.64}$$

$$M^I_{P\Gamma R} = 2.93 - 2.09\tanh[4.18(\frac{I_H}{I_H^B} - 0.62)] \tag{2.65}$$

$$r^B_{P\Gamma R} = 9.1 \tag{2.66}$$

The Sorensen model parameters are summarized in Table 2.1.

Table 2.1: The model parameters [53]

$V_{BC}^G = 3.5\ dl$	$Q_B^G = 5.9\ dl/min$	$T_B^G = 2.1\ min$
$V_{BF}^G = 4.5\ dl$	$Q_H^G = 43.7\ dl/min$	$T_P^G = 5.0\ min$
$V_H^G = 3.5\ dl$	$Q_A^G = 2.5\ dl/min$	$T_P^I = 20\ min$
$V_L^G = 25.1\ dl$	$Q_L^G = 12.6\ dl/min$	$m_0 = 6.33\ U$
$V_G^G = 11.2\ dl$	$Q_G^G = 10.1\ dl/min$	
$V_K^G = 6.6\ dl$	$Q_K^G = 10.1\ dl/min$	
$V_{PC}^G = 10.4\ dl$	$Q_P^G = 12.6\ dl/min$	
$V_{PF}^G = 67.4\ dl$	$Q_B^I = 0.45\ l/min$	
$V_B^I = 0.26\ l$	$Q_H^I = 3.12\ l/min$	
$V_H^I = 0.99\ l$	$Q_A^I = 0.18\ l/min$	
$V_G^I = 0.94\ l$	$Q_K^I = 0.72\ l/min$	
$V_L^I = 1.14\ l$	$Q_P^I = 1.05\ l/min$	
$V_K^I = 0.51\ l$	$Q_G^I = 0.72\ l/min$	
$V_{PF}^I = 6.74\ l$		
$V^\Gamma = 6.74\ l$		

2.3 Type II diabetes model

To develop a model for type II diabetes, the same structure of Sorensen model can be used. However, the parameters of the healthy human body model should be modified based on the blood glucose and insulin concentrations sampled from type II diabetic patients during standard clinical test.

As mentioned in section 1.1.2, type II diabetes mellitus is characterized by several organ malfunctions. These abnormalities are summarized as follows:

- Insulin resistance in peripheral tissues
- Impaired insulin mediated effects on hepatic glucose uptake
- Impaired insulin suppression effects on endogenous glucose production
- Impaired pancreatic insulin secretion both in first phase of release and in overall secretion rate
- Glucose resistance in the liver and peripheral tissues

2.3.1 Selection of model parameters for estimation

The parameters showed in Table 2.1 in section 2.2.4 for a healthy person, represent the physical characteristics of the body, which are the same for diabetic patients. These parameters do not need to be updated in type II diabetes model.

However, from the abnormalities of type II diabetic patients, the parameters within the insulin secretion rate and glucose metabolic rates should be modified. These parameters should be estimated using the available clinical data for type II diabetic patients through a non-linear optimization problem.

Table 2.2 summarizes the abnormalities associated with type II diabetes and their corresponding model equations.

Table 2.2: Abnormalities associated with type II diabetes and their corresponding equations

Abnormalities	Corresponding Equations
Insulin resistance in peripheral tissues	Insulin multiplier in peripheral glucose uptake rate (equation 2.16)
Insulin-induced stimulation of hepatic glucose uptake	Insulin multiplier in hepatic glucose uptake rate (equation 2.28)
Insulin-induced stimulation of hepatic glucose production	Insulin multiplier in hepatic glucose production rate (equation 2.21)
Glucose-induced stimulation of hepatic glucose uptake	glucose multiplier in hepatic glucose uptake rate (equation 2.29)
Glucose-induced stimulation of peripheral glucose uptake	glucose multiplier in peripheral glucose uptake rate (equation 2.31)
Pancreatic insulin secretion rate both in early peak and overall rate	N1 and N2 in the pancreas model (equation 2.58)

Vahidi *et al*. [7, 51] estimated the following parameters in their type II diabetes mellitus model:

- From the glucose sub-model, parameters of the glucose metabolic rates and some parameters of the glucose absorption model have been considered for the parameter estimation. the glucose metabolic rates in the glucose sub-model has the general form of equation 2.9 and the multipliers have the general form of equation 2.10. Considering equation 2.10, a, b, c and d are the parameters of the glucose metabolic rates. To reduce the number of parameters for estimation c and d are selected for the parameter estimation and a and b are considered to be unchanged.

- The glucose absorption model equations are represented by equations 2.32 to 2.38. The model parameters that have been chosen for parameter estimation are k_{12}, k_{min}, k_{max}, and k_{abs}.

- From the insulin sub-model, some parameters from the pancreas model have been chosen for parameter estimation. The pancreas model is represented by equations 2.53 to 2.60 from which N_1, N_2, K, γ, α and β are selected for parameter estimation.

- The hormonal effects of incretins on the pancreatic insulin production are included in equation 2.58. The parameters representing the hormonal effects of incretins on the pancreatic insulin secretion rate are ξ_1 and ξ_2, which are considered for parameter estimation.

- The incretins sub-model is represented by equations 2.39 to 2.42. It has three parameters (i.e. ς, τ_Ψ and $r_{M\Psi C}$), which all of them are selected for the parameter estimation.

2.3.2 Nonlinear optimization problem

Vahidi *et al.* [7, 51] has used a set of available clinical data to estimate the parameters of the model by solving a nonlinear optimization problem. The model parameters are estimated through an iterative optimization algorithm using a sequential quadratic programming (SQP) method. In each iteration, the new values of the estimated parameters are used to solve the model equations.

Estimation of the modified model parameters were carried out by minimizing the deviation of model predictions from the available measurements of peripheral glucose, insulin concentrations. The deviation of model predictions from the measured clinical data is minimized through the following objective function:

$$\min_{\Theta} \sum_{j=1}^{n} [(G^j - \hat{G}^j)^2 + (I^j - \hat{I}^j)^2 + (\Psi^j - \hat{\Psi}^j)^2]. \tag{2.67}$$

where G^j and I^j, and Ψ^j are peripheral glucose, insulin, and incretins concentrations at

time j obtained from the model respectively; $\hat{G}^j$, $\hat{I}^j$, $\hat{\Psi}^j$ are the corresponding clinical measurements; n is the number of samples in the clinical data set; and Θ is the vector of parameters that should be estimated [51].

Different parameters of metabolic rates will be obtained after the optimization procedure for each type II diabetic patient since there are different peripheral glucose, and insulin concentrations profile for different patients.

This optimization problem contains totally four constraints; three constraints for the insulin multipliers in peripheral glucose uptake rate, hepatic glucose uptake rate, and hepatic glucose production rate; and one constraint for the glucose multiplier in hepatic glucose uptake rate.

These constraints express that the value of the multiplier must be set to 1 at basal conditions. The general form of the constraints based on equation 2.10 is:

$$a + b \tanh[c(1 - d)] = 1, \tag{2.68}$$

Chapter 3

A novel and simple self-administered method for assessing insulin sensitivity

3.1 Introduction

Insulin is a key hormone secreted from β-cells in the pancreas that regulates glucose homeostasis. Type II diabetes is characterized by both insulin resistance and decreasing βcell mass [61]. Insulin resistance happens when the sensitivity of peripheral cells to the metabolic action of insulin is decreased due to genetic or environmental factors, obesity, hypertension, dyslipidemias, and/or coronary artery diseases. The ability of insulin to stimulate body glucose disposal can be characterized by an insulin sensitivity index (ISI) [11, 25, 29, 62].

Various methods have been developed for determining the presence and degree of insulin resistance. In Section 1.1.4, some of the common methods usually employed in diabetes research are briefly described. These methods are summarized in the next following sections.

3.1.1 Hyperinsulinemic euglycemic insulin clamp technique

The hyperinsulinemic euglycemic insulin clamp technique has been widely used as a gold standard for understanding insulin resistance in vivo [24]. Defronzo *et al.* [24] in 1979 developed this test. In this test, by a continuous infusion of insulin, the plasma insulin concentration is raised and clamped at around 100 $\mu U/l$. At the same time, by glucose injection via a negative feedback principle, the plasma glucose concentration is kept constant at basal levels. Endogenous glucose production rate is suppressed by high insulin concentration to almost zero. At steady state conditions, the rate of glucose infusion rate is equal to the glucose uptake rate by all body tissues and is therefore a measure of the body insulin sensitivity. This is the only information that can be obtained from this test. This method is labor-intensive, expensive, and limiting for large-scale clinical studies [63].

3.1.2 Modified minimal model (MINMOD) analysis in conjunction with the frequently sampled intravenous glucose tolerance test (FSIVGTT)

More accurate and less labor-intensive than the insulin clamp technique is a modified minimal model (MINMOD) analysis in conjunction with the frequently sampled intravenous glucose tolerance test (FSIVGTT) [32] for the estimation of insulin sensitivity. This method proposed by Yang *et al.* [32] in 1987. In this method, the results of FSIVGTT test is used to determine the parameters of the minimal model [29] and then, obtained parameters are used to define insulin sensitivity and glucose effectiveness indices. They attempted to improve the precision of the estimation of insulin sensitivity (SI) from the minimal model technique by modifying insulin dynamics during a frequently sampled intravenous glucose tolerance test (FSIGT). However, the FSIVGTT is still restrictive for large studies [25, 63].

3.1.3 Homeostasis model assessment (HOMA) of insulin resistance (HOMA-IR)

Homeostasis model assessment (HOMA) of insulin resistance (HOMA-IR), fasting plasma insulin [64], and the fasting-glucose-to-insulin ratio [65] are simple indices of insulin resistance compared with the insulin clamp test. HOMA proposed by Matthews *et al.* [37] in 1985 is a structural computer model of the glucose-insulin feedback system in the homeostatic (overnight-fasted) state. A number of nonlinear empirical equations describing the functions of organs and tissues involved in glucose regulation are included in their model. By solving these equations numerically, glucose, insulin, and C-peptide concentrations are predicted in the fasting steady state for any combination of pancreatic β-cell function and insulin sensitivity (or resistance). From these predictions, the deduction of β-cell function and insulin sensitivity from pairs of fasting glucose and insulin (or C-peptide) measurements can be taken.

Matthews *et al.* [37] demonstrated that in only a few patients with type II diabetes, the homeostasis model assessment of insulin resistance (HOMA-IR) is closely correlated with the insulin sensitivity index assessed by euglycemic clamp. Also it was reported in [66] and [67] that in a relatively greater number of diabetic subjects, HOMA-IR provided a good correlation in the clamp studies. However, some investigators recognized that when the insulin secretion decreases in patients with advanced type II diabetes, the HOMA-IR shows relatively low value since the HOMA-IR is a product of fasting glucose and insulin levels.

3.1.4 Insulin sensitivity indices investigated from oral glucose tolerance test (OGTT)

Recently, several methods have been investigated from oral glucose tolerance test (OGTT). Cederholm and Wibell [68] proposed a formula for ISI that uses the OGTT based on four timed samples of insulin and glucose (at 0, 30, 60, and 120 min). It has fairly good agreement with more complicated procedures, such as the clamp test and the insulin suppression test.

Stumvoll *et al.* [45] disclosed that the insulin sensitivity in non-diabetic subjects can be assessed from OGTT. Simple ISI for type II diabetic patients were derived based on the OGTT by Matsuda and DeFronzo [44]. Their index was correlated to clamp-derived insulin sensitivity.

Gutt *et al.* [48] devised a formula for an insulin sensitivity index, $ISI_{0,120}$ that uses the fasting (0 min) and 120 min post-oral glucose (OGTT) insulin and glucose concentrations. Their data showed that $ISI_{0,120}$ correlated well, when applied prospectively in comparative studies, with the insulin sensitivity index obtained from the euglycemic hyperinsulinemic clamp. Their correlation was demonstrably superior to other indices of insulin sensitivity such as the HOMA formula presented by Matthews *et al.* [37], and performed comparably to the computerized HOMA index.

Although the above methods are relatively easy to conduct, accurate, and adaptable to both population studies and clinical settings, they are not inexpensive, self-monitoring, and convenient since the plasma insulin level must be measured at a specific time as a key variable for calculating these indices in medical labs.

In this chapter, we propose a new ISI estimated from capillary blood glucose measurements. Our approach is to evaluate the feasibility of using the mathematical compartment model proposed by Vahidi et al. [7, 51] to estimate insulin sensitivity.

In the next section, the model of 15 diabetic patients have been developed using the available clinical data from OGTT. In section 3.3, 15 simulated patients' models were used for the development and evaluation of a self-assessment method for obtaining the ISI.

3.2 Clinical data used for model development

The aim of this study is to develop a simple measure of insulin sensitivity by using a self-assessment test without laboratory requirements. From a literature review of OGTT, it was found that the pattern of glucose response to insulin varies from patient to patient. To ensure that the proposed test for estimating the ISI is valid for all available patterns of glucose and insulin concentrations, different sets of blood glucose and insulin measurements must be used for the estimation of the Vahidi model parameters. Different sets of clinical data for type II diabetic patients have been published in the literature from the 2-h 75-g OGTT. Based on the Canadian Diabetes Association 2013 criteria [69], the diagnostic criteria for diabetes are summarized in Table 3.1.

Table 3.1: Diagnosis of diabetes

Type	FPG (mg/dl)	2-h PG (mg/dl)
Normal	<110	<140
Impaired Glucose Tolerance (IGT)	<110	140-199
Impaired Fasting Glucose (IFG)	110-125	<140
Combined IFG and IGT	110-125	140-199
Type II diabetes	≥126	≥200

From our literature survey, it was found that the insulin concentration profile during an OGTT can be grouped in to a few patterns. Hayashi *et al*. [70] derived four possible patterns of insulin profile from a study involving 400 non-diabetic Japanese Americans. They concluded that the insulin concentration pattern during an OGTT strongly predicts

the development of type II diabetes and is correlated with measures of insulin sensitivity. Bakari and Onyemelukwe [71] studied the plasma insulin pattern both in the fasting state and in response to a standard OGTT in 42 type II diabetic Nigerians and 36 healthy control subjects. They found that the type II diabetic patients demonstrated both fasting and post-OGTT hypoinsulinaemia. Therefore, for our model development, 15 available patterns of glucose and insulin concentrations during the 2-h 75-g OGTT for diabetic and non-diabetic subjects were included and presented in details in Table 3.2.

Table 3.2: Mean plasma glucose and insulin levels during OGTT

Subject	Plasma glucose during OGTT (mg/dl)					Plasma insulin during OGTT ($\mu U/ml$)					Reference
	0 *min*	30 *min*	60 *min*	90 *min*	120 *min*	0 *min*	30 *min*	60 *min*	90 *min*	120 *min*	
1	175.86	249.84	315.00	338.40	323.64	4.20	5.50	6.01	6.98	9.92	[71]
2	71.10	135.90	124.92	116.10	101.34	5.72	15.58	13.67	10.48	8.03	[71]
3	75.29	125.71	129.13	108.50	84.67	8.18	30.00	33.05	33.47	16.77	[72]
4	80.00	120.40	110.40	92.10	76.50	7.00	38.40	31.10	21.90	9.30	[72]
5	71.30	130.20	145.00	122.40	91.60	9.20	23.10	34.70	41.90	21.90	[72]
6	74.00	121.00	177.00	180.00	154.00	9.00	13.00	35.00	46.00	41.00	[72]
7	71.00	125.00	134.00	103.00	80.00	7.00	62.00	58.00	36.00	20.00	[72]
8	72.00	118.00	115.00	92.00	62.00	10.00	12.00	35.00	20.00	14.00	[72]
9	89.90	160.2	134.20	-	109.00	11.30	98.90	68.40	-	43.70	[70]
10	90.90	154.80	124.70	-	130.80	11.60	109.80	53.90	-	71	[70]
11	93.30	166.20	171.40	-	122.10	11.70	66.80	103.90	-	58.30	[70]
12	95.50	171.30	193.30	-	159.10	12.70	59.60	86.70	-	118.90	[70]
13	91.30	158.10	148.50	-	144.80	14.90	96.40	74.80	-	130.20	[70]
14	153.40	238.40	292.58	278.68	239.89	6.47	18.88	22.00	20.64	14.57	[73, 74]
15	97.75	164.68	154.54	110.50	87.61	5.52	37.75	42.63	19.58	7.89	[73, 74]

After the Vahidi model had been developed, 15 simulated patients' models were used for the development and evaluation of a self-assessment method for obtaining the ISI. The next section describes the development of the proposed method for obtaining the ISI.

3.3 Proposed self-assessment method for estimation of insulin sensitivity

Several authors proposed various indices for measuring insulin sensitivity by using fasting state or OGTT data and correlated the indices with the data obtained from the hyperinsulinemic euglycemic clamp test. Formulas proposed for calculating the ISI are based on the intercorrelations between the concentrations of glucose and insulin and other parameters. However, they all require the measurements of plasma insulin levels sampled at specific times by laboratory equipment, which is expensive and inconvenient. Therefore, a more practical method for obtaining the ISI is the focus of this research.

A practical test for obtaining the ISI should not require plasma insulin measurements and only need capillary blood glucose measurements. Capillary blood glucose refers to the blood glucose concentration measured from capillary blood vessels. This is most commonly done by a finger prick test by a diabetic patient. The plasma insulin measurement refers to the actual insulin concentration in a persons blood sampled and measured by a lab technician.

For type II diabetic patients, the body is suffering from some insulin resistance and it requires larger amounts of insulin either from the pancreas or from injections to lower their plasma glucose level compared to that of an insulin-sensitive body. For those with severe insulin resistance, the normal physiological response to a given amount of insulin is blunted. As a result, higher levels of insulin are needed to achieve a proper effect.

In light of this, we propose a simple testing approach, in which the simulated patients take a dose of oral glucose ingestion followed by multiple insulin injections at different times. The proposed test is considered clinically acceptable and safe as the insulin dosage can be selected with a large safety margin. We have conducted extensive simulation with different combinations of testing protocols on the fifteen simulated patients using the Vahidi model. After the extensive simulations, we have found that the ISI can be estimated by patients completing a simple testing protocol, which includes two procedures on two separate occasions.

In the first procedure, the fifteen simulated subjects were given a single dose of 75-g glucose. The plasma glucose concentrations of the fifteen subjects were sampled in order to check how their bodies suppress the plasma glucose level with no insulin injection.

In the second procedure, a single dose of 75-g glucose was given to the fifteen simulated subjects. Then, 10 mU/kg insulin was injected twice subcutaneously into the body of the simulated subjects 20 and 50 min after glucose consumption since the major response to a moderate load occurs within 15 min of glucose ingestion [75, 76]. The plasma glucose concentrations of the fifteen subjects were sampled in order to check how their bodies regulate the plasma glucose level with two insulin injections.

After statistical evaluation, it was found that the differences in the plasma glucose concentration profile of each subject from the first and second procedures can be used to define a formula for the ISI. The formula adopted for the estimation of the ISI is described in Section 3.4.2. This section also shows how well the proposed index correlates with the ISI (called M-value) obtained from the euglycemic insulin clamp technique.

3.4 Results and discussion

The Vahidi model includes a set of nonlinear ordinary differential equations and algebraic equations. The model parameters are estimated through an iterative optimization algorithm using an SQP method, as described in Section 2.67. The estimated parameters are then used to solve the Vahidi model equations. The optimization was carried out in MATLAB.

3.4.1 Parameters estimation results

Since different patterns of glucose and insulin concentrations result in different sets of parameters in the Vahidi model, for each subject in Table 3.2, a set of parameters was estimated using the nonlinear optimization algorithm described in Section 2.67. As an example, using the blood glucose and insulin concentration data of subject 1 in Table 3.2, the parameters of the glucose metabolic rates have been considered for the parameter estimation. As the model equations in Section 2.2.1 shows, the glucose metabolic rates in the glucose sub-model has the general form of equation 2.9 and the multipliers have the general form of equation 2.10.

Considering equation 2.10, parameters a, b, c and d in the hepatic glucose production (HGP) rate, the hepatic glucose uptake (HGU) rate, and the peripheral glucose uptake rate (PGU) are selected to be estimated. Also, considering equation 2.58 in Section 2.2.3, the parameters N_1 and N_2 in the pancreatic insulin release model are estimated.

As an example, the estimated model parameters for the glucose and insulin sub-models presented above are shown in Table 3.3 and Table 3.4, respectively for subject 1.

Table 3.3: Parameter estimation results for glucose sub-model (subject 1).

Multiplier in equation (2.10)	a	b	c	d
M^{I}_{PGU}	7.035	6.516	0.15	4.000
$M^{I\infty}_{HGP}$	1.425	1.406	0.607	0.241
$M^{I\infty}_{HGU}$	0.001	2.000	1.500	0.001
M^{G}_{HGU}	5.664	5.658	2.013	1.678

Table 3.4: Parameter estimation results for insulin sub-model (subject 1).

Parameter in equation (2.58)	**Value**
N_1	1.096
N_2	0.654

The model estimation results of the fifteen subjects presented in Table 3.2, are shown in Figures. 3.1 and 3.15.

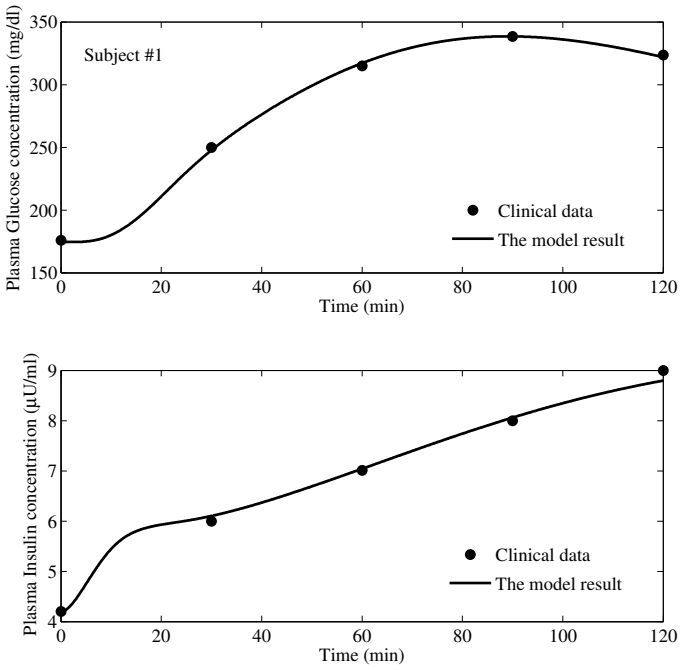

Figure 3.1: Plasma glucose and insulin concentration profile in subject #1, the clinical data (•), the model results (−)

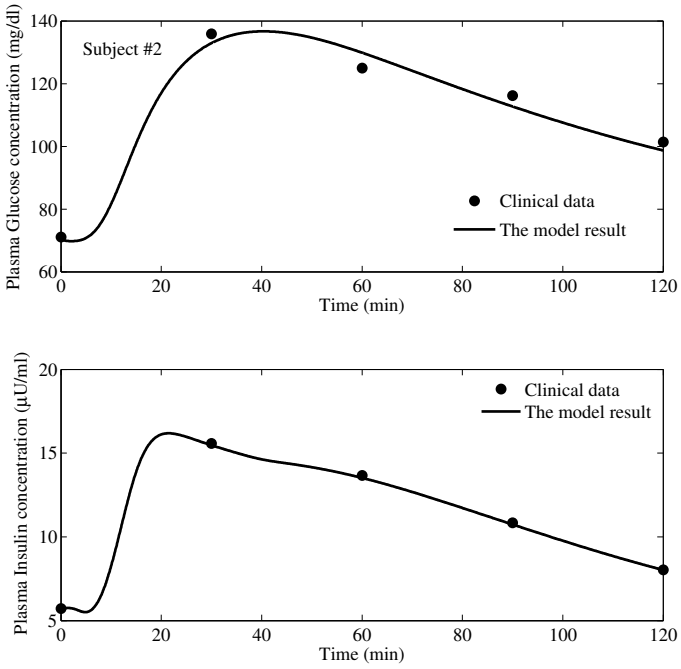

Figure 3.2: Plasma glucose and insulin concentration profile in subject #2, the clinical data (•), the model results (−)

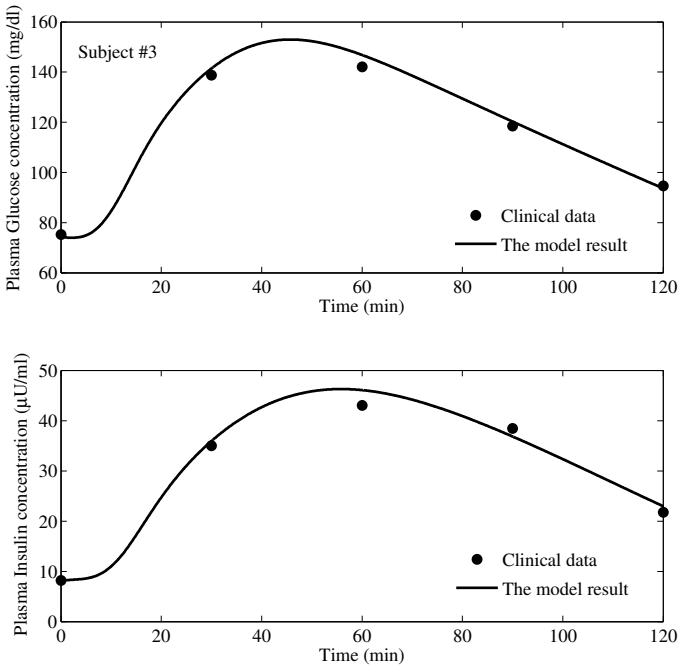

Figure 3.3: Plasma glucose and insulin concentration profile in subject #3, the clinical data (•), the model results (−)

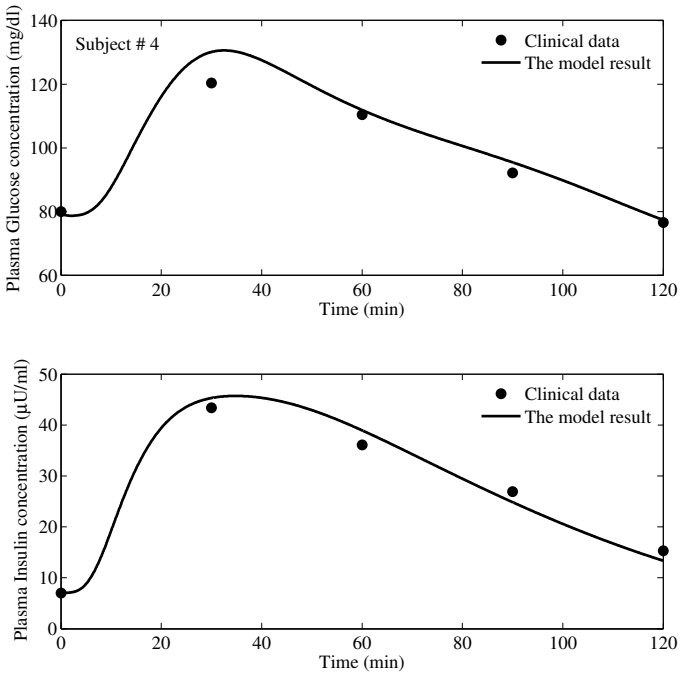

Figure 3.4: Plasma glucose and insulin concentration profile in subject #4, the clinical data (•), the model results (−)

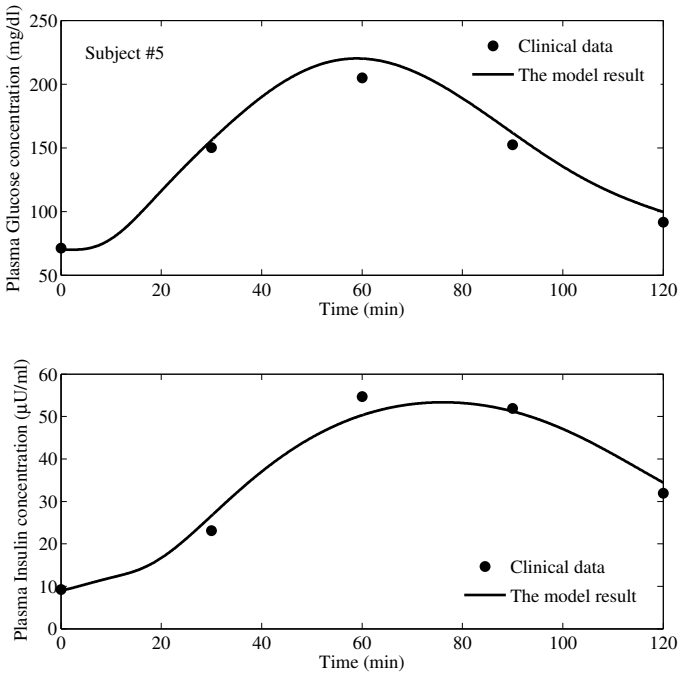

Figure 3.5: Plasma glucose and insulin concentration profile in subject #5, the clinical data (•), the model results (−)

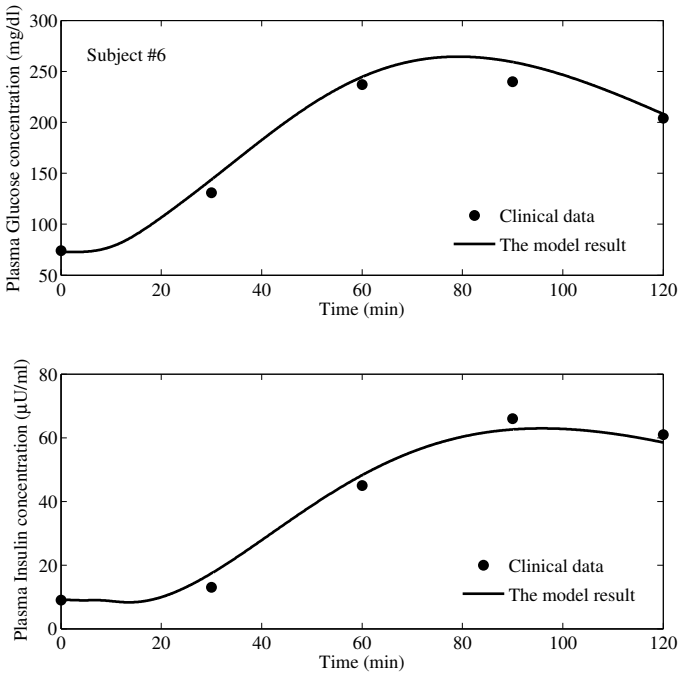

Figure 3.6: Plasma glucose and insulin concentration profile in subject #6, the clinical data (•), the model results (−)

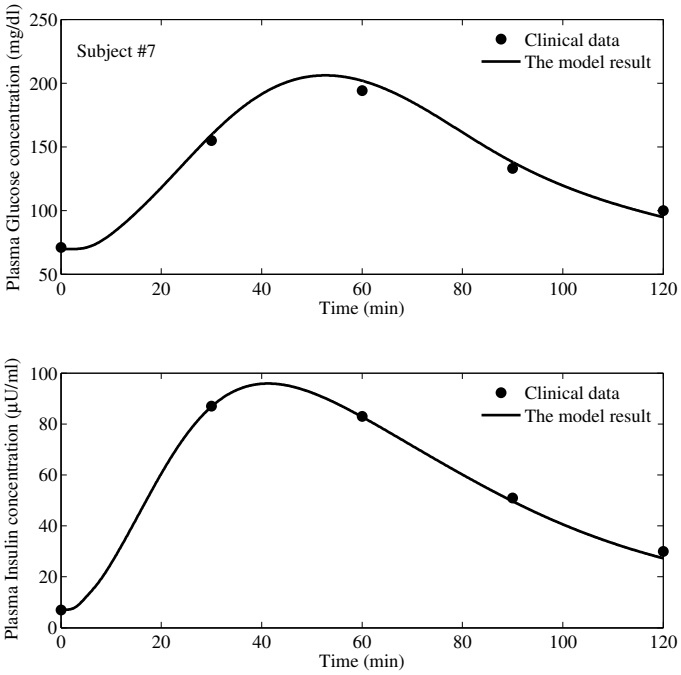

Figure 3.7: Plasma glucose and insulin concentration profile in subject #7, the clinical data (•), the model results (−)

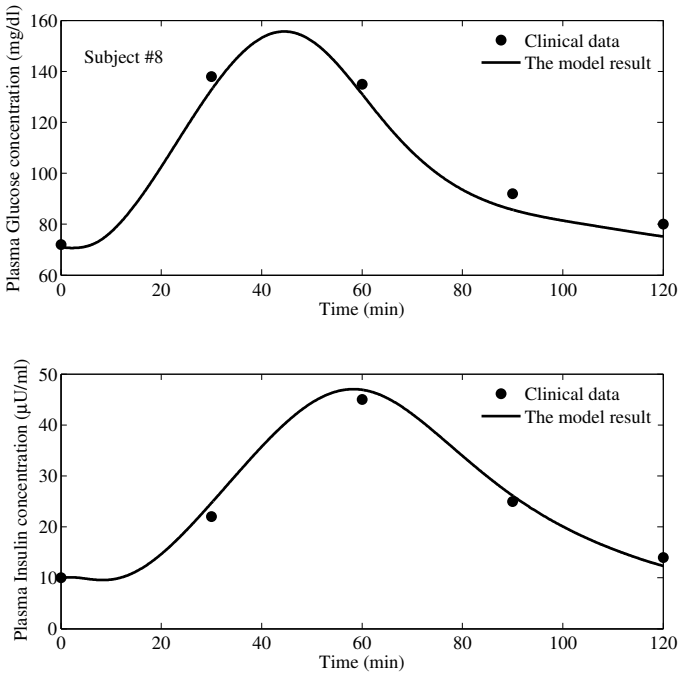

Figure 3.8: Plasma glucose and insulin concentration profile in subject #8, the clinical data (•), the model results (−)

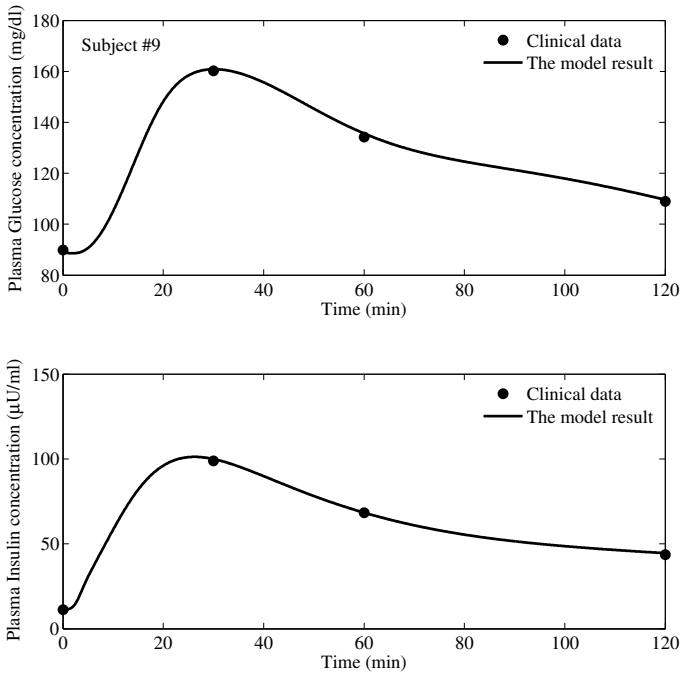

Figure 3.9: Plasma glucose and insulin concentration profile in subject #9, the clinical data (•), the model results (−)

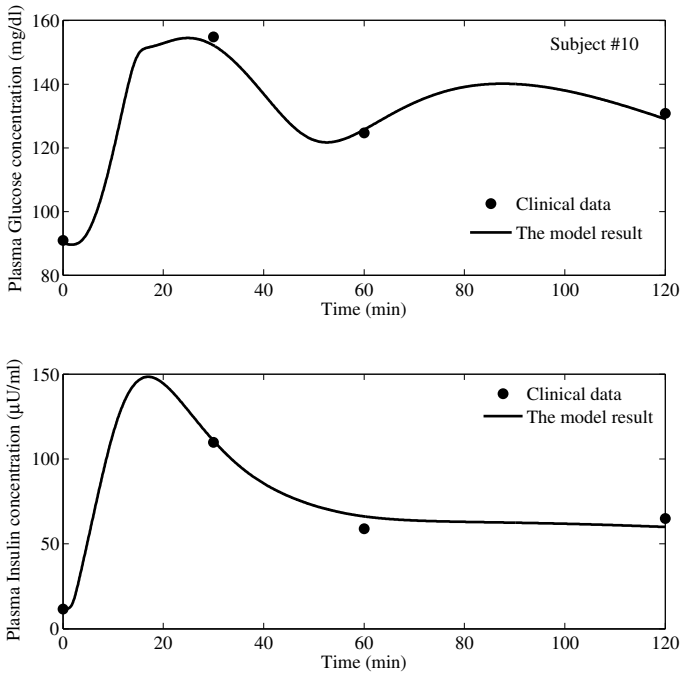

Figure 3.10: Plasma glucose and insulin concentration profile in subject #10, the clinical data (•), the model results (−)

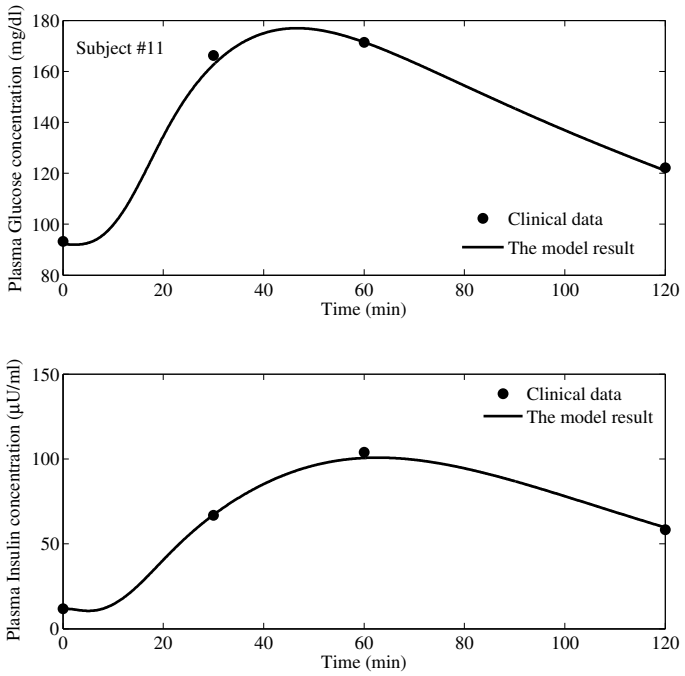

Figure 3.11: Plasma glucose and insulin concentration profile in subject #11, the clinical data (•), the model results (−)

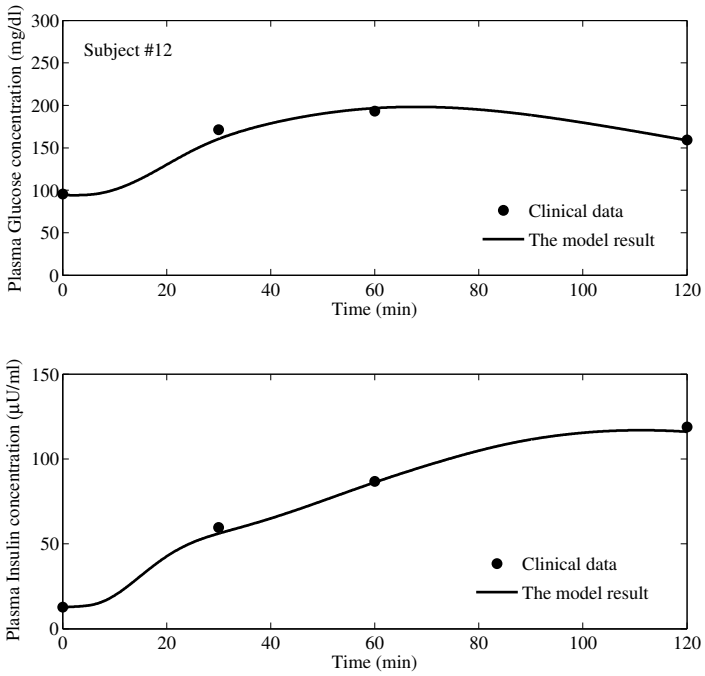

Figure 3.12: Plasma glucose and insulin concentration profile in subject #12, the clinical data (•), the model results (−)

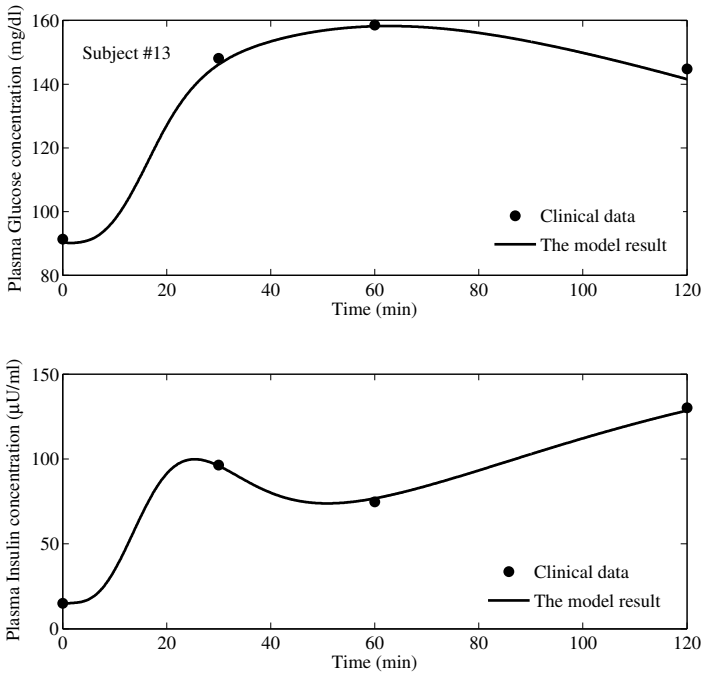

Figure 3.13: Plasma glucose and insulin concentration profile in subject #13, the clinical data (•), the model results (−)

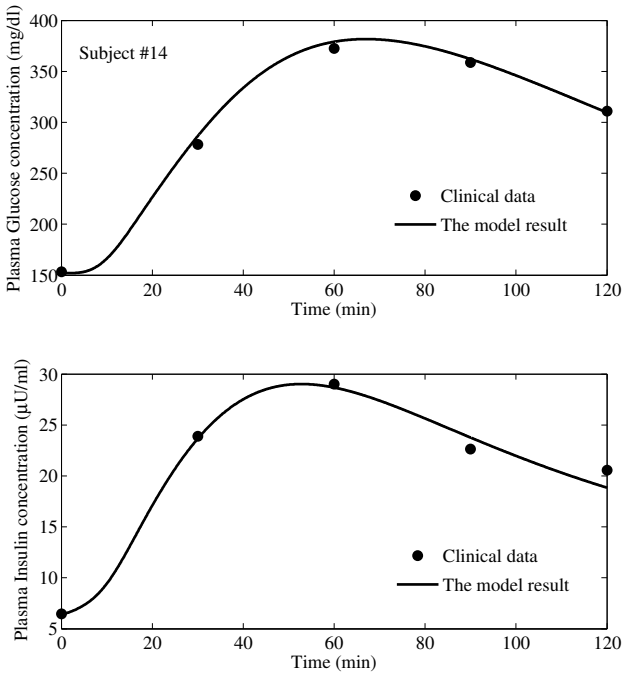

Figure 3.14: Plasma glucose and insulin concentration profile in subject #14, the clinical data (•), the model results (−)

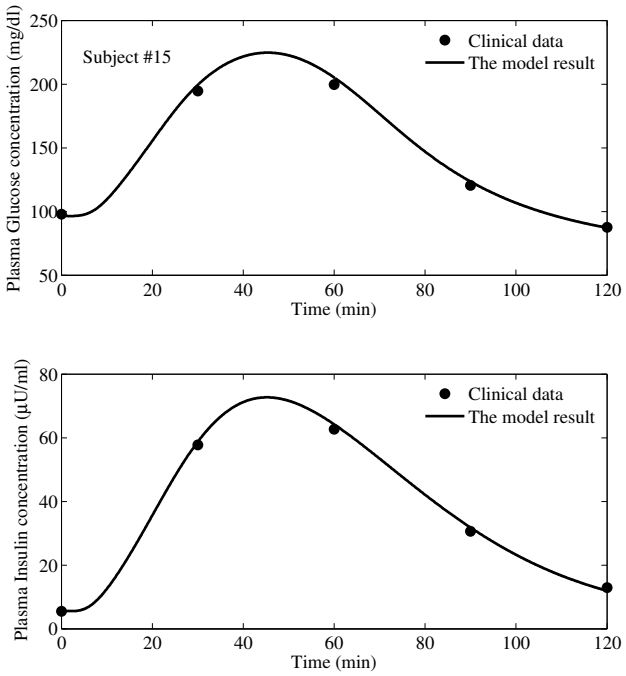

Figure 3.15: Plasma glucose and insulin concentration profile in subject #15, the clinical data (•), the model results (−)

The goodness of fit between the model estimation and the available clinical data set can be calculated using different cost functions in MATLAB. In this study, the goodness of fit is calculated using the mean square error (MSE) as a cost function:

$$MSE = \frac{|x - x_{ref}|}{N_s - 1} \tag{3.1}$$

where x is the glucose or insulin concentration matrix estimated by the model, x_{ref} is the available glucose or insulin concentration from Table 3.2 as the reference, and N_s is the number of actual measured clinical data. From equation (3.1), the overall average goodness of fit for all fifteen subjects is 92%. The simulated trends are reasonably consistent with

the actual clinical data from both a visual inspection and the average goodness of fit.

3.4.2 Quantitative estimation of insulin sensitivity

In order to validate the proposed protocol for estimating the ISI, the M-values from the euglycemic insulin clamp test were obtained for the fifteen subjects from the simulated models. To perform the euglycemic insulin clamp test on the simulated bodies of the fifteen subjects with the Vahidi model, the plasma insulin concentration was acutely raised and maintained at 100 $\mu U/ml$ by a continuous infusion of insulin. Meanwhile, the plasma glucose concentration was held constant at basal levels by a variable glucose infusion in MATLAB. Then, proposed testing protocols described in Section 3.3 were applied to the fifteen simulated subjects.

The plasma glucose concentration profiles of each subject from the first and second procedures are plotted in Figures. 3.16-3.30.

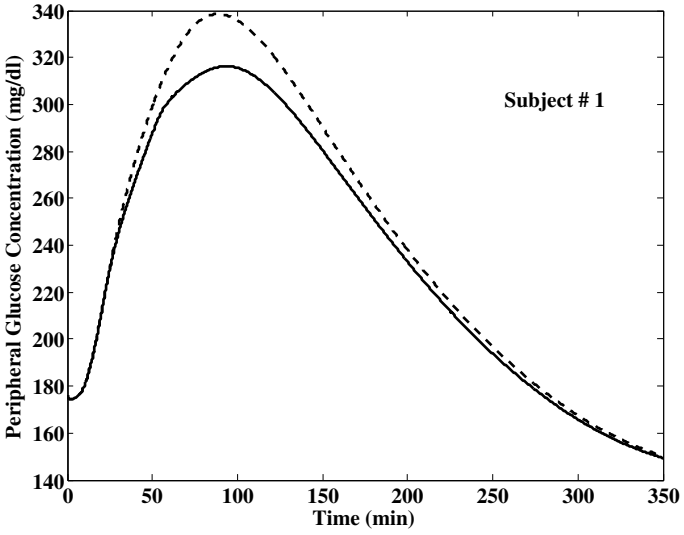

Figure 3.16: Effect of insulin injection in subject #1, two 10 mU/kg insulin injections at 20 and 50 min respectively (-), and no injection (–)

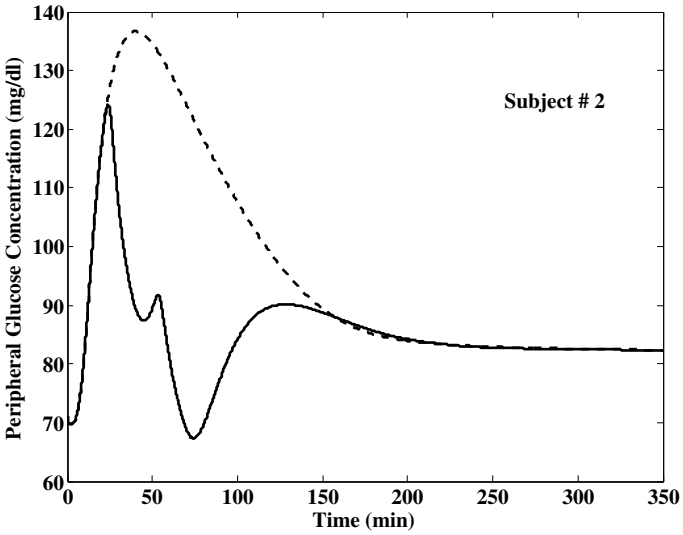

Figure 3.17: Effect of insulin injection in subject #2, two 10 mU/kg insulin injections at 20 and 50 min respectively (-), and no injection (–)

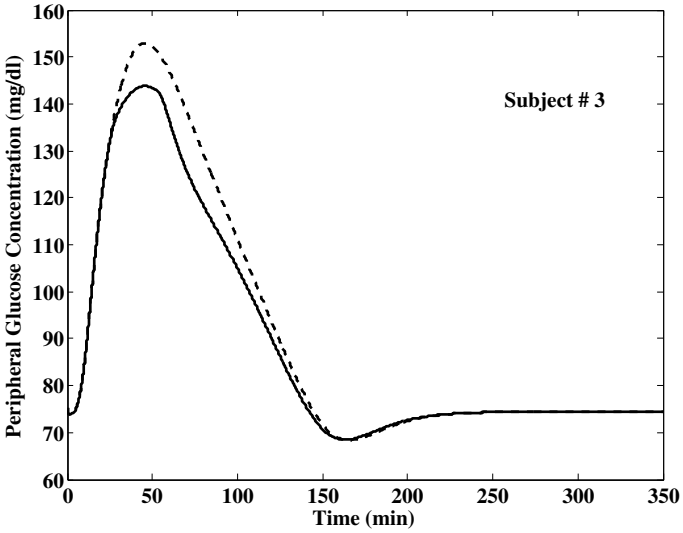

Figure 3.18: Effect of insulin injection in subject #3, two 10 mU/kg insulin injections at 20 and 50 min respectively (-), and no injection (–)

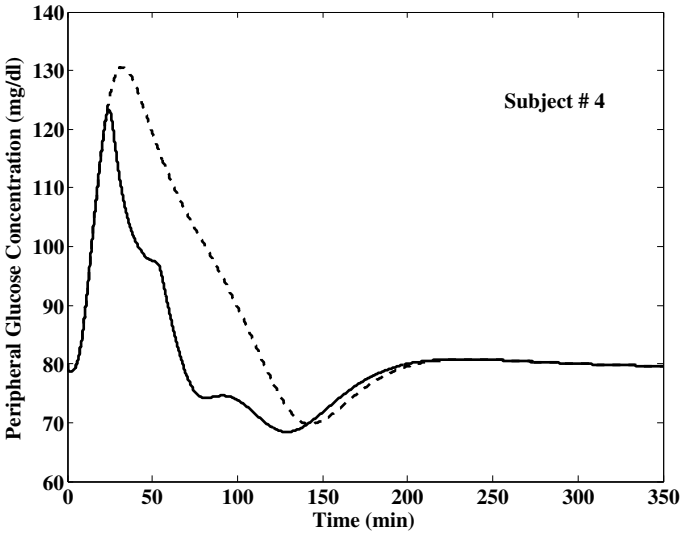

Figure 3.19: Effect of insulin injection in subject #4, two 10 mU/kg insulin injections at 20 and 50 min respectively (-), and no injection (–)

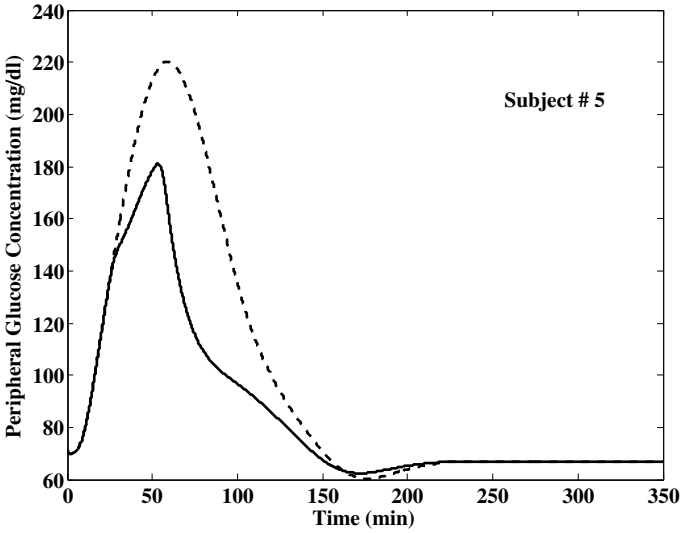

Figure 3.20: Effect of insulin injection in subject #5, two 10 mU/kg insulin injections at 20 and 50 min respectively (-), and no injection (–)

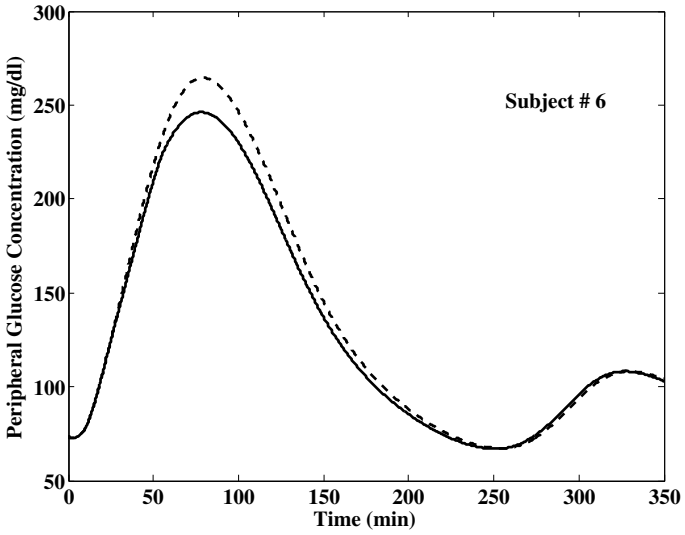

Figure 3.21: Effect of insulin injection in subject #6, two 10 mU/kg insulin injections at 20 and 50 min respectively (-), and no injection (–)

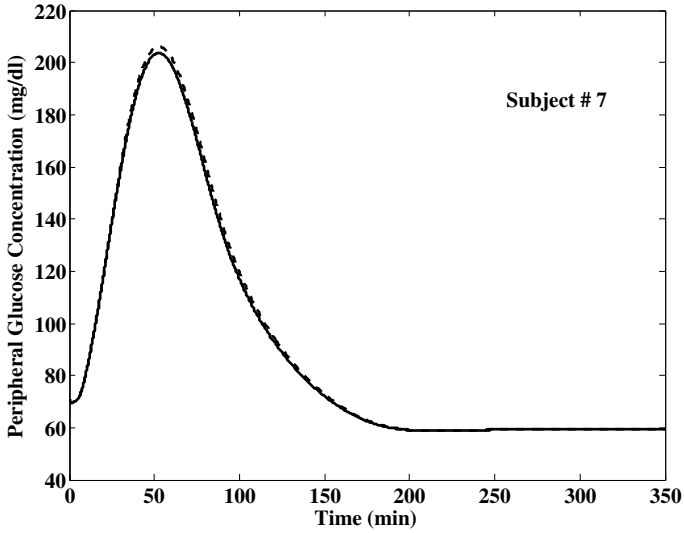

Figure 3.22: Effect of insulin injection in subject #7, two 10 mU/kg insulin injections at 20 and 50 min respectively (-), and no injection (–)

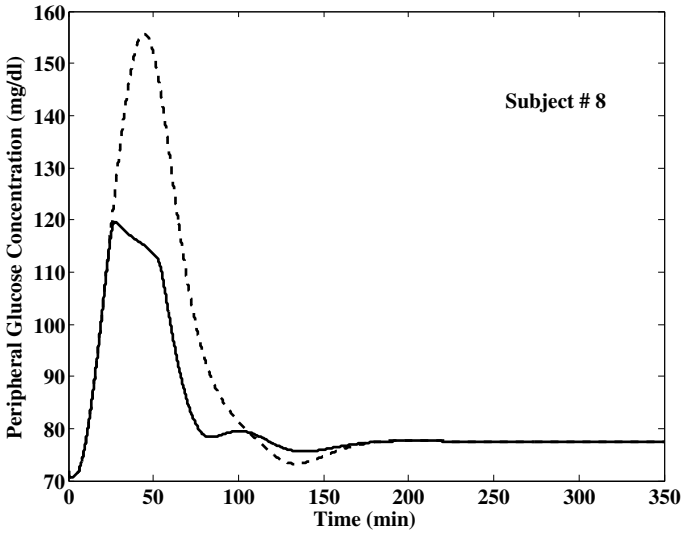

Figure 3.23: Effect of insulin injection in subject #8, two 10 mU/kg insulin injections at 20 and 50 min respectively (-), and no injection (–)

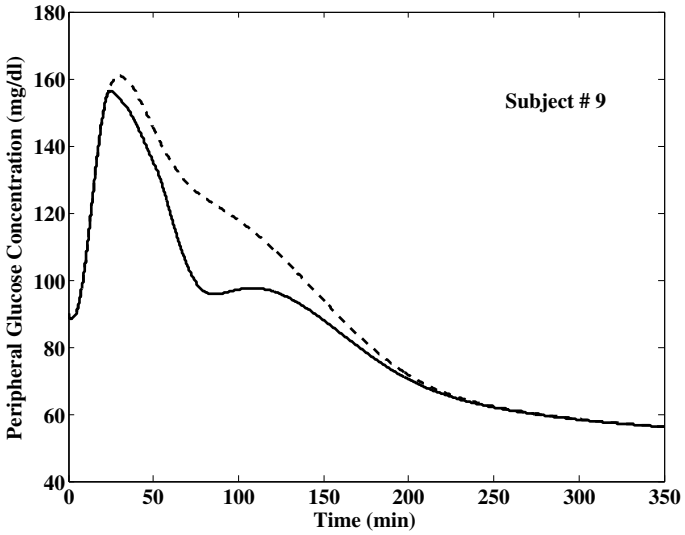

Figure 3.24: Effect of insulin injection in subject #9, two 10 mU/kg insulin injections at 20 and 50 min respectively (-), and no injection (–)

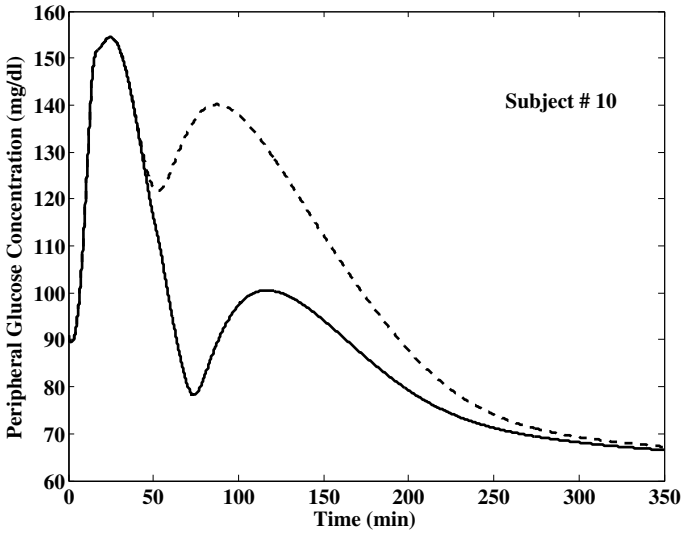

Figure 3.25: Effect of insulin injection in subject #10, two 10 mU/kg insulin injections at 20 and 50 min respectively (-), and no injection (–)

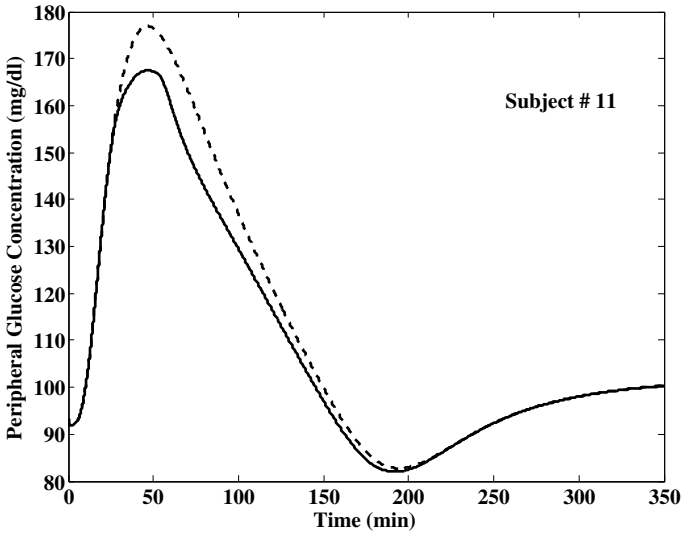

Figure 3.26: Effect of insulin injection in subject #11, two 10 mU/kg insulin injections at 20 and 50 min respectively (-), and no injection (–)

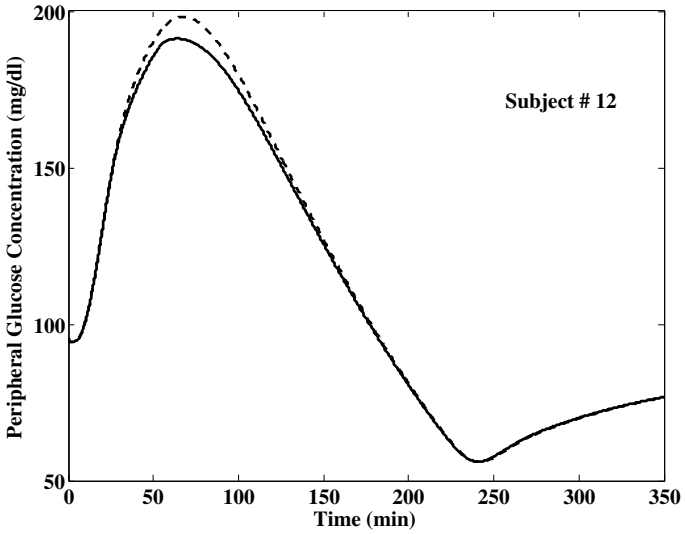

Figure 3.27: Effect of insulin injection in subject #12, two 10 mU/kg insulin injections at 20 and 50 min respectively (-), and no injection (–)

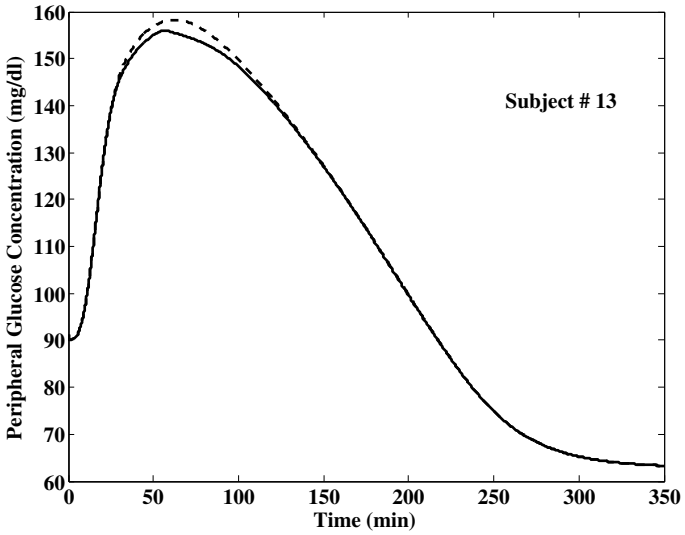

Figure 3.28: Effect of insulin injection in subject #13, two 10 mU/kg insulin injections at 20 and 50 min respectively (-), and no injection (–)

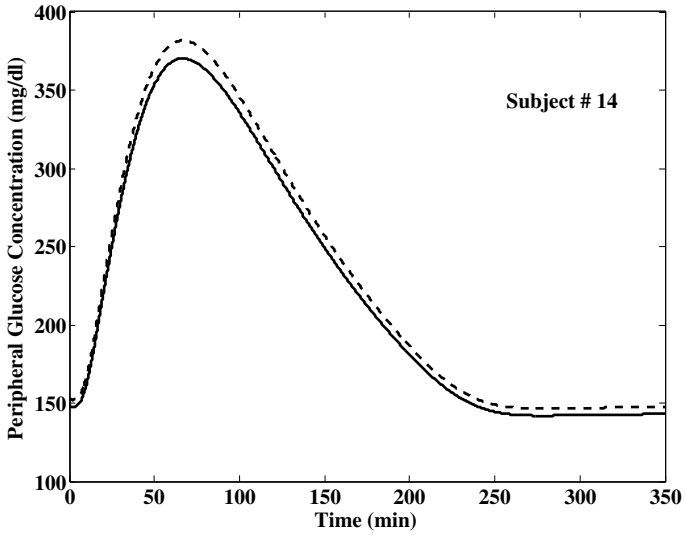

Figure 3.29: Effect of insulin injection in subject #14, two 10 mU/kg insulin injections at 20 and 50 min respectively (-), and no injection (–)

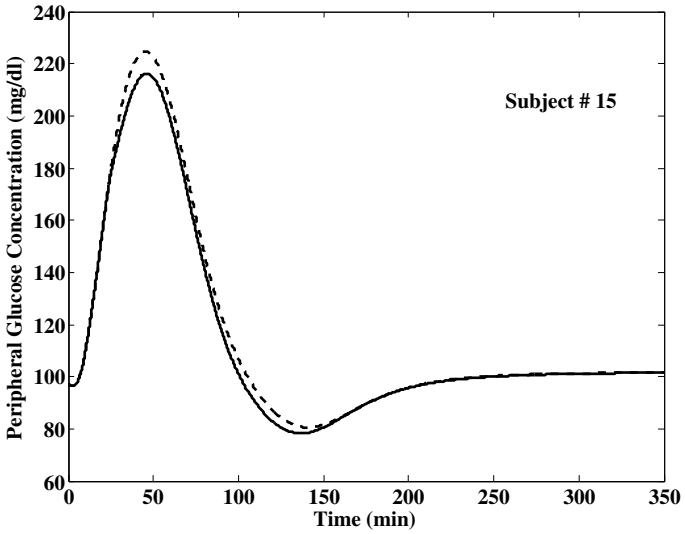

Figure 3.30: Effect of insulin injection in subject #15, two 10 mU/kg insulin injections at 20 and 50 min respectively (-), and no injection (–)

From Figures. 3.16-3.30, the plasma glucose level for insulin-sensitive subjects 2, 4, 5,

8, 9, and 10 were suppressed significantly after the two insulin injections. However, the peripheral glucose concentration profile did not change or were suppressed slightly after the two insulin injections for insulin-resistant subjects 1, 3, 6, 7, 11, 12, 13, 14, and 15.

In the same figure, the maximum differences between plasma glucose levels in the insulin-sensitive subjects occur almost at 60 min and 80 min after glucose consumption because of the two insulin injections. In statistics, multiple linear regression is an approach for modelling the relationship between two or more explanatory variables denoted X and a response variable y by fitting an equation to observed data. To find a new ISI, step-wise multiple regression analysis was performed with the M-value as the dependent variable (y) and the glucose concentrations at fasting (0 min), 60 min, and 80 min after ingestion of 75-g glucose as the three independent variables (X) in MATLAB. The obtained ISI equation from the multiple regression analysis is:

$$\begin{aligned} ISI = {} & 44.071 - 0.1534 \times FPG \\ & - 0.1855 \times G_{60_{min}} + 0.182 \times G_{80_{min}} \\ & - \left(\frac{1.95}{FPG} + \frac{6.81}{G_{60_{min}}} - \frac{5.88}{G_{80_{min}}}\right) \times 10^3 \end{aligned} \tag{3.2}$$

where FPG, $G_{60_{min}}$, and $G_{80_{min}}$ are the peripheral glucose concentrations in mg/dl at fasting (0 min), 60 min, and 80 min after ingestion of a 75-g glucose, respectively.

The means and standard deviations were computed in MATLAB for the defined insulin sensitivity and M-values. Pearsons r coefficient was used for the calculation of correlations between these two measures. The scatter plot of the relationship between the M-value and the ISI from equation ((3.2)) for each subject is shown in Figure. 3.31. Both the Pearsons coefficient ($r = 0.927$) and the p-value ($p = 0.0045$) indicate a strong correlation between the new ISI and the M-value from the euglycemic clamp test.

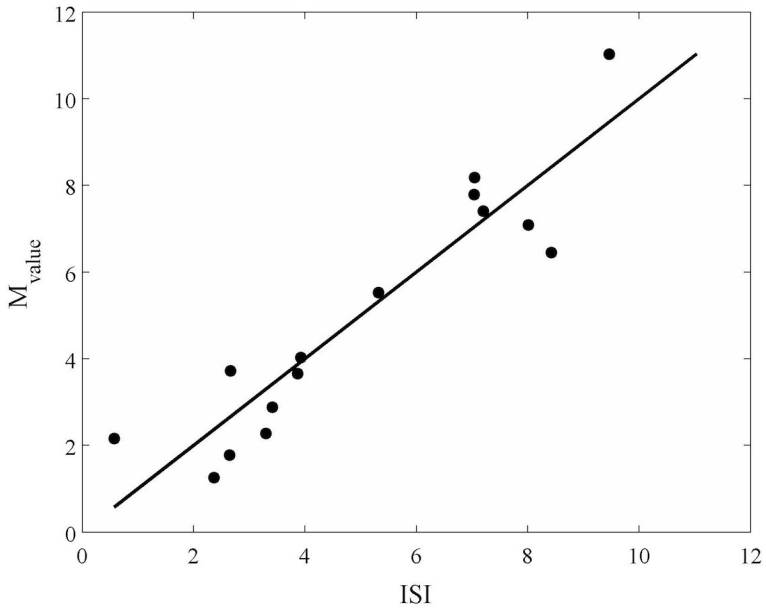

Figure 3.31: Correlation between the ISI and the M-value for the fifteen subjects; $r = 0.927$, $p = 0.0045$

Previous ISIs derived from the OGTT data require the measurements of plasma insulin levels at specific times by laboratory equipment, which is inconvenient, time-consuming, and expensive. The proposed ISI can be estimated from data collected by diabetic patients who need to frequently monitor their status without the need for expensive laboratory facilities.

3.4.3 Comparison of various insulin sensitivity indices obtained from OGTT

The derivations of other indices obtained during the OGTT are briefly presented here. The index of whole-body insulin sensitivity derived by Matsuda and DeFronzo [44] calculates insulin sensitivity from plasma glucose (mg/dl) and insulin (mU/l) concentrations in the fasting state and during the OGTT. Stumvoll *et al.* [45] proposed several ISI equations,

which were obtained from multiple linear regression analysis. The equations calculate the insulin sensitivity from plasma glucose ($mmol/l$) and insulin ($pmol/l$) concentrations during the OGTT. The Gutt index (ISI0,120) [48] was adopted from the ISI proposed by Cederholm and Wibell [68]. The calculation of ISI0,120 ($mgl^2mmol^{-1}mlU^{-1}min^{-1}$) only uses the fasting (0 min) and 120 min concentrations of glucose and insulin during the OGTT.

These three ISIs calculated from the OGTT data are shown in Table 3.5 to compare the correlation of each index with the M-value. Table 3.5 shows the Pearsons correlation of each measurement of insulin sensitivity with the M-value computed in MATLAB. As can be seen from Table 3.5, the correlation of the proposed ISI with the M-values is significantly stronger than those of the other indices, ($r = 0.927$, $p = 0.0045$). Although Table 3.5 shows a very promising and convenient ISI estimation, a proper comparison should be done by applying the proposed ISI protocol to real subjects. This can be a part of future studies research.

Table 3.5: Pearson correlations with M-Value and results of correlation comparisons [1]

Measure	Formula	Correlation with M-value		Reference
$ISI_{Matsuda}$	$\frac{10000}{\sqrt{FPG \times FPI \times G_{mean} \times I_{mean}}}$	$r = -0.43$	$p = 0.1$	[44]
$ISI_{Stumvoll}$	$0.156 - 0.0000459 \times I_{120\ min} - 0.0000321 \times FPI - 0.0054 \times G_{120\ min}$	$r = 0.47$	$p = 0.0794$	[45]
ISI_{Gutt}	$\frac{75000+(FPG-G_{120\ min}) \times 0.19 \times BW}{G_{mean} \times log(I_{mean})}$	$r = -0.2965$	$p = 0.28$	[48]
Proposed ISI	equation (3.2)	$r = 0.927$	$p = 0.0045$	-

Chapter 4

Assessment of type II diabetes mellitus using irregularly sampled measurements with missing data

4.1 Introduction

In diabetic patients, the glucose metabolic rates represent the health status of the liver, muscles and adipose tissues. To measure the glucose metabolic rates in the type II diabetic patients, the measurement of the glucose and insulin concentrations in different parts of the body are needed. However, clinical measurements of all necessary concentrations deep inside different organs or tissues are just not practical or realistic. Therefore, physicians mostly rely on a few measurements from patients' blood and/or capillary glucose measurements at regular or irregular intervals for clinical decisions [77].

Previous studies have shown that important clinical data may be missing owing to different reasons such as inability to record clinical results, infrequent sampling by patients, and illegible hand writing. Lack of complete knowledge about the health status of the diabetic patients poses more problems to physicians in managing type II diabetes while they need time oriented clinical data of past and present status of diabetic patients [78–80].

Since only a few blood glucose measurements per day are available in a non-clinical

setting, developing a predictive model of the blood glucose of a person with type II diabetes mellitus is important. Such a model may provide useful information to diabetic patients of dangerous metabolic conditions, enable physicians to review past therapy, estimate future blood glucose levels, and provide therapy recommendations. It can also be used in the design of a stabilizing control system for blood glucose regulations [81, 82].

Many studies proposed on-line identification of type I diabetes mellitus using neural network modelling approaches [82–85]. Tresp *et al*. [82] developed a predictive model of the blood glucose of a person with type I diabetes mellitus with partially missing clinical data by using a combination of a nonlinear recurrent neural network and a linear error model. However, developing a nonlinear state-space model for type II diabetes mellitus that can easily deal with missing data has received limited attention.

The goal of this work is to develop a blood glucose predictive model for a type II diabetic patient and the model can be estimated by using patient data collected under normal everyday conditions rather than a well-controlled environment typically done in a clinical facility. Such a model should be able to detect dangerous metabolic states of a patient, and optimize the patient's therapy.

In this study, we use online Bayesian estimation framework to estimate a stochastic nonlinear model for type II diabetes mellitus using clinical data with missing data at random intervals. We adopt the detailed nonlinear model developed by Vahidi *et al*. [7, 51] for type II diabetes since the Vahidi model is a much more detailed model comparing with the MINMOD approach. The Vahidi model is able to effectively model individual abnormalities by characterizing distinct compartments as the faulty organs. To artificially create clinical data sets with missing data at random intervals, we then randomly remove 10%, 25% and 50% of the original available data obtained from the Vahidi model. At the end, glucose, insulin, and incretins concentrations, as well as the parameters of different

compartments, are estimated from clinical data with missing data at random intervals. These estimates can then be used to measure the glucose metabolic rates in different organs of the type II diabetic patients.

There is an extensive discussion on estimating the states and the parameters of the nonlinear state-space models from partially missing data using mathematical approaches such as Bayesian filters, Particle filters (PFs), Expectation-Maximization (EM) algorithms, Sequential Importance Resampling (SIR) particle filters [86–89]. In many studies, Baysian estimation has been used in metabolism and physiological modelling [90–92]. Among these methods, we use the SIR based PF proposed by Tulsyan *et al.* [93] for online Bayesian estimation of the states and the parameters of the Vahidi model since it needs less computational cost when a large number of unknown states and parameters must be estimated simultaneously. To do this, a clinical data set, as well as a prior information on the unknown states and parameters of the Vahidi model, are needed. This kind of information can be gathered from physical considerations and population studies.

In this study, the estimation of the Vahidi model parameters are carried out by the SIR particle filtering method for the data sets containing randomly deleted simulated data.

4.2 Mathematical model preparation

The continuous mathematical model of type II diabetes developed by Vahidi *et al.* [7, 51] has been described previously in chapter 2. In order to estimate the unknown parameters of the Vahidi model using particle filtering method, the model must be discretized. To discretize the model, any discretization method is possible to be used. In this study, simply the fixed-step backward difference approximation has been used since it was accurate enough to discretize the model. The following equation represents general discretization

using fixed-step backward difference approximation:

$$\frac{dy}{dx} = \frac{y_i - y_{i-1}}{\Delta x}, \tag{4.1}$$

The above equation is applied to all ordinary differential equations explained in chapter 2. The model can be then rewritten in state space general form as follows:

$$x_{t+1} = f(y_t, \theta_t, u_t) + v_t, \tag{4.2a}$$

$$y_t = g(x_t, \theta_t, u_t) + w_t, \tag{4.2b}$$

where:

- f is the state function representing equations 2.1 to 2.8, 2.20, 2.24, 2.27, 2.43 to 2.49, 2.53, 2.56, 2.57, and 2.61.
- g is the measurement dynamic function representing equations 2.7 and 2.48.
- t is the sampling time index.
- x_t is the vector of states.
- u_t is the vector of inputs.
- y_t is the vector of measurements.
- θ is the vector of model parameters, which are constant values.
- v_t and w_t are state and measurement noise sequences with known probability density functions with zero mean. Since all real systems normally incorporate different environmental noises affecting the measurements and also mathematical models normally have some uncertainties, these noise sequences are added to the model states and outputs to address usual measurement noises and also model uncertainties.

In type II diabetes model g represents the measurement dynamic function variables and $\widehat{y}_t$ is the vector of concentration of either insulin, glucose, or glucagon at sampling time t monitored and recorded by several sensors and measuring devices. These devices record patient's critical variables y_t (output) in response to the test action u_t (input) implemented at some point in time indexed by t. For example, in the intravenous glucose infusion test, insulin concentration measurements as output y_t are recorded at regular intervals against the infused glucose concentration as input u_t. A summary description of this on-line estimation method is provided in the next following sections.

4.3 Response models

In clinical trials, several sensors and measuring devices were used for monitoring the response of a patient to a clinical test. Let us assume that we have a sequence of time-tagged clinical measurements $y_{1:t} = \{y_1, y_2, \ldots, y_t\}$ corresponding to the input action $u_{1:t} = \{u_1, u_2, \ldots, u_t\}$, and that we are interested in predicting the response y_{t+1} for some known input action u_{t+1}. Such predictions are valuable to the physician assessing the health of the patient during clinical trials. To solve this problem, we can assume y_{t+1} is independent of $\{u_{1:t}, y_{1:t}\}$, in which case, the prediction of y_{t+1} is impossible. Alternatively, we can assume y_{t+1} depends on the trend recorded in the past data $\{u_{1:t}, y_{1:t}\}$. For the latter assumption– which is true for any causal system– a response model[1] is useful in predicting the response of a patient to a clinical test.

A reliable response model should not only accurately model a patient's physical and biological response to a clinical test, it should also account for the various uncertainties such as modelling and measurement errors. For example, random measurement errors can

[1] A response model is a mathematical model describing the dynamics of the key internal states of a patient in response to a clinical test.

be modelled by viewing y_t as a random realization of a stochastic process. In this work, we use stochastic state-space models (SSMs) to represent a response model. Mathematically, a SSM can be represented as:

$$x_{t+1} = f(y_t, \theta_t, u_t) + v_t, \tag{4.3a}$$

$$y_t = g(x_t, \theta_t, u_t) + w_t, \tag{4.3b}$$

where x_t describes evolution of the internal states of the patient. Physically, x_t models the complete response of a patient subject to a clinical test. Given the states x_t, inputs u_t and model parameters θ_t at time t, the internal states evolve to x_{t+1}. v_t in equation(4.3a) is the state noise, which accounts for the unknown and unmeasured variations in the states not captured by the response model. Due to the non-zero random state noise v_t, the states are not precisely known. Equation (4.3b) describes how sensor readings y_t relate to the states x_t and parameters θ_t. w_t in equation (4.3b) is the noise term, which accounts for the random sensor noise.

In clinical trials, measurements of only a few critical states are available at our disposal. This is because the high cost or lack of appropriate sensing technology or devices precludes measurement of all but key internal states. The state-space modelling framework is general, and can be used to represent a wide class of response models, including the type II diabetes mellitus response model given in section 2.1.

In this study, we use equation (4.3) for real-time estimation of the critical response variables, such as blood glucose, insulin and incretins concentrations during clinical trial of patients with type II diabetes mellitus. Monitoring these variables is critical as it enables the physicians to review past therapy, estimate future blood glucose levels and provide therapy recommendations. To predict the critical variables using equation (4.3), the model states and parameters, which are typically unknown for a patient need to be estimated first.

Given the state and parameter estimates, the model predictions at t can be computed as:

$$\widehat{y}_t = g(\widehat{x}_t, \widehat{\theta}_t, u_t), \tag{4.4}$$

where $\widehat{y}_t$ is the response predictions and $\widehat{x}_t$ and $\widehat{\theta}_t$ are the parameter and state estimates, respectively. Ideally, given an accurate estimate of the states and parameters, the model predictions should match the clinical measurements as closely as possible. Any standard estimation approach involves fitting the model using available clinical measurements; however, data fitting is not straightforward for SSMs because of the following reasons: 1) the states are stochastic, which makes estimation of both states and parameters challenging and 2) the clinical measurements are assumed to be irregularly sampled. In the next section, we explain how the unknown states and parameters of the response model are estimated.

Remark. There is a much larger appeal to use state-space modelling framework to represent response models. From equation 4.4, it is evident that computing the response predictions using a SSM also requires estimation of all the internal states of the patient. Thus, any method designed to compute the response predictions gives away estimation of all the internal states as a side product. This is of immense value to a physician, considering only a handful of the internal states are actually measured.

4.3.1 States and parameters estimation of the response model

In most real systems, all the physical states are not measurable due to the various inherent restrictions. Therefore, by applying a series of mathematical calculations called "states observer" or "states filtering", unknown model states are estimated by input and output measurements from the real system [7]. For instance, in the type II diabetes model, obtaining measurements of blood glucose and insulin concentrations from different body organs are extremely difficult, dangerous for the subjects and in most of the times clinically im-

possible. However, having this type of information is necessary in evaluating the behaviour of body organs. An alternative is to estimate these concentrations using available measurements from peripheral tissues along with a mathematical model and a states estimator algorithm [7].

If the models is deterministic (the output of the model is fully determined by the parameter values and the initial conditions), the unknown states and parameters are often generated using an observer such as Luenberger observer. Otherwise, for stochastic models (the output of the model is unpredictable due to the influence of a random variable), a filter is used for estimation [94].

In the stochastic state-space model, when the model parameter θ is known, on-line inference about the state process x_t given the observations y_t is a so-called optimal filtering [94]. Kalman filtering methods rely on the model being linear and noise being Gaussian [95]. Extensions to nonlinear systems have also been considered in the literature such as extended Kalman filters (EKF), and unscented Kalman filters (UKF). These suboptimal filters either approximate the nonlinear system through linearization and/or assume that the noise is Gaussian. The approximations are often not satisfactory.

However, Sequential Monte Carlo (SMC) methods, also known as particle methods do not require linearization of the stochastic state-spaces model or Gaussianity of the measurement noises [96]. Particle filtering algorithm are a class of sequential simulation-based algorithms to approximate the posterior distributions of interest. This algorithm is a powerful state estimation method whose accuracy is independent on the degree of model nonlinearity and is able to be improved by increasing the number of particles unlike Kalman filter [94].

In the stochastic state-space model, when the parameter θ is unknown and needs to be estimated from the data either in an on-line or off-line manner, the following methods are

used [94]:

- Bayesian or Maximum Likelihood (ML)
- Off-line (batch) or on-line (recursive)

In the past 15 years, several algorithms have been proposed to solve the simultaneous state-parameter estimation problem in real-time using likelihood and Bayesian derived methods. The recent review paper by Kantas *et al.* [94] provided a detailed exposition of on-line and off-line methods for parameter estimation using Bayesian and likelihood based methods. Simultaneous on-line Bayesian estimators is performed by filtering an extended vector of states and parameters using an adaptive sequential-importance-resampling (SIR) filter with a kernel density estimation method [93].

The existing literature for on-line state-parameter estimation using Bayesian and likelihood based methods assumes that measurement will be available at all sampling time; however, in practice, measurements may not be available at all sampling time instants. Tulsyan *et al.* [93] proposed on-line Bayesian state and parameter estimation in non-linear state- space models (SSMs) with non-Gaussian noise under missing measurements. They used a particle based SIR filtering approach due to the inherent limitations of the EKF and UKF based simultaneous state-parameter estimators. They selected the SIR filter since it is relatively less sensitive to large process noise and is computationally less expensive. Furthermore, the importance weights are easily evaluated and the importance functions can be easily sampled [93].

In the light of aforementioned above, in this study, we apply a particle based SIR filtering approach proposed by Tulsyan *et al.* [93] to estimate the real-time states and parameters of the stochastic nonlinear state-space type II diabetes model under irregularly sampled clinical measurements.

A brief description of the standard particle filter algorithm is presented below to provide the necessary background for the algorithm developed in the following section.

4.3.2 Recursive bayesian estimation

The Sequential Monte Carlo (SMC) approach is a recursive Bayesian estimation method for nonlinear and non-Gaussian filtering problems. In this approach, given a sequence of measurements, the probability density function (PDF) of the current state x_t is estimated. Let us assume that we have a sequence of time-tagged clinical measurements $y_{1:t} = \{y_1, y_2, \ldots, y_t\}$ corresponding to the input action $u_{1:t} = \{u_1, u_2, \ldots, u_t\}$, and we are interested in predicting the density of the state, i.e. $p(x_t|y_{1:t})$, for every iteration. Using the Bayes' theorem and Total law of probability, $p(x_t|y_{1:t})$ can be recursively computed in two steps, which are the update and prediction steps as shown below:

Update Step:

$$p(x_t|y_{1:t}) \propto p_y(y_t|x_t)p(x_t|y_{1:t-1}). \tag{4.5}$$

Prediction Step:

$$p(x_t|y_{1:t-1}) = \int p_x(x_t|x_{t-1})p(x_{t-1}|y_{1:t-1})dx_t. \tag{4.6}$$

It is assumed that the PDF of the initial time step, $p(x_0|y_0)$, is known. Equations (4.5) and (4.6) do not have analytical solutions for nonlinear processes with Gaussian noise. The Sequential Monte Carlo algorithms make these complex integrals tractable through the use of efficient sampling strategies.

4.3.3 Sequential monte carlo (SMC)

The basic idea of SMC is the recursive computation of any given target PDF $\pi(x)$ (e.g., $p(x_t|y_{1:t})$) by generating a set of random particles (samples) and associated weights from the target PDF $\pi(x)$. Furthermore, due to its generality and robustness, it has become an important alternative to the extended Kalman filter (EKF) and unscented Kalman filter (UKF). Unlike Kalman filter method, in the particle filtering method, the exploited approximation does not involve linearization around current estimates [97].

Consider the state space model given by equations (4.3a) and (4.3b). Rather than direct solving the integrals in equations (4.5) and (4.6), the Bayesian recursive estimation is implemented via Monte Carlo sampling. For estimating the PDF, the two pieces of information required at each time step t: the samples x_t^i and their associated weights ω_t^i. From a known density called importance density function, $q(x_t|y_{1:t})$, samples x_t^i are assumed to be generated. The corresponding weights of the samples are defined as:

$$\omega_t^i = \frac{p(x_t^i|y_{1:t})}{q(x_t^i|y_{1:t})} \tag{4.7}$$

and after normalization the weights become:

$$\omega_t^i = \frac{\omega_t^i}{\sum_{i=1}^{N} \omega_t^i} \tag{4.8}$$

where N is the number of samples used. The samples at time step t, $x_t^i \sim q(x_t^i|y_{1:t})$, are computed by multiplying the existing samples, $x_{t-1}^i \sim q(x_{t-1}^i|y_{1:t-1})$, and the new state, $x_t^i \sim q(x_t^i|x_{t-1}^i, y_{1:t})$ if the importance density function is chosen to be factorized such that:

$$q(x_t|y_{1:t}) = q(x_t|x_{t-1}, y_t)q(x_{t-1}|y_{1:t-1}) \tag{4.9}$$

and the updated weight ω_t^i associated with x_t^i can be obtained according to:

$$\omega_t^i \propto \omega_{t-1}^i \frac{p(y_t|x_t^i)p(x_t^i|x_{t-1}^i)}{q(x_t^i|x_{t-1}^i, y_{1:t})} \tag{4.10}$$

It is useful to assume that $q(x_t^i|x_{t-1}^i, y_{1:t}) = q(x_t^i|x_{t-1}^i, y_t)$ when only a filtered estimate of $p(x_t|y_{1:t})$ is required. Then, the importance density only depends on x_{t-1} and y_t. Under this assumption, equation 4.11 can be rewritten as:

$$\omega_t^i \propto \omega_{t-1}^i \frac{p(y_t|x_t^i)p(x_t^i|x_{t-1}^i)}{q(x_t^i|x_{t-1}^i, y_t)} \tag{4.11}$$

and the filtered density $p(x_t|y_{1:t})$ is approximated as follows:

$$p(x_t|y_{1:t}) \approx \sum_{i=1}^{N} \omega_t^i \delta(x_t - x_t^i) \tag{4.12}$$

where $\delta(.)$ is a multi-dimensional Dirac function. x_t^i is the ith sample that approximates the distribution, and the coefficient ω_t^i is the corresponding weight. As $N \to \infty$, the above density approximation approaches the true filtered density $p(x_t|y_{1:t})$. In the next section, a description of real-time Bayesian estimation is provided.

4.4 Online state and parameter estimation in nonlinear state-space models

Our objective is to estimate z_t in real-time using clinical data $\{u_{1:t}; y_{1:t}\}$. Let $z_t = \{x_t, \theta_t\}$ denote an extended vector of unknown states and parameters. It is further assumed that the clinical measurements are recorded at irregular times, such that only a subset of $y_{1:t}$ is available for estimation at t. For notational convenience, we dispense with the input u_t

in the succeeding discussions; however, the method presented in this study holds with the inputs included.

In the Bayesian framework, the variables to be estimated are assumed to be random variables. The states are inherently random due to the noise in equation (4.3a); and the parameters, which are unknown but non-random are assumed to be random, such that $z_t = \{x_t, \theta_t\}$ is a vector of random variables. To set up the Bayesian estimation, we assume z_0 to be distributed with a prior density $p(z_0|y_{1:0})$. Also, we assume the state and measurement noise are independent and identically distributed (i.i.d) zero mean finite variance Gaussian sequences with the probability density functions (PDF) $p_x(.)$ and $p_y(.)$ known *a priori*.

4.4.1 Complete clinical data

First we consider the estimation problem using the complete clinical data set. Assuming $y_{1:t}$ to be available, the real-time Bayesian estimation of z_t at t involves computing the posterior density $p(z_t|y_{1:t})$. Here, $p(z_t|y_{1:t})$ is a probabilistic representation of the statistical information available on z_t conditioned on the clinical measurements $y_{1:t}$. Based on the Bayes' theorem and Total law of probability presented in equations (4.5) and (4.6), $p(z_t|y_{1:t})$ can be recursively computed as shown below:

Update Step:

$$p(z_t|y_{1:t}) \propto p_y(y_t|z_t)p(z_t|y_{1:t-1}). \tag{4.13}$$

Prediction Step:

$$p(z_t|y_{1:t-1}) = \int p_z(z_t|z_{t-1})p(z_{t-1}|y_{1:t-1})dz_t. \tag{4.14}$$

In equation (4.13), $p_y(y_t|z_t)$ is the measurement noise distribution or the likelihood function indicating how likely it is for z_t to have generated the clinical measurement y_t. $p(z_t|y_{1:t-1})$ is a one-step-ahead prior density representing statistical information on z_t prior to the recorded clinical measurement y_t. The prior density $p(z_t|y_{1:t-1})$ is computed using equation (4.14), where $p_z(z_t|z_{t-1})$ is the joint state and parameter noise distribution and $p(z_{t-1}|y_{1:t-1})$ is the posterior distribution at $t-1$.

Starting with $p(z_0|y_{0:1})$, in principle, the recurrence relation between equations (4.13) and (4.14) provides a complete Bayesian solution to the state and parameter estimation problem under complete clinical data. Finally using $p(z_t|y_{1:t})$, the estimate of $\widehat{z}_t$ at t can be computed as the mean of the posterior density, such that the estimate step can be defined as:

$$\widehat{z}_t = \int z_t p(z_t|y_{1:t}) dz_t, \tag{4.15}$$

where $\widehat{z}_t = \{\widehat{x}_t, \widehat{\theta}_t\}$ is the state and parameter estimation at t. Note that other values, such as the mode or median of $p(z_t|y_{1:t})$ can also be selected as the point estimate.

4.4.2 Irregular clinical data

From section 4.4.1, it is evident that if y_t is not measured at t, the posterior density $p(z_t|y_{1:t})$ cannot be computed using equation (4.13). In such situations, the estimates at t, in presence of irregular data can be computed by replacing $p(z_t|y_{1:t})$ in equation (4.15) using the one-step ahead prior density $p(z_t|y_{1:t-1})$.

Now assuming y_{t+1} to be available at $t+1$, the posterior density for z_{t+1}, given clinical measurements $\{y_{1:t-1}, y_t\}$, *i.e.*, $p(z_{t+1}|y_{1:t-1}, y_{t+1})$ can be computed using the Bayes' theorem and the law of total probability, such that the update step shows that:

$$p(z_{t+1}|y_{1:t-1}, y_{t+1}) \propto p(y_{t+1}|z_{t+1})p(z_{t+1}|y_{1:t-1}). \tag{4.16}$$

where $p(z_{t+1}|y_{1:t-1}, y_{t+1})$ is the posterior density for z_{t+1} and $p(z_{t+1}|y_{1:t-1})$ is a two-step ahead prior density computed using the law of total probability, *i.e.*:

$$p(z_{t+1}|y_{1:t-1}) = \int p_z(z_{t+1}|z_t)p(z_t|y_{1:t-1})dz_t. \tag{4.17}$$

Substituting equation (4.14) into equation (4.17) yields the prediction step:

$$p(z_{t+1}|y_{1:t-1}) = \iint p_z(z_{t+1}|z_t)p_z(z_t|z_{t-1})p(z_{t-1}|y_{1:t-1})dz_{t-1:t}. \tag{4.18}$$

Similar to section 4.4.1, having computed $p(z_{t+1}|y_{1:t-1}, y_{t+1})$, the estimate of z_{t+1} can be computed by replacing the density by $p(z_{t+1}|y_{1:t-1}, y_{t+1})$ in equation (4.15). Note that the method proposed in this section is general and can naturally be extended to handle consecutively missing measurements as well.

The Bayesian approach developed in section 4.4 provides an excellent framework for real-time state and parameter estimation under complete and irregular clinical measurements. Computing the Bayesian solution requires evaluation of the multiple integrals in the prediction and estimation steps. Unfortunately, except for linear systems with Gaussian state and measurement noise, or when the states and parameters take on only finite values, the Bayesian solution cannot be solved exactly with finite computing capabilities.

This study uses a sequential Monte-Carlo (SMC)-based adaptive sequential-importance-resampling (SIR) filter proposed by Tulsyan *et al.* [93] to numerically approximate the Bayesian solution. In the next section, using SMC method, the estimation results of states and parameters of the state-space model for type II diabetic patients under various levels of randomly missing clinical data are presented.

4.5 Results and discussion

In this section, the efficiency of the SIR filtering method in handling missing measurements for estimation of the nonlinear stochastic model for type II diabetes mellitus is demonstrated. All the simulations were conducted on a 2.90 GHz CPU with 8 GB RAM Mac using MATLAB 2012b. On-line estimation of states and all the parameters cited in the reference [7] by SIR filtering leads to large memory requirements and computational complexity. To reduce the computation load, only the parameters of type II diabetic subjects that have considerable effects on peripheral glucose, insulin and incretins concentrations were chosen for estimation while keeping all other non-essential model parameters constant.

4.5.1 Clinical data used for model development

The states and the parameters of the Vahidi model were estimated using two different clinical tests, oral glucose tolerance test (OGTT) and isoglycemic intravenous glucose infusion test (IIVGIT) performed by Knop *et al.* [73, 74]. Ten type II diabetic patients (eight men and two women) have been selected for the tests.

A 50 g glucose tolerance test (OGTT test) is performed in the first test and 17 blood samples are taken from the subjects during the test to determine how quickly glucagon suppression occurred. Blood was sampled 15, 10 and 0 minutes before, and after the ingestion of glucose at 5, 10, 15, 20, 30, 40, 45, 50, 60, 70, 90, 120, 150, 180 and 240 minutes.

In the second test, isoglycemic intravenous glucose infusion test (IIVGIT test) is carried out to mimic the plasma glucose profile obtained from the OGTT test. Therefore, the same amount of glucose was injected intravenously to the diabetic subjects in the IIVGIT test. Blood was sampled every 5 minutes [73, 74]. 20 blood samples are taken from the subjects during the second test. Details about the experiments and the subjects' characteristics are

available in [73, 74].

Since the Sorensen model is proposed for a typical 70 kg subject and the clinical data sets, which we used are from subjects with different body weights, all clinical data is scaled to a 70 kg body weight using the following equation:

$$C = (C^C - C^B)\frac{W}{70} + C^B \tag{4.19}$$

where C is the substance concentration, W is the subjects body weight (kg), C^C refers to the concentration from original clinical data, and C^B refers to the concentration at basal condition. The normalized values of the clinical data sets for a 70 kg are provided in Appendix A.

The information included in data sets are peripheral glucose, insulin and incretins (GLP-1 plus GIP) concentrations. The data from both tests are used for estimating the parameters of the model using SIR particle filtering method as follows:

- From the IIVGIT test:
  - Incretins concentrations are not used since no secretion of incretins occurs during the IIVGIT test.
  - Insulin concentrations are used to estimate the parameters of the pancreas model.
- From the OGTT test:
  - The rest of the integrated model parameters including the parameters of the glucose sub-model which also comprises the parameters of the glucose absorption model and the parameters representing the hormonal effects of incretins on the pancreatic insulin production are all estimated using OGTT test data set.

4.5.2 On-line states and parameters estimation results

To apply the SIR particle filtering method, a prior information on the unknown parameters of the Vahidi model from both OGTT and IIVGIT is needed. This information can be obtained from equation (2.67) by minimizing the deviation of model predictions from the available clinical measurements of peripheral glucose, insulin and incretins concentrations described in section 4.5.1.

After the prior information on the unknown parameters obtained, the estimation of the states and parameters of the Vahidi model were estimated using SIR particle filtering method. Firstly, the parameters of the pancreas model were estimated from the isoglycemic intravenous glucose infusion test (IIVGIT) test since no secretion of incretins occurs during the IIVGIT test. In the model parameter estimation, the peripheral insulin concentration in the Vahidi model [7] was considered as a measurement y_k. For implementing the SIR filtering based on the discrepancies between the Vahidi model and the Knop's experimental data, the following parameters were selected:

- The number of particles $N = 5000$
- The sampling time used for discretizing the Vahidi model $\Delta k = 0.4\ min$
- The maximum states noises $v_k \sim \mathcal{N}(0, 0.001)$
- The measurement noise $w_k \sim \mathcal{N}(0, 0.001)$

A priori information on $\{x_0; \theta\}$ includes the lower (LB) and the upper bound (UB) based on the physiological considerations. Four simulation experiments were carried out to evaluate the effectiveness of our proposed method to identify patient models with incomplete data. In the four experiments, 0%, 10%, 25% and 50% of available data simulated from the Vahidi model were removed randomly. For example, when 10% of data were

considered missing, a peripheral insulin concentration at each sampling time was removed from the original data set if a uniformly distributed random variable q in the interval (0,1) is less than 0.1. Similar experiments were done with 25% and 50% missing data [88].

The parameter values after 600 samples from each of these experiments are shown in Table 4.1. The detailed information about these parameters were presented previously in section 2.2.3 from equation 2.53 to 2.58 in detail. For all the experiments, all the parameters except θ_6 and θ_7 converged to the neighbourhood of the original values after a certain number of iterations. θ_6 and θ_7 are not estimated precisely since the sensitivity of the KLD in kernel smoothing algorithm to changes in θ_6 and θ_7 is smaller than its variance.

Table 4.1: Parameter estimation results for insulin sub-model after 600 sampling time during IIVGIT test

Parameters [7]	OriginalValues	Percentage of Missing insulin measurements			
		0%	10%	25%	50%
$\theta_1 : \alpha(min)^{-1}$	0.6152	0.6168	0.5728	0.5803	0.5159
$\theta_2 : \gamma(U/min)$	2.3665	2.3422	2.1860	2.3667	2.5200
$\theta_3 : K(min)^{-1}$	0.0572	0.0565	0.0560	0.0561	0.0544
$\theta_4 : N_1(min)^{-1}$	0.0499	0.0496	0.0519	0.0481	0.0474
$\theta_5 : N_2(min)^{-1}$	0.0001490	0.0001489	0.0001482	0.0001500	0.0001506
$\theta_6 : \xi_1(min)^{-1}$	0.000124	0.000125	0.000126	0.000125	0.000141
$\theta_7 : \xi_2(min)^{-1}$	0.00270	0.00271	0.00280	0.00152	0.00122

Variations of the parameters N_1, N_2, ξ_1 and ξ_2 are shown in Figure. 4.1 and the variations of the parameters α, γ, and K are shown in Figure. 4.2.

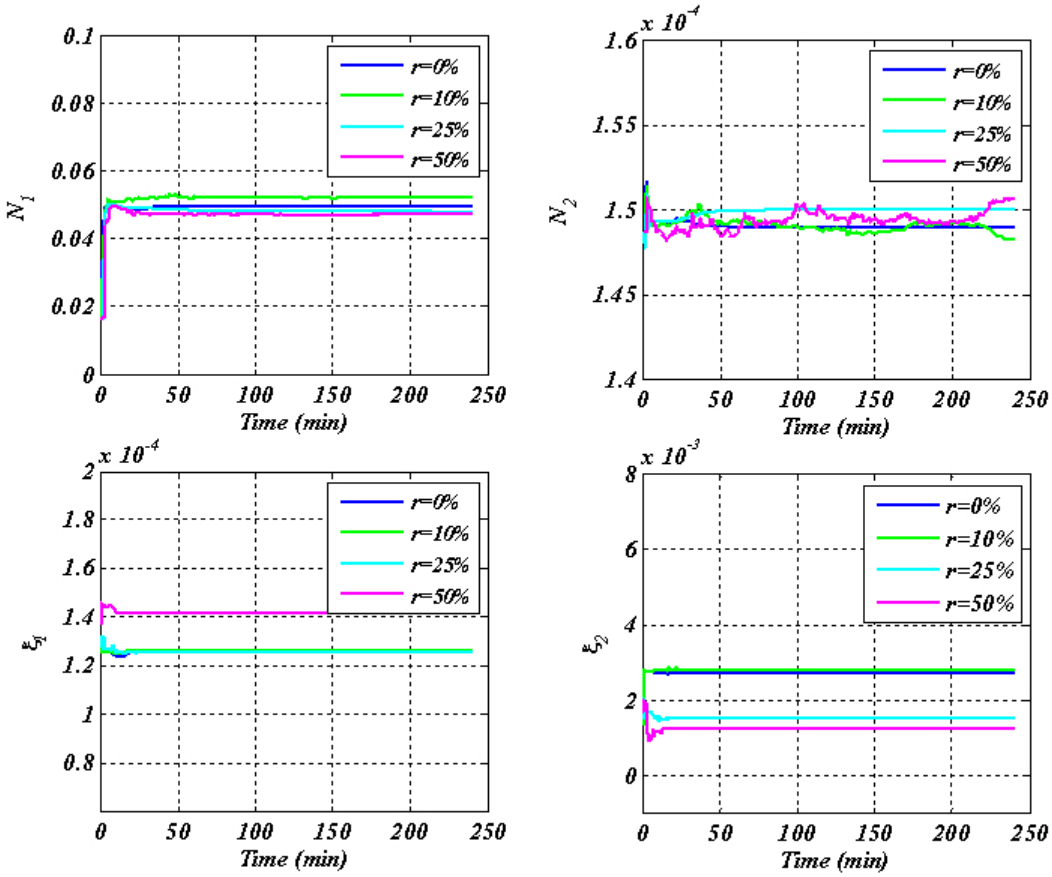

Figure 4.1: Variations of the parameters N_1, N_2, ξ_1 and ξ_2 in the Pancreatic insulin release model

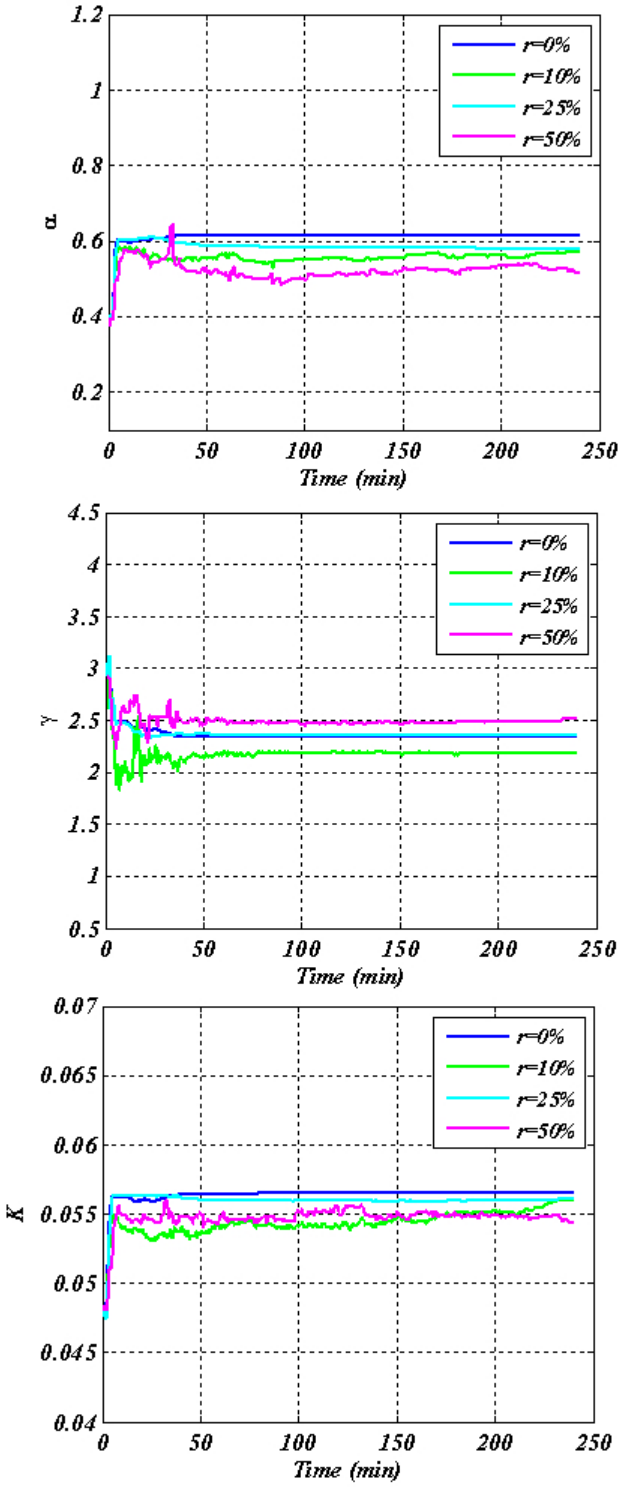

Figure 4.2: Variations of the parameters α, γ, K in the Pancreatic insulin release model

Variations of the peripheral insulin concentrations during the IIVGIT test are shown in Fig. 4.3a in which, r shows the percentage of missing observations. From the Fig. 4.3a, the dynamics of peripheral insulin concentration can be estimated reasonably well with physiological responses in all the experiments even when 50% of the simulated clinical data were absent. Fig. 4.3b presents the goodness of fit between the estimated output and the measured output performed with MATLAB System Identification Toolbox by using normalized root mean square error (NRMSE) as a cost function. Based on the NRMSE measure, the goodness of fit between the simulated peripheral insulin concentration and the available measurements are more than 80%.

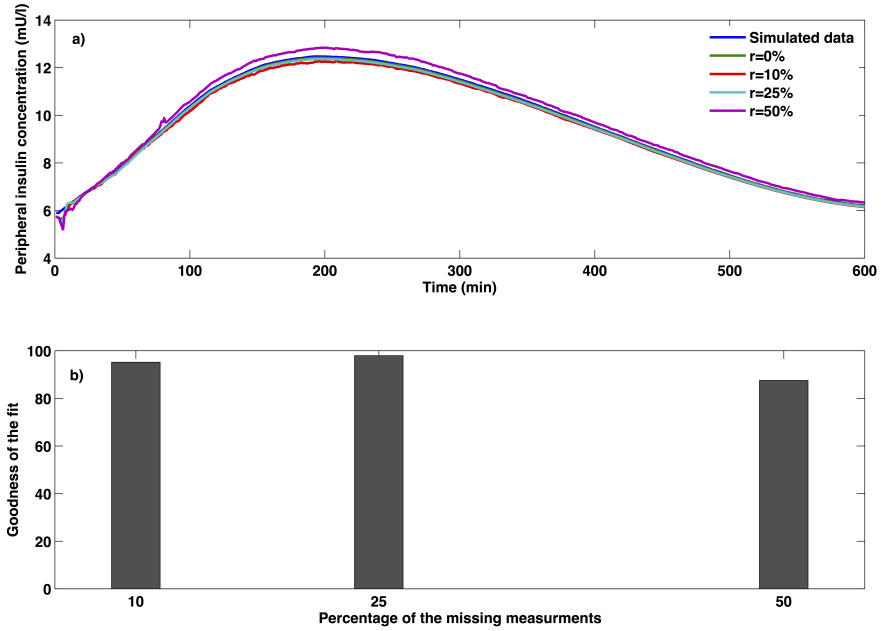

Figure 4.3: Peripheral insulin concentration for type II diabetic subjects during the IIVGIT test

Secondly, from the oral glucose tolerance test (OGTT), the peripheral insulin concentration, peripheral glucose concentration and incretins concentrations were considered as

measurements y_k for estimation of the rest of the model parameters. These parameters consist of the parameters of the glucose sub-model including the parameters of the glucose absorption model and the parameters describing the hormonal effects of incretins on the pancreatic insulin production as described previously in section 2.2.1.

From the glucose sub-model, parameters of the glucose metabolic rates and some parameters of the glucose absorption model have been considered for the parameter estimation. As the model equations in section 2.2.1 shows, the glucose metabolic rates in the glucose sub-model has the general form of equation 2.9 and the multipliers have the general form of equation 2.10. Considering equation 2.10, a, b, c and d are the parameters of the glucose metabolic rates. To reduce the number of parameters for estimation, c and d are selected for the parameter estimation and a and b are considered to be unchanged.

Therefore, parameters c and d in the hepatic glucose production (HGP) rate, the hepatic glucose uptake (HGU) rate, and the peripheral glucose uptake rate (PGU) are selected to be estimated. For implementing the SIR filtering based on the discrepancies between the Vahidi model and the Knop's experimental data, the following parameters were selected:

- The number of particles $N = 20000$
- The sampling time used for discretizing the Vahidi model $\Delta k = 0.1\ min$
- The maximum states noises $v_k \sim \mathcal{N}(0, 0.7)$
- The measurement noise $w_k \sim \mathcal{N}(0, 0.7)$

The parameter values after 2400 samples from each of these experiments are shown in Table 4.2. In all the experiments, the estimated parameters, except θ_1 and θ_4 converged to the neighbourhood of the original values after a certain number of iterations. θ_1 and θ_4 are not estimated precisely since the sensitivity of the KLD in kernel smoothing algorithm to changes in θ_1 and θ_4 is smaller than its variance.

Table 4.2: Variation of the parameters c^G_{HGP}, c^G_{HGU}, $d^{I\infty}_{HGP}$ and K_{12} in glucose sub-model after 2400 sampling time during OGTT test

Parameters [7]	OriginalValues	Percentage of Missing insulin measurements			
		0%	10%	25%	50%
$\theta_1 : c^G_{HGP}$	1.0385	1.0352	1.0885	1.9743	2.0649
$\theta_2 : c^G_{HGU}$	2.03	1.97	1.84	2.23	1.53
$\theta_3 : d^{I\infty}_{HGP}$	0.3648	0.3676	0.3610	0.3625	0.3667
$\theta_4 : K_{12}(min)^{-1}$	0.0783	0.0796	0.0798	0.0842	0.0616
$\theta_5 : c^I_{PGU}$	0.0970	0.0965	0.0965	0.0902	0.1300
$\theta_6 : c^{I\infty}_{HGU}$	3.2606	3.3125	2.9543	2.9625	2.8057
$\theta_7 : d^I_{PGU}$	2.752	2.747	2.724	2.897	2.909
$\theta_8 : d^{I\infty}_{HGU}$	0.0031	0.0030	0.0028	0.0030	0.0038

Variations of the parameters c^G_{HGP}, c^G_{HGU}, $d^{I\infty}_{HGP}$ and K_{12} are shown in Figure. 4.4 and the variations of the parameters c^I_{PGU}, $c^{I\infty}_{HGU}$, d^I_{PGU} and $d^{I\infty}_{HGU}$ are shown in Figure. 4.5.

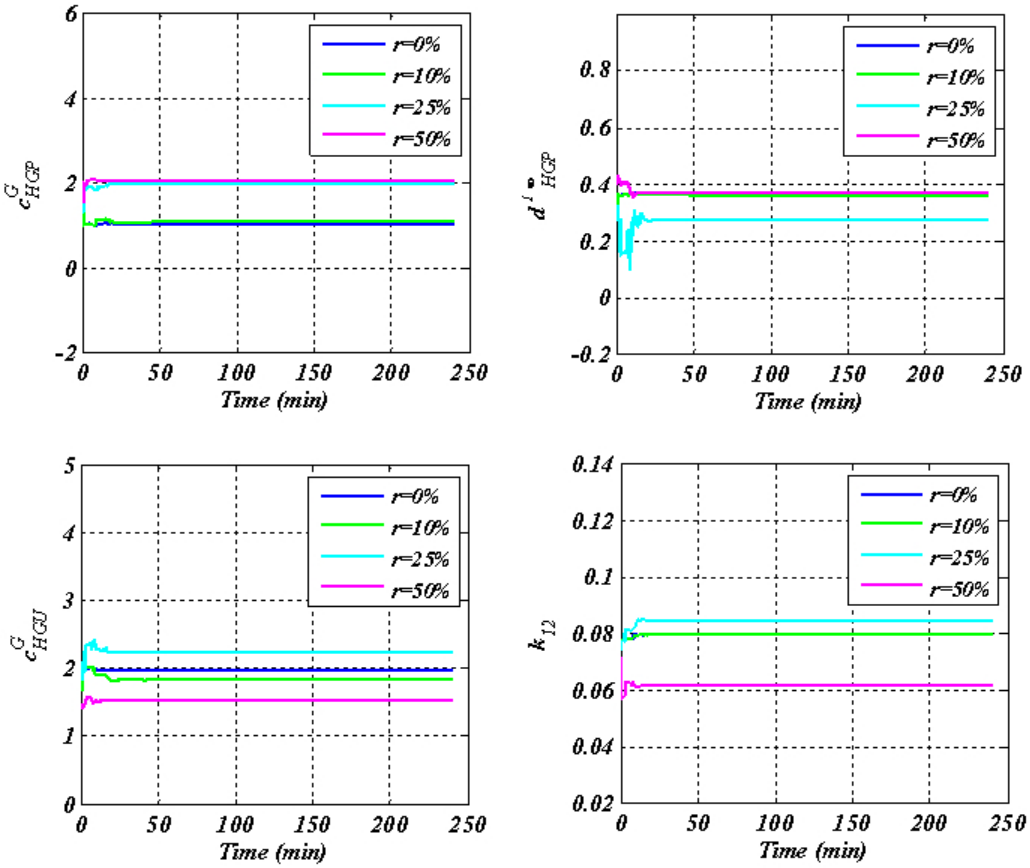

Figure 4.4: Variations of the parameters c^I_{PGU}, $c^{I\infty}_{HGU}$, d^I_{PGU} and $d^{I\infty}_{HGU}$ in glucose sub-model after 2400 sampling time during OGTT test

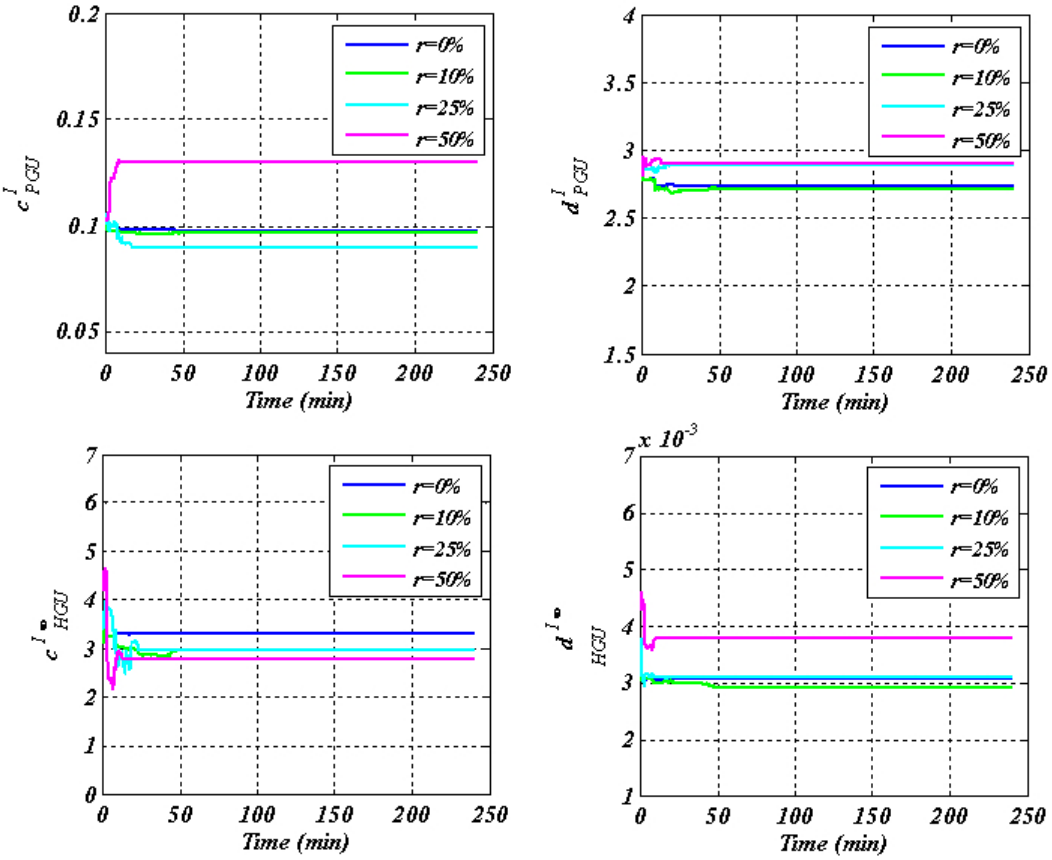

Figure 4.5: Parameter estimation results for glucose sub-model after 2400 sampling time during OGTT test

Variations of the peripheral glucose, insulin, and incretins concentrations during the OGTT test after 2400 iterations are shown in Figs. 5.2a-5.4a. r shows the percentage of missing observations. From the Figs. 5.2a-5.4a, the dynamics of peripheral glucose, insulin, and incretins concentration can be estimated reasonably well with physiological responses in all the experiments even when 50% of the clinical data is missing. Figs. 5.2b-5.4b present the goodness of fit between the estimated output and the measured output performed with MATLAB System Identification Toolbox by using the normalized root mean square error (NRMSE) as a cost function. From Figs. 5.2b-5.4b, the goodness of

fit between the simulated peripheral glucose, insulin and incretins concentration and their available measurements were almost 80% in all the experiments except in Fig. 5.4b when 25% and 50% of peripheral insulin measurements removed randomly. Comparing to Fig. 4.3b in the IIVGIT test , the peripheral insulin concentration was not estimated precisely in the OGTT test since only the parameters of the incretins sub-model and the parameters of the glucose sub-model were estimated in order to reduce the computational complexity.

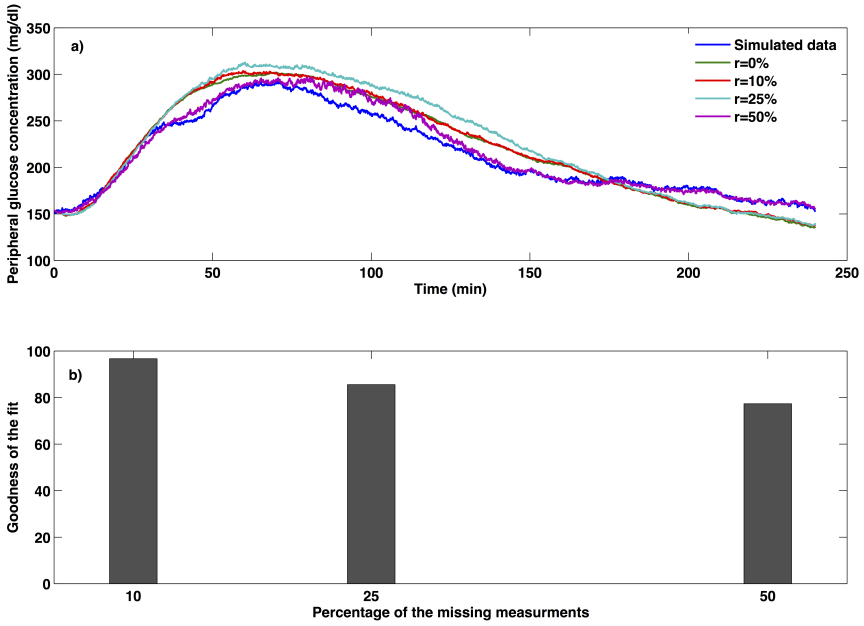

Figure 4.6: Peripheral glucose concentration for type II diabetic subjects during the OGTT test

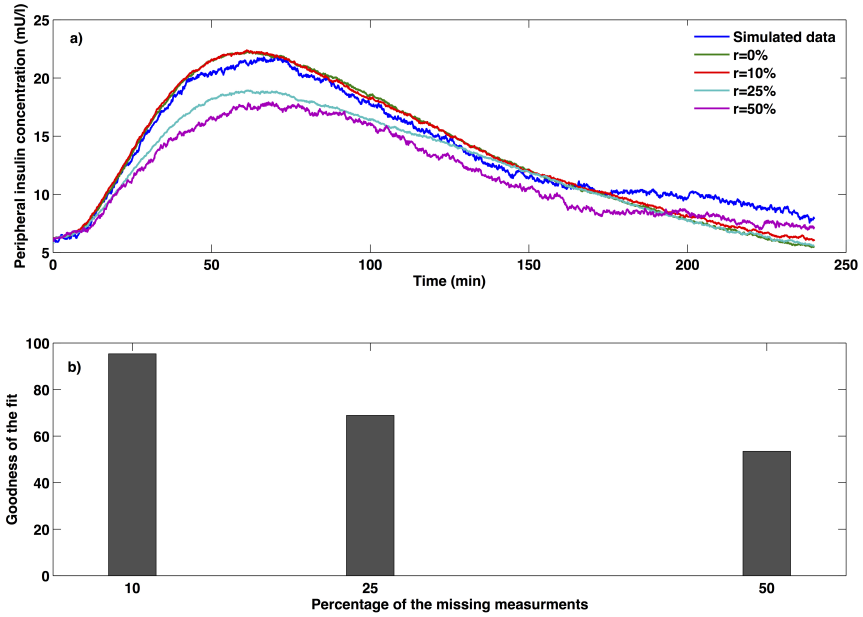

Figure 4.7: Peripheral insulin concentration for type II diabetic subjects during the OGTT test

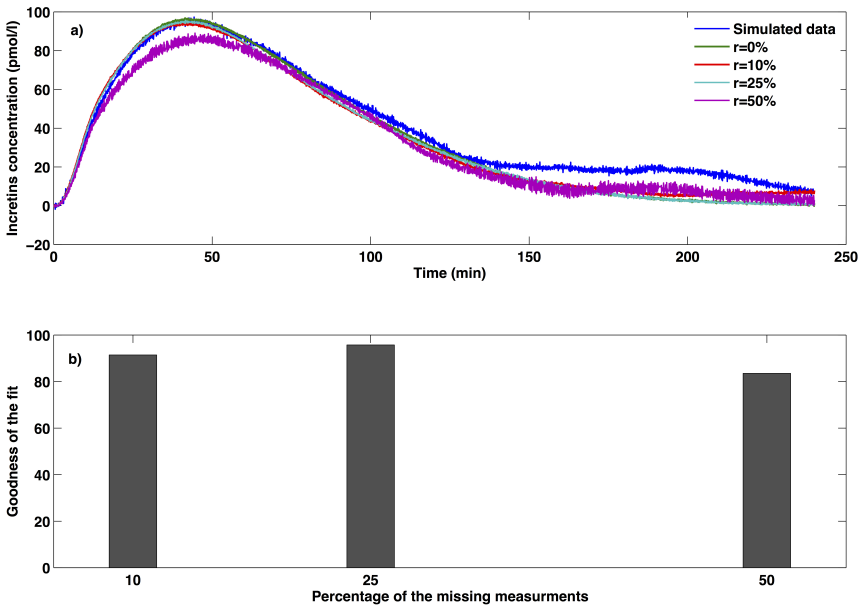

Figure 4.8: Incretins concentration for type II diabetic subjects during the OGTT test

The probability density function of the parameter C^I_{PGU}, one of the parameters of the peripheral glucose uptake rate in the insulin sub-model in [98], is reported in Fig. 5.5. As somewhat expected, the posterior provided by SIR filtering method is concentrated around its original value after about 620 sampling times.

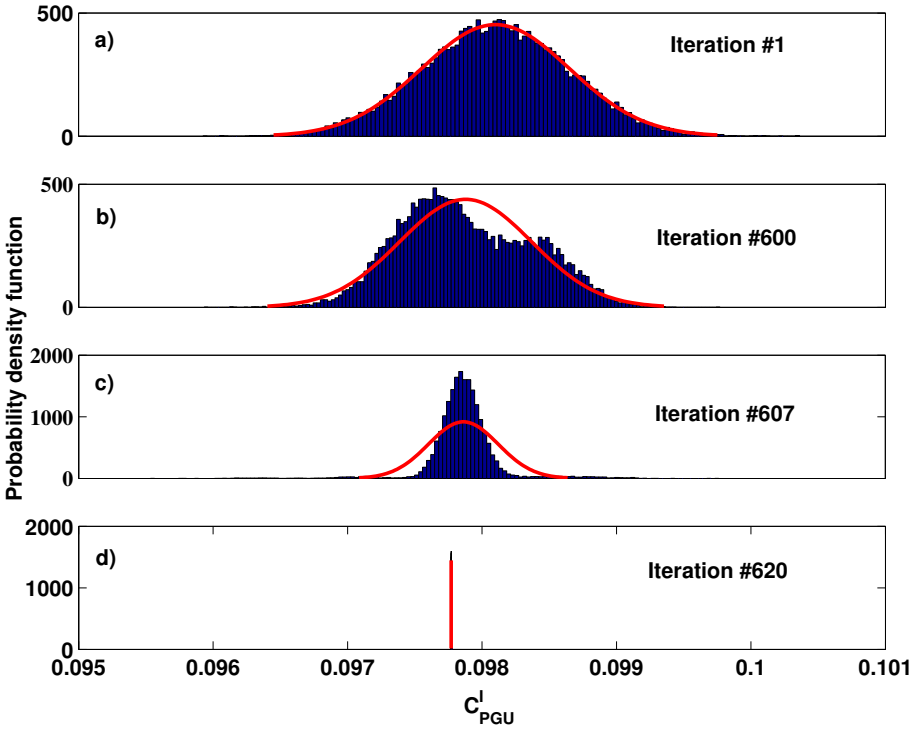

Figure 4.9: The probability density function of c^I_{PGU} from Bayesian identification at sampling time number 1, 600, 607 and 620 (area under each curve is unitary). The y-axis quantity is unit-less.

4.5.3 Application of SIR particle filtering in detection of organ dysfunction in diabetic patients under irregular clinical data

In this section, the application of the adaptive sequential-importance-resampling (SIR) filter in the estimation of the glucose, insulin, and incretins concentrations in different parts of the body under irregularly sampled clinical data is presented. These estimates are used for calculating the glucose metabolic rates in different organs of the type II diabetic patients using irregularly sampled data. Then, by comparing the glucose metabolic rate of each organ in the diabetic patients with the glucose metabolic rate of the same organ in a

normal subject, the abnormal functioning of certain organs is detected and identified.

Using the states and parameters of the Vahidi model estimated in the previous section, the glucose metabolic rates in the peripheral tissues and the liver are calculated from equations (2.9) and (2.10). Figure 5.6 shows the glucose metabolic rates in peripheral tissues and the liver compared with the healthy subjects. According to Figs. 5.6a and 5.6b, the peripheral glucose uptake rate and hepatic glucose uptake rate in type II diabetic patients for all experiments are less than the corresponding values in the healthy subjects due to insulin sensitivity in peripheral tissues and dysfunction in the liver of the diabetic patients. Decreased rate of glucose infusion shows that the overall insulin sensitivity of the body is decreased about 54% in diabetic patients. Even under the presence of 50% missing data, the abnormalities of the liver and adipose tissues are detectable, which provides more physiological information to physicians.

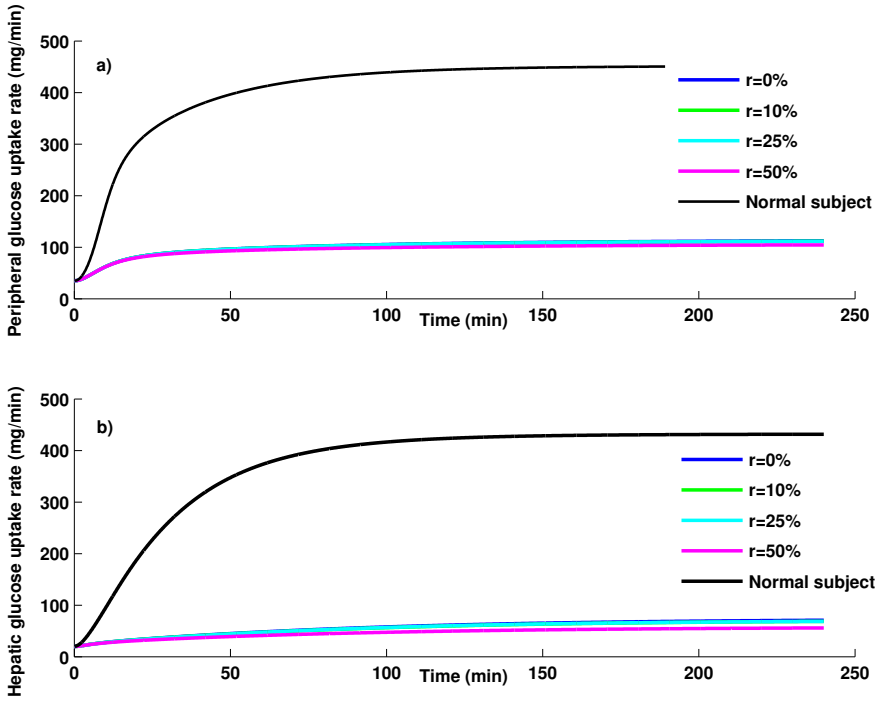

Figure 4.10: Variation of different glucose metabolic rates

4.5.4 strengths and limitations of the SIR particle filtering in clinical practice

The primary practical advantage of the SIR particle filtering method comparing to the traditional statistical methods is its independence from the degree of nonlinearity of the model unlike extended Kalman filtering [77]. An additional advantage in a clinical practice is that the SIR filtering approach is readily adaptable to sequential updating of information obtained from owner history, clinical examination of diabetic patients, and results of different diagnostic tests [99]. It exhibits good performance even for systems with large process or measurement noise.

Furthermore, the accuracy of the particle filtering method can be improved by increas-

ing the number of particles used in the estimation algorithm. However, particles size over 1000 can be computationally intensive and time consuming [88, 99]. The SIR based PF used in this study, needs less computational cost when a large number of unknown states and parameters must be estimated simultaneously since the marginal probability distribution of each parameter and state can be obtained from a posteriori probability distribution of the model parameters and states [92].

Chapter 5

Model-based detection of organ dysfunction and faults in insulin infusion devices for type II diabetic patients

5.1 Introduction

Diabetes is a disease characterized by abnormal glycemic values due to the inability of the pancreas to produce insulin (Type I diabetes) or to the inefficiency of insulin secretion and action (type II diabetes). Patients affected by diabetes need to monitor their glycemic level during all day and control it inside the normal range of 70-180 mg/dl as much as possible.

Glycemic level can be controlled by being in diet, doing exercise and taking oral medication. However, in patients with severe type II diabetes mellitus, insulin treatment is needed like type I diabetes. The insulin treatment can be either multiple daily injection regimens (MDIR) or a continuous subcutaneous insulin infusion (CSII) pump [59]. Recently, new technologies have been developed in order to improve and facilitate diabetes therapy such as [100]:

- sensors for continuous glucose monitoring (CGM), minimally invasive devices, which measure real-time glucose levels and returns the value in every 1 to 5 minutes for up to 7 days.

- pumps for continuous subcutaneous insulin infusion (CSII), which allow a more effective and physiological delivery of insulin. Moreover, the sensor-augmented pump, which are the simple combination of pumps in a single device, makes a further reduction of time spent in hypoglycemia and hyperglycemia.

The availability of CGM sensors and CSII pumps gave the idea of developing an artificial pancreas. These system is based on a closed-loop control algorithm in which CGM measures the glycemic value as a receiving input and the optimal insulin dosage as an output of the controller is infused by CSII pump to keep glycemia in the normal range [100].

The usage of CGM sensors and CSII pumps have made more progress, efficacy and safety in improving the quality of life of people with diabetes compared to the usual multiple daily injection therapy [59, 101]. In such a system, detection of possible failures in either the CGM sensor or CSII pump is crucial for safety.

During day-time while the patient is awake, failures are less critical since they can be fixed by patients. However, in the night-time while the patient is asleep, failures are more dangerous. The possible failures in insulin pump therapy are listed as follows [101]:

- Occlusions in the infusion set; An occlusion is any blockage that prevents the pump from delivering insulin properly. Occlusions may occur for any of the following reasons:

  - If pressure is being applied to the tubing or the infusion site
  - If the cannula has been bent during insertion
  - Kinked insulin pump tubing

  - Crystals forming in the insulin and causing blockages at the cannula

- Disconnection or leakage in the infusion set
- Presence of the bubbles in insulin pumps

If any of the aforementioned issues happen during the insulin pump therapy, the body will not get the intended full insulin dose, which can lead to higher than normal blood glucose level. In addition, even under safe insulin pump therapy, the control of the blood glucose level may fail due to the organ dysfunction progression. Multiple abnormalities in different body organs are listed as follows [77, 102]:

- Resistance of muscles and adipose tissues against the secreted insulin
- Impaired insulin-induced suppression of hepatic glucose production
- Abnormal hepatic glucose uptake rate
- Deficiency in pancreatic insulin production rate

The goal of using fault detection (FD) of glucose-insulin system is to detect the glucose control failure. FD technique has been used previously in many literatures to detect failures in insulin pump therapy for type I diabetes mellitus.

A multivariate statistical technique proposed by Finan *et al.* [103] detects insulin pump leakages and glucose sensor bias. Fecchinetti *et al.* [100] proposed a model-based approach using a Kalman estimator for detecting failures in both continuous subcutaneous insulin infusion (CSII) and continuous glucose monitoring (CGM) to improve safety during overnight glycemic control. Herrero *et al.* [101] proposed utilizing a validated robust model-based fault detection technique based on the interval analysis for detecting disconnections of the insulin infusion set.

All the aforementioned studies used the Bergman minimal model (MINMOD) including three nonlinear differential equations representing variations of plasma insulin and glucose concentrations for type I diabetic patients. However, in this study, we used the detailed nonlinear compartmental type II diabetes model developed by Vahidi *et al.* [51].

In the previous chapter, we estimated the states and the parameters of the Vahidi model using a sequential monte carlo (SMC) filtering method called particle filters. In this chapter, we propose for the first time to our knowledge, the application of the model-based FD algorithm based on a sequential monte carlo (SMC) method to detect either the faults in insulin pump therapy or the organ abnormalities in type II diabetic patients. In the next section, we present definitions of FD and a theoretical background.

5.1.1 Theoretical background on fault detection approaches

There is a large volume of literature on fault detection. In the last four decades, a variety of techniques to solve a number of process monitoring and fault detection problems have been developed. Many of these techniques are described in the survey papers by Basseville [104], Frank [105], Isermann[106], and Willsky [107] and in the books by Willsky [108], Basseville and Nikiforov[109], Pouliezos and Stavrakakis [110] and the references therein. The primary objectives of all FD methods are to detect any deviation from the normal behaviour of the process by providing an alarm tool [111].

There are two approaches for detection of failures [96]:

- Model-based approaches, which are based on a physical model of the process.
- History-based approaches, which rely on large historical data sets.

A model-based approaches often tend to be more powerful and provide a better performance if the process is well modelled [112]. The model-based approaches typically are consist of two procedures [97, 113, 114]:

1. extracting fault symptoms from the process, and residual evaluation

2. decision making based on the residual evaluation

Residual generation in model based approaches is the most important step, which is non-trivial in processes with unmeasured state variables [97, 113, 114]. A schematic representation of model-based fault diagnosis is shown in Figure. 5.1.

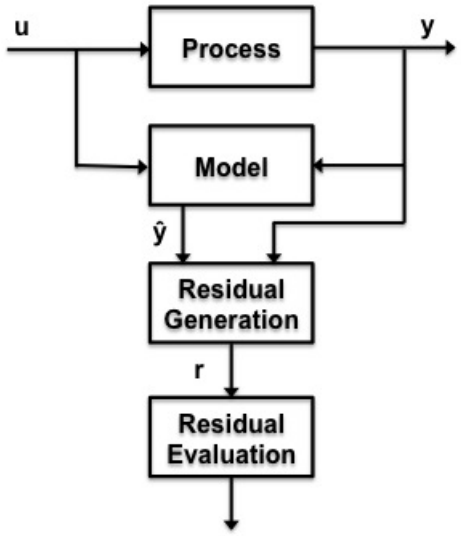

Figure 5.1: Model-based fault diagnosis Scheme [97, 113, 114]

If the models is deterministic, the residuals are often generated using an observer. Otherwise, for stochastic models, a filter has been used. Typically, for residuals generation, the model-based methods rely on the model being linear and noise being Gaussian [95].

The model-based methods have been extended to nonlinear systems in the literature. However, these extensions are based on suboptimal state estimators such as extended Kalman filters (EKF), and unscented Kalman filters (UKF). In these suboptimal filters, the nonlinear system has been approximated through linearization and/or the noise has been assumed Gaussian. The approximations are often not satisfactory and lead to a high

rate of false alarms.

In the light of aforementioned above, we use the model-based FD algorithm based on a sequential monte carlo (SMC) method called particle filter to detect either the faults in insulin pump therapy or the organ abnormalities in type II diabetic patients. The proposed approach does not require linearization of the Vahidi model or Gaussianity of the measurement noises [96].

Since the SMC methods are computationally intensive, their implementation needs the high performance computers. There is some existing literature on the use of SMC for fault detection [96, 115–117]. In these studies, the SMC algorithms proposed are based on the log-likelihood test of observed data under a null and an alternate hypothesis. In these approaches the likelihood function is estimated under both hypotheses and the likelihood function is driven through an approximation that is not applicable to all types of nonlinearities.

In this study, we propose the application of the model-based FD algorithm based on a sequential monte carlo (SMC) method to detect either the faults in insulin pump therapy or the organ abnormalities in type II diabetic patients.

This chapter is organized as follows. In the following section, the model-based fault detection based on the SMC filtering method is discussed. In section 5.3, the proposed technique for detecting disconnection in insulin infusion systems and detecting organs deficiency are explained.

5.2 Problem statement

In order to use the model-based fault detection technique, the discrete format of the Vahidi model described in section 4.2 in equation 4.3 has been used. The measurement and state noises presented in equations (4.3a) and (4.3b) are assumed to enter the process in a

linear fashion in linear processes and, to some extent, in nonlinear processes. Therefore, based on this fundamental assumption, faults can be detected simply by generating and monitoring the prediction errors (or residuals) between the process measurements and model predictions. The one step-ahead predictions from equation (4.3b) can be written as:

$$\hat{y}_t = g(x_{t|t-1}, u_t, \theta) \tag{5.1}$$

where $x_{t|t-1}$ is the one step-ahead prediction of the state, $\hat{y}_t$ is the one-step ahead prediction of the output. Then the prediction error or the residual can be simply written as:

$$\hat{r_t} = y_t - \hat{y}_t \tag{5.2}$$

When there are no changes in the glucose-insulin system, the density function of the residuals, $\hat{r}_t$, must closely follow the measurement noise, w_t. Any deviation of the residuals from this density function implies a fault in the glucose-insulin system.

Measurements of glucose and insulin concentrations in different parts of the body require complex clinical facilities and in some cases may risk the life of the patient. Therefore, clinical measurements of all required concentrations are not possible. The commonly available clinical data include peripheral insulin and glucose concentrations only. Therefore, a straightforward residual analysis, as presented in equations (5.1) and (5.2) is difficult. To overcome this problem, we use a sequential monte carlo (SMC) filtering method called particle filters on a nonlinear model of a group of diabetic patients to estimate the glucose and insulin concentrations in different parts of the body. SMC filtering method previously described in details in section 4.3.3.

5.3 Fault detection of glucose-insulin system

In this section, the efficiency of the sequential monte carlo (SMC) filtering method for failure detection in a glucose-insulin system is demonstrated. To build a model-based fault detection system, we need to have reliable type II diabetes model. In the previous chapter, we used the data provided by Knop *et al.* [73, 74] to estimate the parameters of the Vahidi model. In this chapter, we use the same parameters to simulate the body of the type II diabetic patient, which is under closed-loop insulin pump therapy. The closed-loop simulation assumes that the patient's initial blood glucose is at 115.63 mg/dl. The meal disturbance of 75 gr glucose was introduced at time 500 min. A PI controller with tuning parameters $K_C = 0.22$ and $K_I = 0.44$ is simulated to control the patient's blood glucose level at 90 mg/dl. Fig. 5.2 presents the responses of the PI controller. At time 500 min glucose level increases due to 75 gr meal disturbance. However, the PI controller is able to control the blood glucose level at 90 mg/dl.

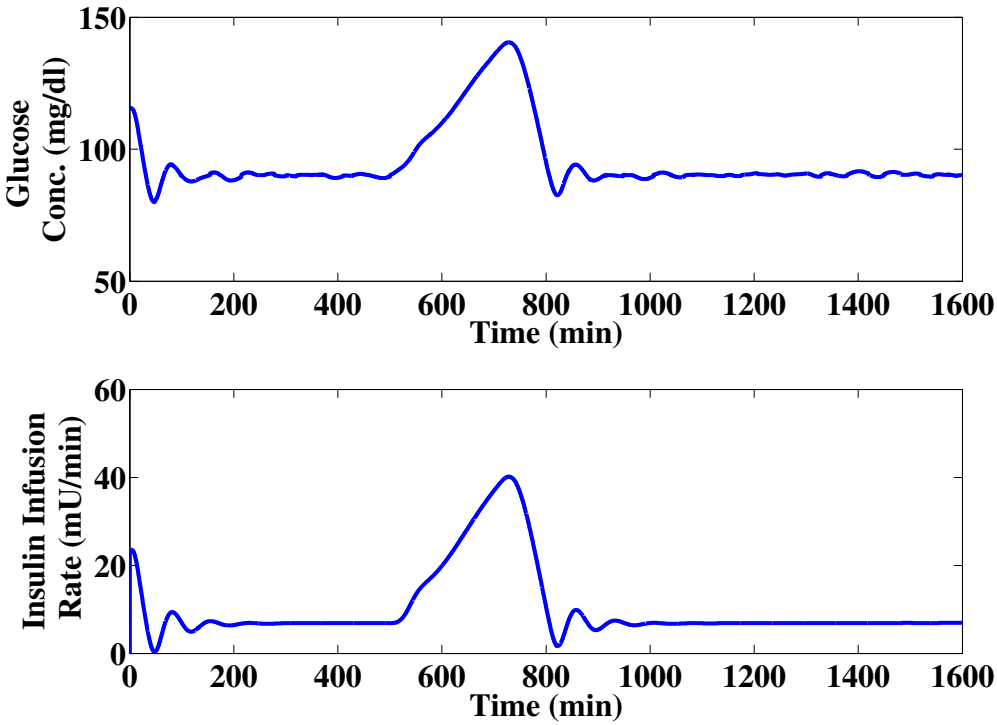

Figure 5.2: Response of the PI controller with a 75 gr meal disturbance at time = 500 min.

In the following sections, four different fault cases are simulated and the SMC filtering method is used to detect the faults. For implementing the SMC filtering, based on the discrepancies between the Vahidi model and the Knop's experimental data, the following parameters were selected:

- The number of particles $N = 25$
- The sampling time used for discretizing the Vahidi model $\Delta t = 0.2\ min$
- The maximum states noises $v_t \sim \mathcal{N}(0, 0.001)$
- The measurement noise $w_t \sim \mathcal{N}(0, 0.001)$

All the simulations were conducted on a 2.90 GHz CPU with 8 GB RAM Mac using MATLAB 2012b.

5.3.1 Detection of insulin pump disconnection (Case 1)

In case 1, we assume that the insulin pump is disconnected 800 *min* after the diabetic patient consumes the 75 *gr* meal at 500 *min*. Figure. 5.3a shows the response of the PI controller when there is no fault and one when the insulin pump is disconnected at time 1300 *min*.

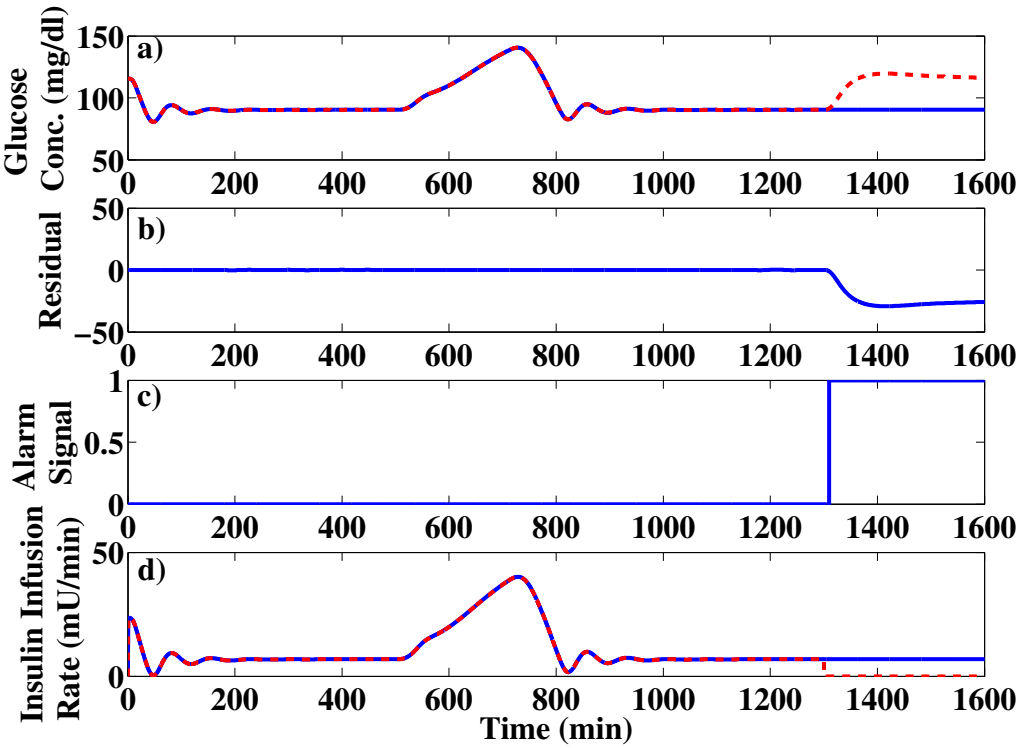

Figure 5.3: Detection of insulin pump disconnection. The blue solid line curve represents no fault and red dashed curve represents fault in Case 1

The residual or prediction error between the measured and the predicted blood glucose

level is shown in Fig. 5.3b. The residual closely follows the measurement noise, w_t before insulin pump gets disconnected. However, it deviates from this density function after time 1300 min.

Figure. 5.3c shows the alarm signal, which stays at zero while the prediction error between predicted and measured blood glucose level is less than 10 mg/dl. Otherwise, it stays at one. Figure. 5.3d shows that the insulin pump is disconnected at time 1300 min and the insulin infusion rate is zero after time 1300 min.

5.3.2 Detection of kinked insulin pump tubing (Case 2)

In case 2, we assume that the insulin pump is kinked 800 min after the diabetic patient consumes the 75 gr meal at 500 min. Figure. 5.4a shows the response of the PI controller when there is no fault and one when the insulin pump is kinked after time 1300 min. To simulate the kinked insulin pump tubing, we assume that the PI controller output (insulin infusion rate) is fluctuated between 0 to 6 mU/min after 1300 min.

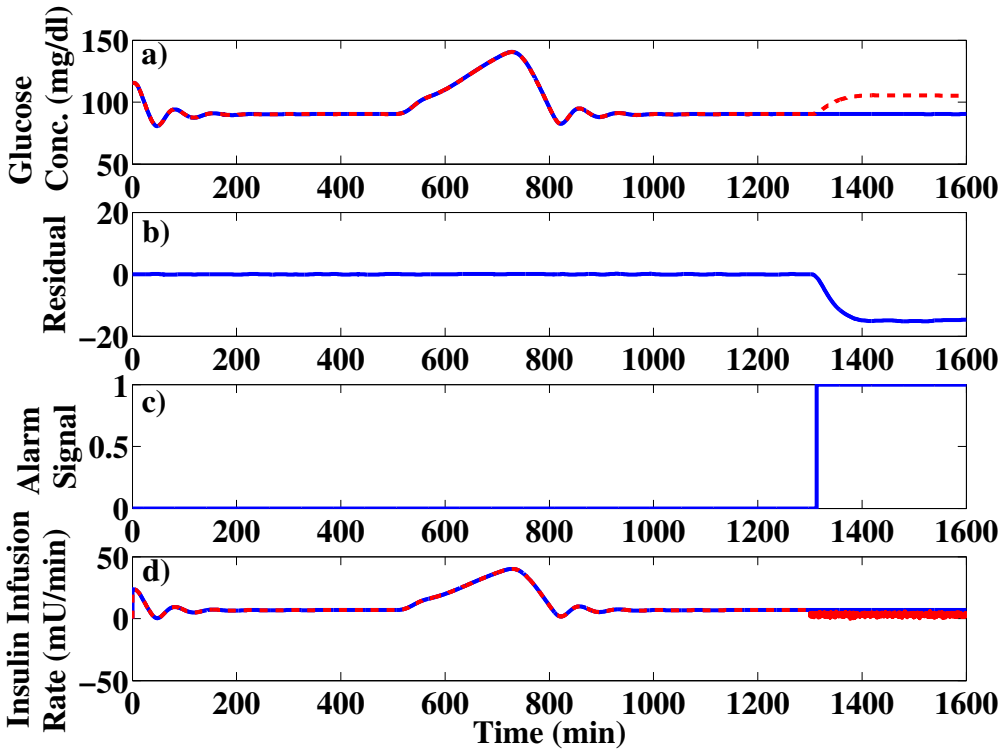

Figure 5.4: Detection of kinked insulin pump tubing. The blue solid line curve represents no fault and red dashed curve represents fault in Case 2

The residual or prediction error between the measured and the predicted blood glucose level is shown in Fig. 5.4b. The residual closely follows the measurement noise, w_t before insulin pump gets kinked. However, it deviates from this density function after time 1300 min.

Figure. 5.4c shows the alarm signal, which stays at zero while the prediction error between predicted and measured blood glucose level is less than 10 mg/dl. Otherwise, it stays at one. Figure. 5.4d shows that the insulin pump is kinked at time 1300 min and the insulin infusion rate is fluctuated.

5.3.3 Detection of organ dysfunction

The glucose metabolic rates in the liver, muscles and adipose tissues represent the behaviour of those organs. From section 2.1, these rates are calculated by measuring the glucose and insulin concentrations in different parts of the body using complex clinical facilities. However, only peripheral insulin and glucose concentrations are available in common clinical data.

In the following sections the glucose concentration in peripheral tissues and the liver are estimated using the SMC filtering method. Then, using the estimated glucose concentrations in peripheral tissue and liver, peripheral glucose uptake rate and hepatic glucose uptake rate are calculated. Decrease in the glucose uptake rate and hepatic uptake rate will provide insight into the insulin resistance of peripheral tissues and liver.

Detection of peripheral insulin resistance (Case 3)

In case 3, we assume that the peripheral glucose uptake rate, r_{PGU}, is decreased by 80% from the previous rate in the simulated patient under insulin pump therapy. The meal disturbance of 75 gr glucose was introduced at time 500 min. Figure. 5.5a shows the response of the PI controller when the insulin sensitivity of the peripheral tissues is decreased by 80%.

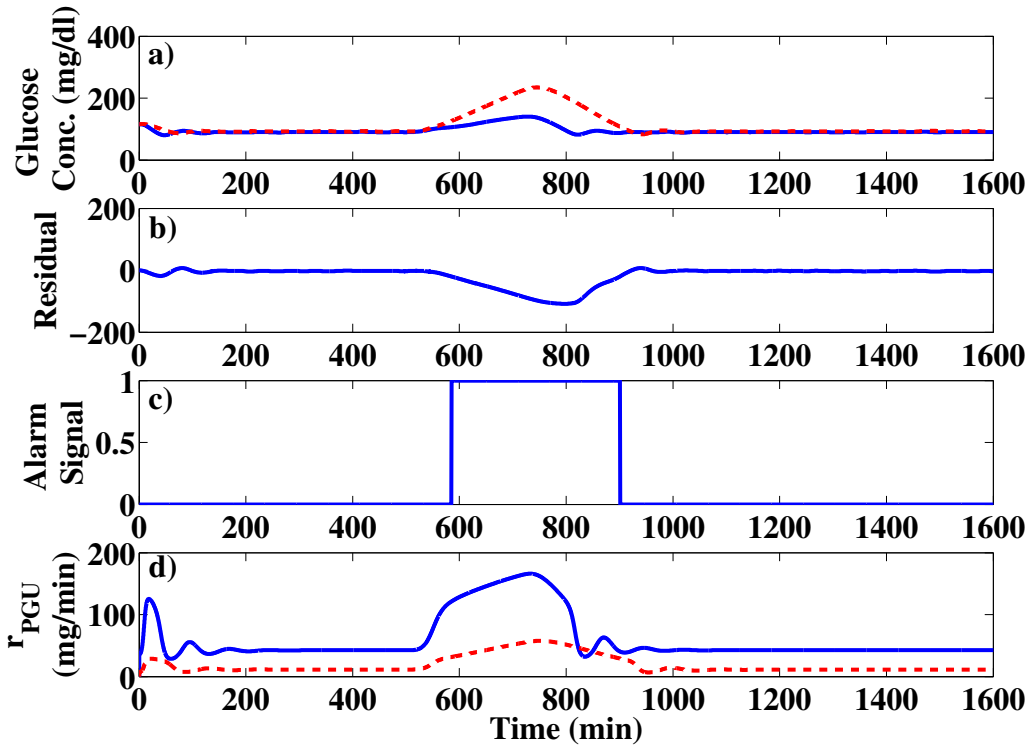

Figure 5.5: Detection of peripheral insulin resistance. The blue solid line curve represents no fault and red dashed curve represents fault in Case 3

The residual or prediction error between the measured and the predicted blood glucose level is shown in Fig. 5.5b. The residual deviates significantly during the meal ingestion. Figure. 5.5c shows the alarm signal, which stays at zero while the prediction error between predicted and measured blood glucose level is less than 10 mg/dl. Otherwise, it stays at one.

In Fig. 5.5d, the profile of the peripheral glucose uptake rate is shown. The increase in blood glucose level during the meal ingestion at time 500 min is due to %80 increase in insulin resistance of the peripheral tissues.

Detection of hepatic insulin resistance (Case 4)

In case 4, we assume that the hepatic glucose uptake rate, r_{HGU}, is decreased by 80% from the previous rate. The meal disturbance of 75 gr glucose was consumed at time 500 min. Figure. 5.6a shows the response of the PI controller when there is no hepatic insulin resistance and one when the hepatic insulin resistance decreased by 80%.

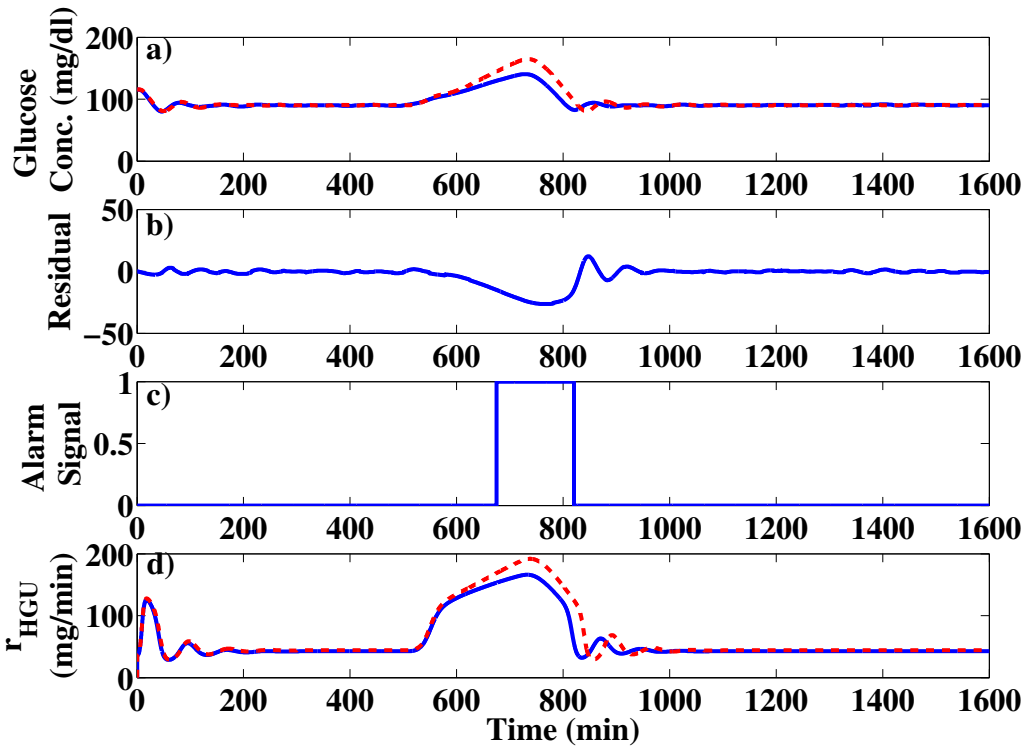

Figure 5.6: Detection of hepatic insulin resistance. The blue solid line curve represents no fault and red dashed curve represents fault in Case 4

The residual or prediction error between the measured and the predicted blood glucose level is shown in Fig. 5.6b. The residual deviates significantly during the meal ingestion. Figure. 5.6c shows the alarm signal, which stays at zero while the prediction error between predicted and measured blood glucose level is less than 10 mg/dl. Otherwise, it stays at

one.

In Fig. 5.6d, the profile of the hepatic glucose uptake rate is shown. The increase in blood glucose level during the meal ingestion at time 500 *min* is due to %80 increase in hepatic insulin resistance.

Chapter 6

Conclusions and recommendations

6.1 Summary

This thesis focuses on assessment of type II diabetes mellitus using compartmental mathematical modelling. The outcomes of this research are summarized in the following sections.

6.1.1 A simple self-administered method for assessing insulin sensitivity in type II diabetic patients

Chapter 3 presented a simple self-administered method for assessing insulin sensitivity in type II diabetic patients. In this chapter, the feasibility of using the mathematical compartment model proposed by Vahidi et al. [7, 51] to estimate insulin sensitivity has been evaluated. Fifteen sets of OGTT data from diabetic patients published in the literature have been used to estimate the Vahidi model parameters. From the estimated model parameters, a simple method for conveniently estimating insulin sensitivity by patients themselves has been developed and evaluated. It is shown that the proposed method yields an ISI measure, which is strongly correlated with the M-value obtained from the euglycemic clamp test (r =0.927, p= 0.0045).

6.1.2 Assessment of type II diabetes mellitus using irregularly sampled measurements with missing data

In chapter 4, we have identified the nonlinear states and the parameters of glucose, insulin and incretins sub-model developed by Vahidi et.al [7] for type II diabetes mellitus in the presence of 10%, 25% and 50% of randomly missing clinical observations by employing the Sequential Importance Resampling (SIR) filtering method. The motivation for this study originates from the lack of complete knowledge about the health status of the diabetic patients. In addition, only a few blood glucose measurements per day are available in a non-clinical setting due to different reasons like unreadable hand writing, inability to record clinical results, and infrequent sampling by patients.

It is shown that by implementing an on-line SIR particle filtering method to the Vahidi model developed for type II diabetes mellitus, we are able to estimate the dynamics of the plasma glucose, insulin and incretins concentration under the presence of maximum 50% available clinical data. In addition, the goodness of fit between the simulated peripheral glucose, insulin and incretins concentration and their available measurements were almost 80% in the most of the experiments. The results of this study can be used to inform type II diabetic patients of their medical conditions, enable physicians to review past therapy, estimate future blood glucose levels, provide therapeutic recommendations and even design a stabilizing control system for blood glucose regulation.

6.1.3 Model-based detection of organ dysfunction and faults in insulin infusion devices for type 2 diabetic patients

In chapter 5, we have used the type II diabetes model developed by Vahidi et.al [51]. We employed model-based fault detection technique based on a Sequential Monte Carlo (SMC) filtering method for detecting faults in insulin infusion system and detecting organ

dysfunction. The proposed approach has been demonstrated (in silico) to be an effective tool for detecting disconnection faults in insulin infusion systems and detecting organ deficiencies. In the future work, we intend to extend this work to develop an algorithm capable of detecting and isolating faults simultaneously in a glucose-insulin system.

6.2 Recommendations for future work

Various medications are available for type II diabetic subjects such as insulin, sulfonylureas, meglitinides, biguanides and thiazolidinediones that decrease the blood glucose level in type II diabetic patients. Specific type of medication is prescribed to the diabetic patients based on the type and severity of abnormalities. Therefore, the information obtained from the developed type II diabetes model would be helpful in prescribing a suitable medication for the diabetic patients. In addition, the chance of prescribing an efficient medication for the patients in a safe and cost effective way has been increased.

In the light of aforementioned above, the research area, which can be taken into more consideration is the study of development of pharmacokinetic-pharmacodynamic (PK-PD) models for different medicines. The term "pharmacokinetics" refers to a branch of pharmacology studying the fate of an external substance administered to a live organism. The term "pharmacodynamic" refers to another branch of pharmacology examining the biochemical and physiological effects of a medicine on a live organism. The PK-PD models study the effect of different medicines on the patients safely without any administration that may be harmful for the patients.

A pharmacokinetic model can be attached to the type II diabetes model representing how the medication is distributed into the body organs and consumed by them. For the pharmacodynamic part, structural modification should be attached into the type II diabetes model to represent the effects of the medication on body organs. I have contributed in

developing a pharmacokinetic pharmacodynamic model for metformin and four types of insulin (regular, NPH, lente and ultralente) whose preliminary results have been published in [76]. Similarly, PK-PD models for other medications can be developed for studying the effects of them on lowering the blood sugar level.

Bibliography

[1] Melissa Barazandegan, Fatemeh Ekram, Ezra Kwok, and Bhushan Gopaluni. Simple Self-Administered Method for Assessing Insulin Sensitivity in Diabetic Patients. *J. Med. Biol. Eng.*, 36(2):197–205, apr 2016.

[2] Melissa Barazandegan, Fatemeh Ekram, Ezra Kwok, Bhushan Gopaluni, and Aditya Tulsyan. Assessment of type II diabetes mellitus using irregularly sampled measurements with missing data. *Bioprocess Biosyst. Eng.*, 38(4):615–629, oct 2015.

[8] Dan Niculescu. *Williams Textbook of Endocrinology*, volume 4. Elsevier Inc., 2008.

[53] J T Sorensen. *A physiologic model of glucose metabolism in man and its use to design and assess improved insulin therapies for diabetes.* PhD thesis, Massachusetts Institute of Technology, 1985.

[7] Omid Vahidi. *Dynamic Modeling of Glucose Metabolism for the Assessment of Type II Diabetes Mellitus.* Phd thesis, The University of British columbia, 2013.

[51] O. Vahidi, K.E. Kwok, R.B. Gopaluni, and L. Sun. Developing a physiological model for type II diabetes mellitus. *Biochem. Eng. J.*, 55(1):7–16, jun 2011.

[97] F. Alrowaie, K.E. Kwok, and R.B. Gopaluni. An algorithm for fault detection in stochastic non-linear state-space models using particle filters. *2011 Int. Symp. Adv. Control Ind. Process.*, (1):60–65, 2011.

[113] F. Alrowaie, R.B. Gopaluni, and K.E. Kwok. Fault detection and isolation in stochastic non-linear state-space models using particle filters. *Control Eng. Pract.*, 20(10): 1016–1032, oct 2012.

[114] Feras A Alrowie. *Fault Isolation and Alarm Design in Non-linear Stochastic Systems*. Phd thesis, The University of British Columbia, 2015.

[3] Canadian Diabetes Association. Diabetes facts. 2009.

[4] LC Groop, E Widen, and E Ferrannini. Insulin resistance and insulin deficiency in the pathogenesis of Type 2 (non-insulin-dependent) diabetes mellitus: errors of metabolism or of methods. *Diabetologia*, 1:1326–1331, 1993.

[5] A Basu, R Basu, P Shah, A Vella, C M Johnson, K S Nair, M D Jensen, W F Schwenk, and R a Rizza. Effects of type 2 diabetes on the ability of insulin and glucose to regulate splanchnic and muscle glucose metabolism: evidence for a defect in hepatic glucokinase activity. *Diabetes*, 49(2):272–83, feb 2000.

[6] International Diabetes Federation. United for Diabetes Campaign: Key Messages. Technical report, International Diabetes Federation, Brussels, Belgium, 2007.

[9] Ralph a DeFronzo. Pathogenesis of type 2 diabetes mellitus. *Med. Clin. North Am.*, 88(4):787–835, ix, 2004.

[10] Philip E. Cryer. Hypoglycemia in type 1 diabetes mellitus, 2010.

[11] R a DeFronzo. The triumvirate: beta-cell, muscle, liver. A collusion responsible for NIDDM. *Diabetes*, 37(6):667–687, jun 1988.

[12] P Iozzo, F Geisler, V Oikonen, M Maki, T Takala, O Solin, E Ferrannini, J Knuuti,

and P Nuutila. Insulin stimulates liver glucose uptake in humans: An F-18-FDG PET study. *J. Nucl. Med.*, 44(5):682–689, 2003.

[13] E Ferrannini, D C Simonson, L D Katz, G Reichard, S Bevilacqua, E J Barrett, M Olsson, and R a DeFronzo. The disposal of an oral glucose load in patients with non-insulin-dependent diabetes. *Metabolism.*, 37(1):79–85, 1988.

[14] Peter J Campbell, J Mandarino, and John E Gerich. with NIDDM and 14 nondiabetic normal volunteers with no family history of diabetes mellitus. Their clinical and metabolic features. 37(1):15–21, 1988.

[15] Ralph A. DeFronzo, Eleuterio Ferrannini, and Donald C. Simonson. Fasting hyperglycemia in non-insulin-dependent diabetes mellitus: Contributions of excessive hepatic glucose production and impaired tissue glucose uptake. *Metabolism*, 38(4): 387–395, 1989.

[16] R Basu, W F Schwenk, and R A Rizza. Both fasting glucose production and disappearance are abnormal in people with "mild" and "severe" type 2 diabetes. *Am. J. Physiol.*, 287(1):E55–E62, 2004.

[17] Rita Basu, Visvanathan Chandramouli, Betty Dicke, Bernard Landau, and Robert Rizza. Obesity and type 2 diabetes impair insulin-induced suppression of glycogenolysis as well as gluconeogenesis. *Diabetes*, 54(7):1942–1948, 2005.

[18] M a Pfeifer, J B Halter, and D Porte. Insulin secretion in diabetes mellitus. *Am. J. Med.*, 70(3):579–588, 1981.

[19] K S Polonsky, B D Given, L J Hirsch, H Tillil, E T Shapiro, C Beebe, B H Frank, J A Galloway, and E Van Cauter. Abnormal patterns of insulin secretion in non-insulin-dependent diabetes mellitus. *N. Engl. J. Med.*, 318(19):1231–1239, 1988.

[20] P-J Guillausseau, T Meas, M Virally, M Laloi-Michelin, V Médeau, and J-P Kevorkian. Abnormalities in insulin secretion in type 2 diabetes mellitus. *Diabetes Metab.*, 34(2):43–48, 2008.

[21] A. A. Alzaid, S. F. Dinneen, D. J. Turk, A. Caumo, C. Cobelli, and R. A. Rizza. Assessment of insulin action and glucose effectiveness in diabetic and nondiabetic humans. *J. Clin. Invest.*, 94(6):2341–2348, 1994.

[22] S. Del Prato, M. Matsuda, D. C. Simonson, L. C. Groop, P. Sheehan, F. Leonetti, R. C. Bonadonna, and R. A. DeFronzo. Studies on the mass action effect of glucose in NIDDM and IDDM: Evidence for glucose resistance. *Diabetologia*, 40(6):687–697, 1997.

[23] Michael F. Nielsen, Rita Basu, Steven Wise, Andrea Caumo, Claudio Cobelli, and Robert A. Rizza. Normal glucose-induced suppression of glucose production but impaired stimulation of glucose disposal in type 2 diabetes: Evidence for a concentration-dependent defect in uptake. *Diabetes*, 47(11):1735–1747, 1998.

[24] RA DeFronzo. Glucose clamp technique : a method for quantifying insulin secretion and resistance. *Am. J. Physiol. - Endocrinol. Metab.*, 237:214–223, 1979.

[25] Arie Katz, SS Nambi, and Kieren Mather. Quantitative insulin sensitivity check index: a simple, accurate method for assessing insulin sensitivity in humans. *J. Clin. Endocrinol. Metab.*, 85(7):2402–2410, 2000.

[26] S. W. Shen, G. M. Reaven, and J. W. Farquhar. Comparison of impedance to insulin-mediated glucose uptake in normal subjects and in subjects with latent diabetes. *J. Clin. Invest.*, 49(12):2151–2160, 1970.

[27] Y. Harano, H. Hidaka, K. Takatsuki, S. Ohgaku, M. Haneda, S. Motoi, K. Kawagoe, Y. Shigeta, and H. Abe. Glucose, insulin, and somatostatin infusion for the determination of insulin sensitivity in vivo. *Metabolism*, 27(9):1449–1452, sep 1978.

[28] D. Pei, C. N. O. Jones, R. Bhargava, Y. D. I. Chen, and G. M. Reaven. Evaluation of octreotide to assess insulin-mediated glucose disposal by the insulin suppression test. *Diabetologia*, 37(8):843–845, aug 1994.

[29] Bergman. Quantitative estimation of insulin sensitivity. *Am. Phisiological Soc.*, 236 (6):E667–E677, 1979.

[30] J. C. Beard, R. N. Bergman, W. K. Ward, and D. Porte. The insulin sensitivity index in nondiabetic man: Correlation between clamp-derived and IVGTT-derived values. *Diabetes*, 35(3):362–369, 1986.

[31] R N Bergman, R Prager, a Volund, and J M Olefsky. Equivalence of the insulin sensitivity index in man derived by the minimal model method and the euglycemic glucose clamp. *J. Clin. Invest.*, 79(3):790–800, mar 1987.

[32] Y J Yang, J H Youn, and R N Bergman. Modified protocols improve insulin sensitivity estimation using the minimal model. *Am. J. Physiol.*, 253(6 Pt 1):E595–602, dec 1987.

[33] DIANE T. FINEGOOD, IRENE M. HRAMIAK, and JOHN DUPRE. A Modified Protocol for Estimation of Insulin Sensitivity with the Minimal Model of Glucose Kinetics in Patients with Insulin-Dependent Diabetes*. *J. Clin. Endocrinol. Metab.*, 70(6):1538–1549, jun 1990.

[34] M J Quon, C Cochran, S I Taylor, and R C Eastman. Direct comparison of standard

and insulin modified protocols for minimal model estimation of insulin sensitivity in normal subjects. *Diabetes Res*, 25(4):139–149, 1994.

[35] Mohammed F. Saad, Garry M. Steil, Wagdy W. Kades, Maged F. Ayad, Wagih A. Elsewafy, Rima Boyadjian, Sujata D. Jinagouda, and Richard N. Bergman. Differences between the tolbutamide-boosted and the insulin-modified minimal model protocols. *Diabetes*, 46(7):1167–1171, 1997.

[36] R N Bergman, L S Phillips, and C Cobelli. Physiologic evaluation of factors controlling glucose tolerance in man: measurement of insulin sensitivity and beta-cell glucose sensitivity from the response to intravenous glucose. *J. Clin. Invest.*, 68(6): 1456–1467, 1981.

[37] DR Matthews, JP Hosker, AS Rudenski, BA Naylor, DF Treacher, and RC Turner. Homeostasis model assessment: insulin resistance and beta-cell function from fasting plasma glucose and insulin concentrations in man. *Diabetologia*, 28:412–419, 1985.

[38] JC Levy, DR Matthews, and MP Hermans. Correct Homeostasis Model Assessment (HOMA) Evaluation Uses the Computer Program. *Diabetes Care*, 21(12):2191–2192, 1998.

[39] Tara M. Wallace, Jonathan C. Levy, and David R. Matthews. Use and abuse of HOMA modeling, 2004.

[40] Kieren J. Mather, A. Evay Hunt, Helmut O. Steinberg, Giancarlo Paradisi, Ginger Hook, Arie Katz, Michael J. Quon, and Alain D. Baron. Repeatability characteristics of simple indices of insulin resistance: Implications for research applications. *J. Clin. Endocrinol. Metab.*, 86(11):5457–5464, 2001.

[41] Hui Chen, Gail Sullivan, Lilly Q Yue, Arie Katz, and Micheal J Quon. QUICKI is a useful index of insulin sensitivity in subjects with hypertension. *Am. J. Physiol. Endocrinol. Metab.*, 284(4):E804–E812, 2003.

[42] AJG Hanley, Ken Williams, and Clicerio Gonzalez. Prediction of Type 2 Diabetes Using Simple Measures of Insulin Resistance Combined Results From the San Antonio Heart Study, the Mexico City Diabetes Study, and the Insulin Resistance Atherosclerosis Study. *Diabetes*, 52:463–469, 2003.

[43] H. Chen, G. Sullivan, and M. J. Quon. Assessing the Predictive Accuracy of QUICKI as a Surrogate Index for Insulin Sensitivity Using a Calibration Model. *Diabetes*, 54 (7):1914–1925, jul 2005.

[44] M Matsuda and RA DeFronzo. Insulin Sensitivity Indices Obtained From Oral Glucose Tolerance Testing Comparison with the euglycemic insulin clamp. *Diabetes Care*, 22(9):1462–1470, 1999.

[45] M Stumvoll, a Mitrakou, W Pimenta, T Jenssen, H Yki-Järvinen, T Van Haeften, W Renn, and J Gerich. Use of the oral glucose tolerance test to assess insulin release and insulin sensitivity. *Diabetes Care*, 23(3):295–301, mar 2000.

[46] a Avignon, C Boegner, D Mariano-Goulart, C Colette, and L Monnier. Assessment of insulin sensitivity from plasma insulin and glucose in the fasting or post oral glucose-load state. *Int. J. Obes. Relat. Metab. Disord.*, 23(5):512–7, 1999.

[47] a Mari, G Pacini, E Murphy, B Ludvik, and J J Nolan. A model-based method for assessing insulin sensitivity from the oral glucose tolerance test. *Diabetes Care*, 24 (3):539–548, 2001.

[48] M Gutt, C L Davis, S B Spitzer, M M Llabre, M Kumar, E M Czarnecki, N Schneiderman, J S Skyler, and J B Marks. Validation of the insulin sensitivity index (ISI(0,120)): comparison with other measures. *Diabetes Res. Clin. Pract.*, 47(3): 177–84, mar 2000.

[49] F Belfiore, S Iannello, and G Volpicelli. Insulin sensitivity indices calculated from basal and OGTT-induced insulin, glucose, and FFA levels. *Mol. Genet. Metab.*, 63 (2):134–41, 1998.

[50] Fatemeh Ekram. *Blood Glucose Regulation in Type II Diabetic Patients*. Phd thesis, The University of British Columbia, 2016.

[52] J R Guyton, R O Foster, J S Soeldner, M H Tan, C B Kahn, L Koncz, and R E Gleason. A model of glucose-insulin homeostasis in man that incorporates the heterogeneous fast pool theory of pancreatic insulin release. *Diabetes*, 27(10):1027–1042, 1978.

[54] Victor W Bolie. Coefficients of normal blood glucose regulation. *J. Appl. Physiol.*, 16(5):783–788, 1961.

[55] E Ackerman and LC Gatewood. Model studies of blood-glucose regulation. *Bull. . . .*, 27:21–37, 1965.

[56] C Cobelli and A Mari. Validation of mathematical models of complex endocrine-metabolic systems. A case study on a model of glucose regulation. *Med. Biol. Eng. Comput.*, 21(4):390–9, jul 1983.

[57] Roman Hovorka, Valentina Canonico, Ludovic J Chassin, Ulrich Haueter, Massimo Massi-Benedetti, Marco Orsini Federici, Thomas R Pieber, Helga C Schaller, Lukas Schaupp, Thomas Vering, and Malgorzata E Wilinska. Nonlinear model predictive

control of glucose concentration in subjects with type 1 diabetes. *Physiol. Meas.*, 25 (4):905–920, 2004.

[58] Chiara Dalla Man, Michael Camilleri, and Claudio Cobelli. A system model of oral glucose absorption: validation on gold standard data. *IEEE Trans. Biomed. Eng.*, 53(12 Pt 1):2472–2478, 2006.

[59] F. Ekram, L. Sun, O. Vahidi, E. Kwok, and R. B. Gopaluni. A feedback glucose control strategy for type II diabetes mellitus based on fuzzy logic. *Can. J. Chem. Eng.*, 9999:1–7, mar 2012.

[60] Herbert D Landahl and Gerold M Grodsky. Comparison of models of insulin release. *Bull. Math. Biol.*, 44(3):399–409, 1982.

[61] GC Weir and S Bonner-Weir. Five stages of evolving β-cell dysfunction during progression to diabetes. *Diabetes*, 53(December):S16–S21, 2004.

[62] Gerald M. Reaven, Hans Lithell, and Lewis Landsberg. Hypertension and Associated Metabolic AbnormalitiesThe Role of Insulin Resistance and the Sympathoadrenal System. *N. Engl. J. Med.*, 334:374–381, 1996.

[63] G M Steil, a Volund, S E Kahn, and R N Bergman. Reduced sample number for calculation of insulin sensitivity and glucose effectiveness from the minimal model. Suitability for use in population studies. *Diabetes*, 42(2):250–6, feb 1993.

[64] M Laakso. How good a marker is insulin level for insulin resistance? *Am. J. Epidemiol.*, 137(9):959–65, may 1993.

[65] R S Legro, D Finegood, and a Dunaif. A fasting glucose to insulin ratio is a useful measure of insulin sensitivity in women with polycystic ovary syndrome. *J. Clin. Endocrinol. Metab.*, 83(8):2694–8, aug 1998.

[66] M Emoto, Y Nishizawa, K Maekawa, Y Hiura, H Kanda, T Kawagishi, T Shoji, Y Okuno, and H Morii. Homeostasis model assessment as a clinical index of insulin resistance in type 2 diabetic patients treated with sulfonylureas. *Diabetes Care*, 22 (5):818–22, 1999.

[67] Enzo Bonora, Giovanni Targher, Maria Alberiche, Riccardo C. Bonadonna, Francesca Saggiani, Marina B. Zenere, Tiziano Monauni, and Michele Muggeo. Homeostasis model assessment closely mirrors the glucose clamp technique in the assessment of insulin sensitivity: Studies in subjects with various degrees of glucose tolerance and insulin sensitivity. *Diabetes Care*, 23(1):57–63, 2000.

[68] J Cederholm and L Wibell. Insulin release and peripheral sensitivity at the oral glucose tolerance test. *Diabetes Res. Clin. Pract.*, 10(2):167–75, oct 1990.

[69] Jean-Marie Ekoé, Zubin Punthakee, Thomas Ransom, Ally P.H. Prebtani, and Ronald Goldenberg. Screening for Type 1 and Type 2 Diabetes. *Can. J. Diabetes*, 37:S12–S15, apr 2013.

[70] Tomoshige Hayashi, Edward J Boyko, Kyoko Kogawa Sato, Marguerite J McNeely, Donna L Leonetti, Steven E Kahn, and Wilfred Y Fujimoto. Patterns of insulin concentration during the OGTT predict the risk of type 2 diabetes in Japanese Americans. *Diabetes Care*, 36(5):1229–35, may 2013.

[71] AG Bakari and GC Onyemelukwe. Plasma insulin response to oral glucose tolerance test in type-2 Nigerian diabetics. *East Afr. Med. J.*, 81(9):463–467, 2004.

[72] RJ Jarrett, IA Baker, H Keen, and NW Oakley. Diurnal variation in oral glucose tolerance: blood sugar and plasma insulin levels morning, afternoon, and evening. *Br. Med. J.*, 1(January):199–201, 1972.

[73] Filip K Knop, Tina Vilsbøll, Patricia V Højberg, Steen Larsen, Sten Madsbad, Aage Vølund, Jens J Holst, and Thure Krarup. Reduced incretin effect in type 2 diabetes: cause or consequence of the diabetic state? *Diabetes*, 56(8):1951–1959, 2007.

[74] F K Knop, T Vilsbøll, S Madsbad, J J Holst, and T Krarup. Inappropriate suppression of glucagon during OGTT but not during isoglycaemic i.v. glucose infusion contributes to the reduced incretin effect in type 2 diabetes mellitus. *Diabetologia*, 50(4):797–805, may 2007.

[75] DJ Chisholm, JD Young, and L Lazarus. The gastrointestinal stimulus to insulin release: I. Secretin. *J. Clin. Invest.*, 48(8):1453–60, aug 1969.

[76] Fatemeh Ekram, Melissa Barazandegan, Ezra Kwok, and Bhushan Gopaluni. Evaluation of treatment regimens for blood glucose regulation in type II diabetes using pharmacokinetic-pharmacodynamic modeling. In *2015 34th Chinese Control Conf.*, pages 8519–8524. IEEE, jul 2015.

[77] O Vahidi, RB Gopaluni, and KE Kwok. Detection of organ dysfunction in type II diabetic patients. *Am. Control Conf.*, 3:4769–4774, 2011.

[78] Akash Rajak and Kanak Saxena. Achieving realistic and interactive clinical simulation using case based TheraSim's therapy engine dynamically. *Proc. Natl. Conf. . . .*, 2010.

[79] CM Machan. *Type 2 diabetes mellitus and the prevalence of age-related cataract in a clinic population.* Ms.c., MS.c. Thesis, University of Waterloo, 2012.

[80] Wei Qi Wei, Cynthia L Leibson, Jeanine E Ransom, Abel N Kho, and Christopher G Chute. The absence of longitudinal data limits the accuracy of high-throughput

clinical phenotyping for identifying type 2 diabetes mellitus subjects. *Int. J. Med. Inform.*, jul 2012.

[81] Thomas Briegel and Volker Tresp. A Nonlinear State Space Model for the Blood Glucose Metabolism of a Diabetic (Ein nichtlineares Zustandsraummodell fur den Blutglukosemetabolismus eines Diabetikers). *at-Automatisierungstechnik*, 50(5):228–236, 2002.

[82] V Tresp and T Briegel. A solution for missing data in recurrent neural networks with an application to blood glucose prediction. *Adv. Neural Inf. Process. Syst.*, 10: 971–977, 1998.

[83] V Tresp, T Briegel, and J Moody. Neural-network models for the blood glucose metabolism of a diabetic. *Neural Networks, IEEE ...*, 10(5):1204–13, jan 1999.

[84] AK El-Jabali. Neural network modeling and control of type 1 diabetes mellitus. *Bioprocess Biosyst. Eng.*, 27(2):75–9, apr 2005.

[85] SG Mougiakakou. Neural network based glucose-insulin metabolism models for children with type 1 diabetes. *... Med. ...*, 1(Mm):3545–8, jan 2006.

[86] Shima Khatibisepehr and Biao Huang. Dealing with irregular data in soft sensors: Bayesian method and comparative study. *Ind. Eng. Chem. Res.*, 47(22):8713–8723, nov 2008.

[87] AP Dempster, NM Laird, and DB Rubin. Maximum likelihood from incomplete data via the EM algorithm. *J. R. Stat. Soc. Ser. B*, 39(1):1–38, 1977.

[88] R. B. Gopaluni. A particle filter approach to identification of nonlinear processes under missing observations. *Can. J. Chem. Eng.*, 86(6):1081–1092, dec 2008.

[89] Jing Deng and Biao Huang. Bayesian method for identification of constrained non-linear processes with missing output data. *Am. Control Conf.*, 3:96–101, 2011.

[90] Gianluigi Pillonetto, Giovanni Sparacino, Paolo Magni, Riccardo Bellazzi, and Claudio Cobelli. Minimal model S(I)=0 problem in NIDDM subjects: nonzero Bayesian estimates with credible confidence intervals. *Am. J. Physiol. Endocrinol. Metab.*, 282 (3):E564–73, mar 2002.

[91] C Cobelli, A Caumo, and M Omenetto. Minimal model SG overestimation and SI underestimation: improved accuracy by a Bayesian two-compartment model. *Am. J. Physiol.*, 277(3 Pt 1):E481–E488, 1999.

[92] G Sparacino. Maximum-likelihood versus maximum a posteriori parameter estimation of physiological system models: the C-peptide impulse response case study. *. . . , IEEE Trans.*, 47(6):801–11, jun 2000.

[93] Aditya Tulsyan, Biao Huang, R. Bhushan Gopaluni, and J. Fraser Forbes. On simultaneous on-line state and parameter estimation in non-linear state-space models. *J. Process Control*, 23(4):516–526, apr 2013.

[94] N. Kantas, A. Doucet, S. S. Singh, and J. M. Maciejowski. An overview of sequential Monte Carlo methods for parameter estimation in general state-space models. *IFAC Symp. Syst. Identif.*, (Ml):774–785, 2009.

[95] P.M. Frank and X. Ding. Survey of robust residual generation and evaluation methods in observer-based fault detection systems. *J. Process Control*, 7(6):403–424, 1997.

[96] V. Kadirkamanathan, P. Li, M. H. Jaward, and S. G. Fabri. Particle filtering-based fault detection in non-linear stochastic systems. *Int. J. Syst. Sci.*, 33(4):259–265, 2002.

[98] O Vahidi and KE Kwok. Development of a physiological model forpatients with type 2 diabetes mellitus. *... Control Conf. (ACC ...*, pages 2027–2032, 2010.

[99] IA Gardner. The utility of Bayes' theorem and Bayesian inference in veterinary clinical practice and research. *Aust. Vet. J.*, 80(12):10–13, 2002.

[100] Andrea Facchinetti, Simone Del Favero, Giovanni Sparacino, and Claudio Cobelli. Detecting failures of the glucose sensor-insulin pump system: Improved overnight safety monitoring for Type-1 diabetes. In *Proc. Annu. Int. Conf. IEEE Eng. Med. Biol. Soc. EMBS*, pages 4947–4950, 2011.

[101] Pau Herrero, Remei Calm, and J Vehí. Robust Fault Detection System for Insulin Pump Therapy Using Continuous Glucose Monitoring. *J. Diabetes Sci. Technol.*, 6 (5):1131–1141, 2012.

[102] Omid Vahidi, R. Bhushan Gopaluni, and Ezra Kwok. Detection of Abnormalities in Type II Diabetic Patients Using Particle Filters. *J. Med. Biol. Eng.*, 35(2):188–201, 2015.

[103] Daniel A. Finan, Wendy C. Bevier, Howard Zisser, Cesar C. Palerm, Lois Jovanovic, Francis J. Doyle III and Dale E. Seborg. An experimental evaluation of PCA monitoring strategies for type 1 diabetes subjects. In *AIChE New York Meet.*, 2006.

[104] Michaele Basseville. Detecting changes in signals and systems-A survey. *Automatica*, 24(3):309–326, 1988.

[105] Paul M Frank. Fault diagnosis in dynamic systems using analytical knowledge-based redundancy A survey and some new results. *Automatica*, 26(3):459–474, 1990.

[106] Rolf Isermann. Process fault detection based on modeling and estimation methods–A survey. *Automatica*, 20(4):387–404, 1984.

[107] Alan S. Willsky. A survey of design methods for failure detection in dynamic systems. *Automatica*, 12(6):601–611, 1976.

[108] Alan S Willsky. Detection of Abrupt Changes in Dynamic Systems. In M. Basseville and A. Benveniste, editors, *Detect. Abrupt Chang. Signals Dyn. Syst.*, pages 27–49. Springer, 1986.

[109] M Basseville and I V Nikiforov. *Detection of Abrupt Changes*, volume 2 of *Prentice Hall information and system sciences series*. Citeseer, 1993.

[110] A.D. Pouliezos and G.S. Stavrakakis. *Real time fault monitoring of industrial processes*. Kluwer Academic Publishers, USA, 1994.

[111] Bingyong Yan, Zuohua Tian, and Songjiao Shi. A novel distributed approach to robust fault detection and identification. *Int. J. Electr. Power Energy Syst.*, 30(5): 343–360, jun 2008.

[112] Jie Chen and Ron J Patton. *Robust model-based fault diagnosis for dynamic systems*, volume 11 of *Kluwer International Series on Asian Studies in Computer and Information Science*. Kluwer Academic Publishers, 1999.

[115] V. Kadirkamanathan, P. Li, M.H. Jaward, and S.G. Fabri. A sequential Monte Carlo filtering approach to fault detection and isolation in nonlinear systems. In *Proc. 39th IEEE Conf. Decis. Control (Cat. No.00CH37187)*, volume 5, pages 4341–4346. IEEE, 2000.

[116] Venkat Venkatasubramanian and Raghunathan Rengaswamy. A review of process fault detection and diagnosis Part I : Quantitative model-based methods. *Comput. Chem. Eng.*, 27:293–311, 2003.

[117] Venkat Venkatasubramanian, Raghunathan Rengaswamy, and Surya N Kavuri. A review of process fault detection and diagnosis: Part ii: Qualitative models and search strategies. *Comput. Chem. Eng.*, 27(3):313 – 326, 2003.

Appendix A

The numerical values of the clinical data sets used in chapter 4 are provided here in detailed. These values are normalized by the body weight of the subjects shown in Table A.1.

Table A.1: Gender and body weight of diabetic subjects [7]

	Subject									
	1	**2**	**3**	**4**	**5**	**6**	**7**	**8**	**9**	**10**
Body weight Kg	73.0	81.0	106.0	74.0	53.0	65.5	77.5	69.0	69.0	69.5
Gender	M	M	M	M	F	F	M	M	M	M

Table A.2: Normalized GLP-1 concentration data set ($pmol/l$) of diabetic subjects for OGTT [7]

Time (min)	**Subject**										**Mean**
	1	**2**	**3**	**4**	**5**	**6**	**7**	**8**	**9**	**10**	
0	17.7	19.7	18.0	18.3	15.7	11.7	22.7	8.0	9.7	9.3	15.1
15	41.0	28.2	30.1	15.9	28.8	14.8	25.3	9.0	9.0	16.0	21.8
30	26.4	42.0	36.2	32.8	28.8	48.5	33.0	29.7	13.9	19.9	31.1
45	29.5	36.3	36.2	18.0	36.4	65.3	27.5	35.6	16.9	30.8	33.2
60	36.8	28.2	39.2	22.2	29.5	45.7	25.3	22.8	17.9	29.9	29.7
90	22.2	16.6	30.1	18.0	20.5	20.4	23.0	18.8	22.8	21.9	21.4
120	12.8	10.8	33.1	11.6	13.6	15.7	24.1	12.9	13.9	16.0	16.5
150	9.7	10.8	39.2	14.8	21.2	18.5	23.0	13.9	10.5	14.0	17.6
180	14.9	13.1	28.6	21.2	16.7	14.8	14.2	16.9	7.0	15.0	16.2
240	9.7	14.3	19.5	16.9	11.4	12.0	9.8	10.0	10.0	16.0	12.9

Table A.3: Normalized GIP concentration data set ($pmol/l$) of diabetic subjects for OGTT test [7]

Time (min)	**Subject**										**Mean**
	1	**2**	**3**	**4**	**5**	**6**	**7**	**8**	**9**	**10**	
0	9.0	6.7	9.0	36.0	16.3	12.3	30.3	8.7	11.7	42.3	18.2
15	89.3	80.0	127.1	77.2	61.5	47.6	125.2	26.7	19.9	100.6	75.5
30	59.1	118.1	133.2	144.9	67.6	78.5	107.5	32.7	45.5	110.5	89.7
45	83.0	95.0	115.0	142.8	72.9	55.1	108.6	28.7	57.3	111.5	87.0
60	69.5	95.0	90.8	113.2	61.5	60.7	105.3	35.6	62.3	118.5	81.2
90	72.6	39.5	68.1	66.7	59.2	40.1	78.7	26.7	51.4	93.6	59.7
120	33.0	22.1	31.7	40.2	24.4	30.7	41.0	15.9	24.8	32.1	29.6
150	15.3	11.7	9.0	18.0	13.1	17.6	20.0	8.0	17.4	21.2	15.1
180	10.0	11.7	10.5	19.1	10.0	14.8	8.9	10.0	10.0	24.1	12.9
240	6.9	10.5	12.0	10.6	12.3	9.2	17.8	9.0	7.1	12.2	10.8

Table A.4: Normalized peripheral glucose concentration data set ($mmol/l$) of diabetic subjects for OGTT test [7]

Time (min)	**Subject**										**Mean**
	1	**2**	**3**	**4**	**5**	**6**	**7**	**8**	**9**	**10**	
0	8.4	9.1	7.5	10.4	7.6	7.3	8.3	6.2	12.0	8.4	8.5
5	8.1	8.8	6.7	9.9	7.2	6.7	8.0	6.1	11.6	8.3	8.1
10	8.8	9.9	8.3	10.8	8.5	7.5	8.1	6.6	12.5	8.7	9.0
15	10.0	11.3	9.6	11.5	9.3	8.3	9.3	8.0	12.8	9.7	10.0
20	11.1	13.2	10.7	12.5	10.1	9.1	10.7	7.9	14.1	10.8	11.0
30	12.3	15.8	13.6	16.4	11.0	11.4	14.4	10.0	15.1	12.5	13.2
40	13.2	18.0	14.6	17.6	12.0	13.0	15.3	11.2	16.8	14.5	14.6
50	14.7	18.6	16.4	18.6	12.7	12.7	16.4	11.7	17.5	15.8	15.5
60	16.3	19.4	17.3	19.6	13.1	12.7	17.0	11.5	18.5	16.9	16.3
70	16.8	19.6	16.3	19.6	13.4	11.3	16.8	11.6	19.1	17.7	16.2
90	18.4	16.7	15.5	19.3	12.7	9.6	13.5	11.3	20.2	17.5	15.5
120	17.5	14.0	13.3	17.4	10.9	7.8	10.1	9.7	19.2	13.6	13.3
150	16.4	12.0	10.2	15.4	8.6	5.8	8.3	7.6	17.5	11.0	11.3
180	14.3	9.6	7.7	14.0	7.5	5.2	7.1	6.5	16.2	9.0	9.7
240	12.2	7.2	5.7	12.4	6.4	5.3	5.4	5.5	14.7	6.4	8.1

Table A.5: Normalized peripheral insulin concentration data set ($pmol/l$) of diabetic subjects for OGTT test [7]

Time (min)	**Subject**										**Mean**
	1	**2**	**3**	**4**	**5**	**6**	**7**	**8**	**9**	**10**	
0	43	50	126	48	52	32	27	17	22	33	45
10	33	71	102	42	68	34	34	14	29	39	46
20	75	122	216	29	122	89	68	40	37	62	86
30	109	153	379	67	114	197	99	77	34	83	131
40	66	202	399	55	152	202	99	91	57	59	138
50	68	180	408	81	201	155	133	59	53	102	144
60	81	184	446	75	199	196	152	48	47	102	153
70	73	85	393	50	161	198	179	57	35	165	140
90	82	107	414	65	175	173	129	59	36	194	143
120	49	111	378	52	107	102	74	38	24	78	101
150	63	87	250	63	60	38	40	28	24	64	72
180	50	69	184	42	66	26	30	14	33	65	58
240	38	44	81	46	42	30	14	5	22	28	35

Table A.6: Normalized peripheral glucose concentration data set ($mmol/l$) of diabetic subjects for IIVGIT test [7]

Time (min)	**Subject**										**Mean**
	1	**2**	**3**	**4**	**5**	**6**	**7**	**8**	**9**	**10**	
0	9.3	10.8	7.5	10.4	6.7	7.4	7.2	5.5	12.4	8.8	8.6
5	8.7	11.0	6.4	9.7	7.5	6.3	6.3	4.8	11.9	8.3	8.1
10	9.1	11.1	8.9	10.7	8.3	7.7	8.2	6.6	12.3	8.6	9.1
15	9.7	11.1	10.7	11.9	9.2	9.2	9.7	8.0	13.5	10.5	10.3
20	10.4	13.3	12.0	12.1	9.9	9.5	10.3	8.7	14.0	11.4	11.2
25	10.8	14.3	13.1	12.8	10.3	9.7	10.6	9.3	14.0	11.8	11.7
30	11.4	15.4	15.2	14.0	11.3	10.5	12.3	10.5	15.3	13.1	12.9
35	12.3	16.0	16.1	13.5	12.3	10.8	13.1	10.5	15.7	13.8	13.4
40	13.2	17.0	18.7	15.9	13.3	11.5	15.4	11.3	16.6	14.3	14.7
45	14.0	17.7	18.7	17.8	14.3	11.9	16.7	10.1	16.8	14.6	15.3
50	14.6	18.3	18.6	18.6	14.4	13.8	17.4	12.2	17.3	15.7	16.1
60	16.3	19.0	17.9	19.4	14.1	13.9	16.9	12.1	18.0	17.4	16.5
70	16.9	19.8	17.2	19.9	12.8	12.4	16.9	12.3	19.1	17.9	16.5
90	17.4	18.0	14.9	20.2	11.5	9.6	15.2	12.9	19.7	17.8	15.7
120	17.9	15.1	12.3	18.1	10.3	7.4	11.9	11.8	19.9	14.9	13.9
150	16.1	12.9	9.8	16.2	8.8	6.0	8.2	9.9	18.2	12.5	11.9
180	15.0	11.0	8.3	13.8	7.3	5.3	7.1	8.3	17.1	10.4	10.4
240	12.6	8.8	5.8	12.3	6.1	5.2	5.2	6.3	15.3	7.3	8.5

Table A.7: Normalized peripheral glucose concentration data set ($mmol/l$) of diabetic subjects for IIVGIT test [7]

Time (min)	**Subject**										**Mean**
	1	**2**	**3**	**4**	**5**	**6**	**7**	**8**	**9**	**10**	
0	9.3	10.8	7.5	10.4	6.7	7.4	7.2	5.5	12.4	8.8	8.6
5	8.7	11.0	6.4	9.7	7.5	6.3	6.3	4.8	11.9	8.3	8.1
10	9.1	11.1	8.9	10.7	8.3	7.7	8.2	6.6	12.3	8.6	9.1
15	9.7	11.1	10.7	11.9	9.2	9.2	9.7	8.0	13.5	10.5	10.3
20	10.4	13.3	12.0	12.1	9.9	9.5	10.3	8.7	14.0	11.4	11.2
25	10.8	14.3	13.1	12.8	10.3	9.7	10.6	9.3	14.0	11.8	11.7
30	11.4	15.4	15.2	14.0	11.3	10.5	12.3	10.5	15.3	13.1	12.9
35	12.3	16.0	16.1	13.5	12.3	10.8	13.1	10.5	15.7	13.8	13.4
40	13.2	17.0	18.7	15.9	13.3	11.5	15.4	11.3	16.6	14.3	14.7
45	14.0	17.7	18.7	17.8	14.3	11.9	16.7	10.1	16.8	14.6	15.3
50	14.6	18.3	18.6	18.6	14.4	13.8	17.4	12.2	17.3	15.7	16.1
60	16.3	19.0	17.9	19.4	14.1	13.9	16.9	12.1	18.0	17.4	16.5
70	16.9	19.8	17.2	19.9	12.8	12.4	16.9	12.3	19.1	17.9	16.5
90	17.4	18.0	14.9	20.2	11.5	9.6	15.2	12.9	19.7	17.8	15.7
120	17.9	15.1	12.3	18.1	10.3	7.4	11.9	11.8	19.9	14.9	13.9
150	16.1	12.9	9.8	16.2	8.8	6.0	8.2	9.9	18.2	12.5	11.9
180	15.0	11.0	8.3	13.8	7.3	5.3	7.1	8.3	17.1	10.4	10.4
240	12.6	8.8	5.8	12.3	6.1	5.2	5.2	6.3	15.3	7.3	8.5

Table A.8: Normalized peripheral insulin concentration data set ($pmol/l$) of diabetic subjects for IIVGIT test [7]

Time (min)	**Subject**										**Mean**
	1	**2**	**3**	**4**	**5**	**6**	**7**	**8**	**9**	**10**	
0	27	74	111	46	45	33	17	7	17	32	41
10	21	73	90	46	47	44	21	26	18	30	42
20	22	84	152	36	47	51	28	28	11	30	49
30	20	80	209	43	63	55	31	26	12	36	57
40	18	98	244	45	62	78	39	31	16	47	68
50	22	106	297	57	67	99	44	30	19	49	79
60	25	101	334	75	79	126	73	25	15	66	92
70	27	105	259	91	64	117	71	23	17	47	82
90	37	101	349	75	70	108	62	24	20	42	89
120	36	95	294	64	84	68	72	19	23	62	82
150	41	100	197	47	56	53	55	21	21	16	61
180	50	110	161	53	40	21	29	17	24	16	52
240	30	50	91	35	31	19	17	10	20	27	33

Table A.9: : Intravenous glucose infusion amount (g) to diabetic subjects during IIVGIT test [7]

Time (min)	**Subject**										**Mean**
	1	**2**	**3**	**4**	**5**	**6**	**7**	**8**	**9**	**10**	
0-15	1.53	0.2	13.8	2.4	8	3.2	6	6.4	2.8	2.6	4.7
15-30	4.41	11	10.6	6.4	8.8	7.6	11.2	10	7.8	8.2	8.62
30-45	9.21	8.6	17.4	13.2	12.4	11.6	12.8	3.8	8.4	8.4	10.62
45-60	7.48	8.6	4.8	12.2	3.8	7.8	8	7.8	8.2	11.2	8.02
60-75	5.95	6.6	2.8	7.6	1.4	0.8	4.8	5.8	9.2	8.6	5.38
75-90	4.99	1.4	0.8	3.2	2	0.4	2	4.2	7.2	6.2	3.26
90-105	6.33	0	0.2	2	2.8	0.2	0.2	3	7	0.4	2.24
105-120	0.96	0	0	2	3	0.4	0	1.4	0.4	0	0.82
120-135	0.58	0	0	0.6	3.2	0.2	0	0	0.2	0	0.48
135-150	0.38	0	0	0.4	0	0.2	0	0	0	0	0.1
150-165	0.58	0	0	0	0	0	0	0	0	0	0.06
165-180	0	0	0	0	0	0	0	0	0	0	0
180-195	0.19	0	0	0	0	0	0	0	0	0	0.02
195-240	0	0	0	0	0	0	0	0	0	0	0
Total	42.6	36.4	50.4	50	45.4	32.4	45	42.4	51.2	45.6	44.32